ABB

ENVISAT–1
GROUND SEGMENT

MIPAS
Michelson Interferometer for Passive Atmospheric Sounding

Algorithm Technical Baseline Document (ATBD) for MIPAS Level 1B Processing

Program Document No: **PO-TN-BOM-GS-0012**
Issue: **2** **Revision:** **-**
Date: **14 October 2016**

	Function	Name	Signature	Date
Prepared by	R&D Scientist	Richard L. Lachance		
Revised by	Software Engineer	Ginette Aubertin		
Approved by				
Approved by	PM	Gaétan Perron		

ABB Inc. • Automation Division
3400 Rue Pierre-Ardouin • Québec, Québec G1P 0B2 CANADA • Phone (418) 877-2944 • Fax (418) 877-2834

TABLE OF CONTENTS

TABLE OF CONTENTS 1
DOCUMENT CHANGE RECORD 4
1. INTRODUCTION 6
1.1 Purpose of document 6
1.2 Scope 6
1.3 Documents 7
1.4 Definitions 8
1.4.1 Calibration 8
1.4.2 Validation 8
1.4.3 Characterization 9
1.4.4 Verification 10
1.4.5 Observational Data 10
1.4.6 Auxiliary Data 10
1.4.7 Measurement Data 10
1.4.8 Other Instrument Specific Terms and Definitions 10
1.4.9 MIPAS Data products from ESA 11
1.5 Acronyms 12
2. Ground Processing Description 14
2.1 Measurement principle 14
2.2 Details about instrument detectors 15
2.3 Types of measurements 16
2.3.1 Description of the related measurement types 16
3. Ground Processing principles 18
3.1 Objective of the Ground Processing 18
3.2 Overview of Ground Processing needs 19
3.2.1 Instrument Operation vs. Data Acquisition / Downlink Scenario 19
3.3 Basic radiometric relations 19
3.3.1 General Calibration Equation 20
3.3.2 MIPAS Specific Calibration Equation 21
3.4 Special considerations 23
3.4.1 Fringe count errors detection and correction 23
3.4.2 Non-linearity correction 27
3.4.3 Spectral calibration 28
3.4.4 Complex numerical filtering 30
3.4.5 SPE and PAW responsivity scaling 33
3.5 Identification of the Ground Processing functions 34
4. Ground Processing Functions and Description 38
4.1 LOAD DATA 40
4.1.1 Objective 40
4.1.2 Definition of variables 42
4.1.3 Detailed structure and formulas 44
4.1.4 Computational sequence 46
4.2 CALCULATE OFFSET CALIBRATION 48
4.2.1 Objective 49

4.2.2 Definition of variables....50
4.2.3 Detailed structure and formulas....53
4.2.4 Computational sequence....60
4.3 CALCULATE GAIN CALIBRATION....62
4.3.1 Objective....63
4.3.2 Definition of variables....65
4.3.3 Detailed structure and formulas....69
4.3.4 Computational sequence....80
4.4 CALCULATE SPECTRAL CALIBRATION....83
4.4.1 Objective....84
4.4.2 Definition of variables....85
4.4.3 Detailed structure and formulas....87
4.4.4 Computational sequence....92
4.5 CALCULATE RADIANCE....94
4.5.1 Objective....94
4.5.2 Definition of variables....95
4.5.3 Detailed structure and formulas....99
4.5.4 Computational sequence....110
4.6 CALCULATE ILS RETRIEVAL....113
4.6.1 Objective....114
4.6.2 Definition of variables....115
4.6.3 Detailed structure and formulas....117
4.6.4 Computational sequence....122
4.7 CALCULATE POINTING....123
4.7.1 Objective....123
4.7.2 Definition of Variables....124
4.7.3 Detailed structure and formulas....125
4.7.4 Computational Sequence....127
4.8 CALCULATE GEOLOCATION....129
4.8.1 Objective....129
4.8.2 Definition of Variables....130
4.8.3 Detailed structure and formulas....133
4.8.4 Computational Sequence....139
4.9 MAIN PROCESSING SUBFUNCTIONS....141
4.9.1 Spikes detection....141
4.9.2 Interpolation....147
4.9.3 Fringe count error detection and correction....154
4.9.4 Non-linearity correction....158
4.9.5 Equalization and combination....160
4.9.6 Peak fitting....161
4.10 AUXILIARY SUBFUNCTIONS....163
4.10.1 Fast Fourier transforms....163
4.10.2 Alias unfolding....165
4.10.3 Linear fitting....168
4.10.4 Parabolic fitting....170
4.10.5 Linear interpolation....172
4.10.6 Parabolic interpolation....174
4.10.7 Simplex minimization....176

4.10.8 Determination of the goodness of fit 179

5. Ground Processing Accuracies 182
5.1 Sources of processing errors 182
5.1.1 Algorithm accuracy 182
5.1.2 Finite precision 182
5.2 General assumptions 184
5.2.1 Key Instrument performance requirements 184

APPENDIX A ILS Algorithm 185
A.1 Input Parameters 185
A.2 Formulas 186
A.2.1 Integration on a Finite Field of View 186
A.2.2 Laser Misalignment and Shear 187
A.2.3 Optical Speed Profile 187
A.2.4 Sampling Perturbation at Turn Around 187
A.2.5 Drift of Laser Frequency 188
A.2.6 White Frequency Noise on Laser Signal 188
A.2.7 Overall Modulation and ILS 188

APPENDIX B Additional Functionality ALGORITHMs 189
B.1 ANALYZE INTERFEROGRAM 189
B.1.1 Definition of variables 189
B.1.2 Formulas 189
B.2 RAW TO NOMINAL 191
B.2.1 Definition of variables 191
B.2.2 Formulas 191
B.3 INTRODUCE FCE 193
B.3.1 Definition of variables 193
B.3.2 Formulas 193
B.4 COADD INTERFEROGRAMS 194
B.4.1 Definition of variables 194
B.4.2 Formulas 195

DOCUMENT CHANGE RECORD

Issue	Revision	Date	Chapter / Paragraph Number, Change Description (and Reasons)
1	-	16 Sep 1998	First release of document. Version based on Issue 4A (27 February 1998) of document "Detailed Processing Model and Parameter Data List Document (DPM/PDL) for MIPAS Level 1B Processing" (PO-RP-BOM-GS-0003). The Detailed Structure and Formulas sections have been combined for all ground segment functions. Note that the present processing scheme of FCE handling is still under revision and not definitive.
1	A	29 May 2001	Update of document to be in-line with issue 4D (20 April 2001) of DPM PO-RP-BOM-DS-0003.
1	B	15 Oct 2002	Update of document to be in-line with issue 4F (15 Oct 2002) of DPM PO-RP-BOM-DS-0003.
1	C	15 Nov 2006	Update of document to be in-line with issue 4L (1 July 2006) Deletion of paragraphs (section 3.4.1.3) and modification of the note concerning systematic FCE of previous offset (section 4.2.4.12). Update of ILS algorithm to handle new MIPAS resolution Update of algorithm to perform reduction of resolution by software on calibration measurements (section 4.1.4) Change Load Data when ISP auxiliary data missing Support offline processing with restituted attitude file Calculate quadratic terms for spectral calibration Report ILS shift frequency Reduce interferogram to avoid undersampling the spectrum for scene obtained at 8.2 MPD.
1	D	24 May 2013	Update of document to be in-line with issue 5D (18 March 2013) of DPM PO-RP-BOM-DS-0003. Improved spike detection/correction algorithm Improved offset validation algorithm Improved altitude determination

2	-	14 Oct 2016	Update of document to be in-line with issue 6 (14 October 2016) of DPM PO-RP-BOM-DS-0003.

1. INTRODUCTION

1.1 Purpose of document

The purpose of this document is to describe the Level 1B algorithms needed for the ground segment in order to produce meaningful data meeting all the requirements of the MIPAS instrument. The present Algorithm Technical Baseline Document (ATBD) is destined to the user community and all MIPAS related people.

MIPAS (Michelson Interferometer for Passive Atmospheric Sounding) is an ESA developed instrument to be operated on board ENVISAT-1 as part of the first Polar Orbit Earth Observation Mission program (POEM-1). MIPAS will perform limb sounding observations of the atmospheric emission spectrum in the middle infrared region.

Level 1B data is geolocated, radiometrically and spectrally (frequency) calibrated spectra with annotated quality indicators.

1.2 Scope

This document describes the MIPAS instrument specific processing required at the ground segment. This work concerns the processing at the ground segment of the MIPAS instrument data. It covers only the processing up to Level 1B data products specific to the MIPAS instrument. It covers the processing needs for all data being sent to ground when the instrument is operational, including observational and auxiliary data, for all measurements performed by the instrument, with the exception of the processing of data generated in raw data mode, SPE self test mode and in LOS calibration mode. It is assumed that the data entering the processing chain is identical to the data leaving the instrument on board.

The Envisat–1 ground segment is composed of three parts: the Payload Data Segment (PDS), the Flight Operation Segment (FOS) and the User Data Segment (UDS). This work is related only to the PDS. Therefore, the processing of the data produced when the instrument is under test or characterization, e.g. during the Commissioning Phase, is excluded.

A special case is the use of the raw data mode of the instrument, allowed only when the platform is in direct view of a receiving station. This mode is intended only for instrument testing. Thus, data produced in the raw data mode is not covered here. Finally, the processing required for the preparation of new up-loadable data tables, for changing the instrument operational configuration, is also excluded.

1.3 Documents

Refer to the MIGSP STD [RD 23] for issue number of the documents pertaining to the latest version of the MIGSP S/W.

Reference documents

No	Reference	Title
[RD 1]	PO-RS-DOR-SY-0029	MIPAS Assumptions on the Ground Segment
[RD 2]	PO-TN-BOM-MP-0019	Non-linearity Characterization and Correction
[RD 3]	PO-RS-DOR-MP-0001	MIPAS Instrument Specification
[RD 4]	PO-TN-BOM-GS-0006	MIPAS In-flight Spectral Calibration and ILS retrieval
[RD 5]	PO-PL-BOM-MP-0009	Instrument Level Calibration and Characterization Plan
[RD 6]	PO-PL-DAS-MP-0031	In-Flight Calibration Plan
[RD 7]	PO-TN-BOM-GS-0010	MIPAS Level 1B Processing Input/Output Data Definition
[RD 8]	PO-RP-DAS-MP-0036	Conversion Algorithms for MIPAS Auxiliary Data
[RD 9]	PO-ID-DOR-SY-0032	Payload to Ground Segment Interface Control Document
[RD 10]	PO-TN-DAS-MP-0001	Instrument Timeline
[RD 11]	PO-TN-BOM-GS-0007	MIPAS Observational Data Validation
[RD 12]	PO-RS-BOM-MP-0001	On-ground Signal Processing Requirement Specifications
[RD 13]	PO-RP-BOM-MP-0001	MIPAS Performance Analysis
[RD 14]	PO-TN-ESA-GS-0361	ENVISAT-1 reference definitions document for mission related software
[RD 15]	PO-TN-BOM-GS-0005	Detection of spurious spikes in an interferogram
[RD 16]	PO-TN-BOM-MP-0017	Technical Note on Fringe Count Error
[RD 17]	PO-ID-DAS-MP-0010	Instrument Measurement Data Definition
[RD 18]	PO-IS-GMV-GS-0557	ENVISAT-1 Mission CFI Software, PPF_LIB Software User Manual
[RD 19]	PO-IS-GMV-GS-0558	ENVISAT-1 Mission CFI Software, PPF_ORBIT Software User Manual
[RD 20]	PO-IS-GMV-GS-0559	ENVISAT-1 Mission CFI Software, PPF_POINTING Software User Manual
[RD 21]	H. E. Revercomb, H. Buijs, H. B. Howell, D. D. Laporte, W. L. Smith, and L. A. Sromovsky, “Radiometric calibration of IR Fourier transform spectrometers: solution to a problem with the High-Resolution Interferometer Sounder”, Appl. Opt., Vol. 27, No 15, pp. 3210–3218, Aug. 1988.	
[RD 22]	PO-RP-BOM-MP-0003	Detailed Processing Model and Parameter Data List Document (DPM/PDL) for MIPAS Level 1B Processing
[RD 23]	PO-MA-BOM-GS-0002	MIGSP Software Transfer Document

1.4 Definitions

In this section, we review some of the basic terms used in the document. For each term, we provide (in *italics*) the definition established by the mission prime, if such a definition exists. Then, if necessary, we present an interpretation of the definition for the MIPAS instrument ground segment.

1.4.1 Calibration

Calibration, in the sense as used within the ENVISAT–1 program, is the procedure for converting instrument measurement output data into the required physical units.

For MIPAS, the output of the ground processor is an atmospheric spectrum showing radiance as a function of wavenumber. Calibration refers not only to the assignment of absolute radiance values to the y-axis but also to the assignment of absolute wavenumbers to the x-axis. The calibration procedure is defined by the three major elements:

- A scenario for measurement data acquisition,
- A set of auxiliary data, as acquired during on-ground characterization or from the subsystem/platform during the measurement,
- A method for computing the calibrated data using the measurement and characterization data.

Three types of calibration for MIPAS can thus be identified:

Radiometric Calibration: The process of assigning absolute values in radiance units, (noted [r.u.] expressed in $W/(cm^2\ sr\ cm^{-1})$) to the intensity axis (y-axis) with a specified accuracy. The radiometric calibration implies the knowledge of a certain spectral calibration.

Spectral Calibration: The process of assigning absolute values in cm^{-1} to the wavenumber axis (x-axis) with a specified accuracy.

LOS Calibration: The process of assigning an absolute LOS pointing value to a given atmospheric spectrum with a specified accuracy.

1.4.2 Validation

Validation has no specific definition for the program. In the present document, we will use this term according to the following definition.

Validation is the procedure for converting instrument measurement data into a representative indicator of the quality of the measurement. It consists of:

- A set of pre-established reference data. This data shall be available for the ground segment. It may be deduced from characterization measurements (characterization for validation) or it may be obtained analytically.
- A method for computing the quality indicator of a given measurement using the reference data.

In this document the following types of validation may be distinguished:

System validation: Procedure for converting the relevant auxiliary data into quality indication.

Observation validation: Procedure for converting observational data into quality indication.

The final indicator of the quality of the measurement data takes into account both types of validation.

1.4.3 Characterization

Characterization is the direct measurement, or derivation from measurements, of a set of technical and functional parameters, valid over a range of conditions to provide data necessary for calibration, ground processor initialization and verification.

Characterization measurements can be classified according to their purposes

- Characterization for calibration: These are all measurements used in the calibration procedure besides actual scene measurements. These measurements may be acquired on ground or in flight. Since by definition, the data from these measurements are used in the calibration procedure, they all need to be available to the ground segment.
- Characterization for verification: Verification is defined below. In the context of characterization, verification refers only to performance requirements.
- Characterization for ground processor initialization: These are the data used in the ground processing and stored at ground segment prior to launch. In these, we can distinguish
  - Pre-flight characterization for calibration: Characterization measurements taken on ground and used in the calibration procedure. The data from these measurements may have been acquired at instrument level using the GSE (e.g. the spectral calibration) or at subsystem level by the subsystem contractor (e.g. the on-board blackbody radiance calibration).
  - Pre-flight characterization for verification: Not applicable to the MIPAS ground segment. There are no pre-flight verification measurements needed by the ground processor.
  - Pre-flight characterization for validation: Characterization measurements taken on ground and used in the validation procedure. The data from these measurements may have been acquired at instrument level using the GSE (e.g. deep space interferogram reference data) or at subsystem level by the subsystem contractor (e.g. reference data for validation of detector temperature).

Determination: Determination is a special case of a characterization where the quantity is not measured as a function of any parameter, i.e. a single value is recorded.

1.4.4 Verification

Verification is the sum of all activities performed to demonstrate fulfillment of a requirement.

In principle, verification should be applied to all requirements in MIPAS requirement specifications and other applicable documents therein. There are several types of requirements, for example electrical requirements, mechanical requirements, etc. In the present document, we are only concerned by instrument performance requirements.

Characterization measurements for performance verification produce outputs in the form of an actual numerical value (or vector of values). By comparison of these measurements with numerical values representing the requirement, the performance verification process produces binary outputs of the type *pass/no pass*. Therefore, it requires a measurement accuracy equal to the expected magnitude of the specification of the requirement being verified.

1.4.5 Observational Data

Observational data is all raw sensor data acquired by the instrument after digitization.

By this is meant the data points from the source signal. In the case of MIPAS, the source signal can be an interferogram or the radiometric signal from a star crossing the FOV.

1.4.6 Auxiliary Data

Auxiliary data is all data to be provided by an instrument or an external source to allow full interpretation and evaluation of its observational data.

Auxiliary data is defined for the present document as all the additional data required by the ground segment for the generation and delivery of ground segment data products and coming neither from the space segment nor from the ground segment. These data are intended to be rarely changed. They include templates for data validation, look-up tables for data conversion, etc.

Also all additional data, apart from observational data sent to the ground segment by the instrument to allow full interpretation of its observational data.

1.4.7 Measurement Data

Measurement data is all (processed) observational and auxiliary data delivered by the instrument to the PPF Data Handling Assembly.

1.4.8 Other Instrument Specific Terms and Definitions

<u>Interferometer Sweep</u>

An interferometer sweep is the data recording for a single interferogram.

Elevation Scan Sequence

An elevation scan sequence comprises a sequence of interferometer sweeps within a fixed time interval at variable elevation and azimuth with respect to the MIPAS local normal reference frame.

The number of interferometer sweeps per elevation scan sequence can be commanded in the range from 1 to 75. A typical elevation scan sequence consists of 16 interferometer sweeps for operation with high spectral resolution. For operation with lowest spectral resolution, the typical elevation scan sequence consists of 75 interferometer sweeps.

The instrument can perform these typical elevation scan sequences within less than 75 seconds, not including the time required for an offset calibration.

The azimuth angle shall be adjustable during an elevation scan sequence within a limited range, but not during an interferometer sweep.

1.4.9 MIPAS Data products from ESA

Level	Description
Level 0	Unprocessed raw data with annotated quality and orbit information
Level 1A	Reconstructed interferograms from individual spectral channels (not archived)
Level 1B	Geolocated, radiometrically and spectrally (frequency) calibrated spectra with annotated quality indicators.
Level 2	Profiles of pressure, temperature, O_3, H_2O, CH_4, N_2O, and HNO_3
L2/Meteo	Subset of Level 2: pressure, temperature, O_3 and H_2O with < 3 hours of delivery time.

1.5 Acronyms

ADC	Analog to Digital Converter
AIT	Assembly, Integration, and Test
API	Application Process Identifier
APS	Absolute Position Measurement Sensor
ATBD	Algorithm Technical Baseline Document
BB	Blackbody
ASCM	Adaptive Scaling (non-linear) Correction Method
CCM	Cross-Correlation Method
CBB	MIPAS on-board Calibration Blackbody
CFI	Customer Furnished Items
DFH	Data Field Header
DPM	Detailed Processing Model
DPU	Detector and Preamplifier Unit
DS	Deep Space
ESA	European Space Agency
ESU	Elevation Scan Unit
FCE	Fringe Count Error
FFT	Fast Fourier Transform
FOS	Flight Operation Segment
FOV	Field Of View
FWHM	Full Width at Half Maximum
HWHM	Half Width at Half Maximum
ICU	Instrument Control Unit
IFoV	Instantaneous Field of View
IGM	Interferogram
ILS	Instrument Line Shape
INT	Interferometer
IR	Infrared
LOS	Line Of Sight
MPD	Maximum Path Difference
NESR	Noise Equivalent Spectral Radiance
OBT	On-Board Time
OPD	Optical Path Difference
PAW	Pre-Amplifier Warm
PC	Photo Conductive (detector)
PCD	Product Confidence Data
PDL	Parameter Data List
PDS	Payload Data Segment
PFM	Peak Finding Method
R&S&L	Radiometrically, Spectrally and Locally calibrated
RMS	Root Mean Square
SAA	South Atlantic Anomaly
SNR	Signal to Noise Ratio
SPC	Spectrum
SPE	Signal Processing Electronics

SPH	Source Packet Header
TBC	To Be Confirmed
TBD	To Be Determined
UDS	User Data Segment
ZPD	Zero Path Difference

μw	Microwindow
r.u.	Radiance units: $\frac{W}{\mathrm{cm}^2\,\mathrm{sr}\,\mathrm{cm}^{-1}}$
n.u.	No Units

2. GROUND PROCESSING DESCRIPTION

2.1 Measurement principle

MIPAS is a Michelson Interferometer based on the principle of Fourier Transform and designed to measure with high resolution and high spectral accuracy the emission of infrared radiation from the atmosphere in the spectral range from 4.15 to 14.6 μm (685 – 2410 cm^{-1}). At the core of the instrument is a Fourier transform spectrometer which measures with one stroke the spectral features of the atmosphere within the entire spectral range with high spectral resolution (less or equal than 0.035 cm^{-1} FWHM unapodized) and throughput. The spectrometer transforms the incoming spectral radiance, i.e. the *spectrum*, into a modulated signal, the *interferogram*, where all infrared wavenumbers in the band of interest are present simultaneously. The output from the spectrometer consists of one such interferogram for each observed scene.

The MIPAS instrument is designed to observe the horizon with an instantaneous field of view which corresponds at the tangent point to 3 km in vertical direction and 30 km in horizontal direction. MIPAS is equipped with two scan mirrors which allow to make measurements in either of two pointing regimes. One regime covers horizontally a 35 deg range in anti-flight direction (rearward) whilst the other one covers a 30 deg wide range sideways in anti-sun direction. The majority of measurements will be made in rearward viewing, as the observation geometry provides good coverage including the polar regions. For special events monitoring, the instrument can be commanded in both rearward and sideways viewing geometries. The vertical pointing range covers the tangent height from 5 to 150 km. One basic elevation scan sequence will comprise sixteen high resolution atmospheric scene measurements (or up to 75 scene measurements but with reduced spectral resolution (1/10)) and will take about 75 seconds. A typical elevation scan will start at about 50 km tangent height and descend in 3 km steps to 5 km. As the initial angles and the step sizes of the azimuth and elevation scan mirror are programmable any other elevation scan sequence can be realized.

In order to properly calibrate the radiometric output from the instrument, it is also necessary to acquire regularly, during the course of the mission, two additional types of measurements of well-defined targets. The first one is done with an internal high-precision calibration blackbody. For the second measurement, the instrument is simply looking at the deep space, that represents a source of low (negligible) radiance. Following the acquisition, the ground segment has to perform a Fourier Transform of the interferograms and a calculation of the instrument response, based on the calibration measurements, in order to recover the original spectrum in calibrated units. No special measurement is taken on board for precise spectral calibration because it is assumed that spectral calibration will be possible using known features in the measured spectra themselves. Finally, it is necessary to perform calibration measurements to assess line-of-sight pointing errors. For that purpose, the instrument is operated as a simple radiometer measuring the signal from stars crossing the instrument field of view.

2.2 Details about instrument detectors

The MIPAS interferometer has a dual port configuration, i.e. it has two input ports and two output ports. Only one input port is actually needed to acquire data from a given scene. Thus, the second input port is designed to look at a cold target in order to minimize its contribution to the signal. The signals detected at both output ports are, in principle, similar and can be combined in order to improve signal-to-noise ratio. This setup has also the advantage of providing a certain redundancy. If a detector fails on one output port, the corresponding detector of the other port still provides useful data.

The role of the Detector and Preamplifier Unit (DPU) is to convert the infrared radiation into electrical signal. The MIPAS detectors are designed to cover the spectral range from 685 cm^{-1} to 2410 cm^{-1}. Eight detectors are used and the spectral range is split into five bands, each band being covered by one(two) specific detector(s). The spectral ranges of the detectors are depicted in the following tables:

Single detector ranges:

Detector	Optical Range [cm^{-1}]
A1	685 – 995
A2	685 – 1193
B1	995 – 1540
B2	1193 – 1540
C1 & C2	1540 – 1780
D1 & D2	1780 – 2410

Spectral bands and contributing detectors in Nominal Operation:

Band	Detector	Decimation factor	Optical Range [cm^{-1}]
A	A1 & A2	21	685 – 980
AB	B1	38	1010 – 1180
B	B2	25	1205 – 1510
C	C1 & C2	31	1560 – 1760
D	D1 & D2	11	1810 – 2410

The requirements for the SPE are to provide backups should either channels B1 or B2 be lost. This is done by widening the filters bandwidth on another channel (A2 or B1 respectively) to effectively allow frequencies from two bands to pass through. Thus, one channel produces two bands. The bands A and AB can be extended to the following ranges:

Band	Detector	Optical Range [cm^{-1}]
A	A2	685 – 1180
AB	B1	1010 – 1510

2.3 Types of measurements

In this section, we want to separate the different measurements taken by the instrument according to the physical meaning of the measurement and therefore according to the content of the observational data acquired. In other words, we differentiate the measurements according to what the instrument is looking at.

MIPAS acquires data in two different operational modes. Default is the *measurement mode*. In this mode either IR-radiation from the atmosphere, from the deep space or sequentially from the deep space and from an internal blackbody source is entering the spectrometer. Nominal measurement means measurement of radiation originating from the atmosphere with high resolution. Looking at the deep space provides a negligible IR-input signal, i.e. the measured interferogram is related to self-emission of the instrument. This offset is subtracted from the scene measurement during on-ground data processing. Deep space measurements are performed frequently (once every *four* elevation scan) in order to account for changing self-emission of the instrument due to temperature variations in the orbit. Offset measurements are performed at reduced resolution (1/10). For radiometric (gain) calibration, the instrument is sequentially looking at the deep space and at an internal blackbody. In order to improve the signal to noise ratio and consequently the achievable gain calibration accuracy, many interferograms from the deep space and the internal blackbody reference source are recorded and co-added on the ground. Radiometric calibration measurements are performed at reduced resolution (1/10).

2.3.1 Description of the related measurement types

Of all the following listed measurement types, only the scene measurements contain the desired scientific information, i.e. spectra of the atmosphere. All other measurements are characterization measurements for calibration. Using the results from these characterization measurements, the calibration procedure is applied to the scene measurements.

The spectral calibration is a special case since no dedicated measurements are taken for that purpose. In fact, the characterization data for spectral calibration is derived from normal scene measurements.

Scene Measurements

MIPAS will take measurements of the atmosphere at different altitudes. The elevation range is scanned in discrete steps using the elevation mirror. A single scene measurement is taken at each elevation value.

Deep Space Measurements

The instrument itself is contributing to the observed spectrum. In order to remove this contribution, it is necessary to take a measurement of a “cold” scene, i.e. a scene with negligible radiance. Since the instrument contribution is varying, mainly because of temperature orbital variations, this offset measurement shall be repeated regularly. It is used for the radiometric calibration, with a subtraction of the instrument contribution (self-emission) from the scene measurements and blackbody measurements.

Reference Blackbody Measurements

Measurements of an internal calibration source, a well characterized blackbody source, are performed to characterize the instrument responsivity (or gain). These measurements are also repeated regularly because of the expected responsivity variations. A complete determination of the instrument gain is composed of several blackbody measurements combined with an equivalent number of deep space measurements. Used for the radiometric calibration.

3. GROUND PROCESSING PRINCIPLES

3.1 Objective of the Ground Processing

The functions described in this Section are assumed to be implemented in the Ground Segment necessary for processing of the MIPAS scene, deep space, and calibration measurements data.

The incoming data may be acquired during scene, deep space and blackbody. Incoming data therefore need to be processed differently and each will generate different type of output, namely calibrated spectra, calibration data, and data for interpretation of spectra (e.g. the expected instrument LOS pointing for each scene measurement).

An additional Ground Processing task is the generation of input data required for instrument operations.

The main objectives of the ground processing are:

- Pre-process and store all incoming data;
- Convert calibration measurements into calibration data to be used for calibration of scene measurements;
- Convert scene measurements into calibrated spectra;
- Processing of LOS tangent point geolocation data (taking into account pointing errors);
- Generate operations related input data.

In accordance with these main objectives, the overall ground processing can be separated into dedicated functions which are described in the next section. The following table summarizes the assumed products that are expected to result from ground processing.

Product	Remarks
Calibrated spectra	Radiometrically, spectrally, and geometrically corrected measurement data of the scene in physical units.
Calibration data	Gain and offset calibration data.

Table 3.1-1 List of Ground Segment products

3.2 Overview of Ground Processing needs

Generally speaking, the ground processing system has to mathematically retransform the scene interferograms from the MIPAS instrument into spectral information useful to scientists, considering all relevant data from calibration measurements, from characterization measurements for calibration and from characterization measurements for validation in order to yield fully calibrated spectra. All this information will enable to retrieve atmospheric key parameters. Ground processing shall include:

- Processing of calibration measurements including
  - Deep space measurements for offset subtraction from scene
  - Blackbody measurements
  - Deep space measurements for offset subtraction from blackbody
- Processing of scene measurements for spectral calibration
- Processing of scene measurements for generating fully calibrated spectra

The input data to the MIPAS ground processing will contain interferograms of the observed IR sources (atmosphere, blackbody, offset, deep space).

3.2.1 Instrument Operation vs. Data Acquisition / Downlink Scenario

The on-board recording of MIPAS data and the data downlink to different ground stations is performed independently of the actual measurements performed. The Level 1B ground processor has therefore to cope with raw data packages (Level 0 data) which do not start necessarily with an offset calibration or the first sweep in a limb sequence.

It is assumed that the Level 1B algorithm processes only complete elevation scans and that if Level 0 data do not start with an offset measurement, the first available valid offset data are used for radiometric calibration.

3.3 Basic radiometric relations

The basic mathematical relation between interferograms and spectra is the Fourier transform. The general relationship between an interferogram and its equivalent spectrum can be expressed as:

$$\bar{S}(\sigma) = F\{I(x)\} \tag{1}$$

where the left side of the equation (spectral domain) denotes the spectrum as a function of wavenumber (σ), and the right side (spatial domain) denotes the Fourier transform of the interferogram as a function of the optical path (x). As the measured interferogram is not symmetrical (because of dispersions effects in the beamsplitter and electronics), the resulting spectrum will be complex (represented here by the overbar notation).

The computer implementation of the discrete Fourier transform uses the standard Fast Fourier Transform (FFT) algorithms. We will denote the transformation as

$$\bar{S} = \mathrm{FFT}\{I\} \tag{2}$$

When using numerical Fourier transforms, special care must be taken about special particularities of the numerical implementation (see Section 4.10.1 for more details). Also, when dealing with decimated interferograms, *alias unfolding* (also called Spectrum Unscrambling or Spectrum Re-ordering) must be performed in order to remove the down conversion to a zero IF (intermediate Frequency) introduced at the satellite level (See Section 4.10.1 for more details).

3.3.1 General Calibration Equation

The basic approach for determining absolute radiance measured by a FTIR spectrometer is the same as that used for filter radiometers and has been used successfully for other interferometric applications [RD 21]. The detectors and electronics are designed to yield in principle an output which is linear in the incident radiance for all wavenumbers in the optical passband of the instrument, and two reference sources are viewed to determine the slope and offset which define the linear instrument response at each wavenumber.

The measurement obtained by the system is proportional to the spectral power distribution at the detector. The latter is composed of the emission coming from each input port, along with thermal emission of the spectrometer.

Using the following notation,

	Cold Blackbody	**Hot Blackbody**	**Scene Meas.**	**Units**
Theoretical spectrum radiance	L^C	L^H	L^M	W / (cm^2 sr cm^{-1})
Observed spectrum radiance	S^C	S^H	S^M	Arbitrary (digitalization units)

the measurement can be expressed as:

$$\bar{S}^M = \bar{G}(L^M + \bar{O}) \tag{3}$$

where $\bar{S}^M(\sigma)$ is the calculated complex spectrum from the measurement (arbitrary units, commonly referred to as digitalization units [d.u.]).

$L^M(\sigma)$ is the true incident spectral radiance from the *scene* (in [r.u.]).

$\bar{G}(\sigma)$ is the overall spectral responsivity of the instrument, referred to as *gain*. it is a complex function to include interferogram phase delays,

$\bar{O}(\sigma)$ is the instrument emission, referred to as *offset*, it is the stray radiance, including all modulated radiance that does not come from the scene (in [r.u.]).

Overbars refer here to complex quantities, comprising a real and an imaginary part.

To be more precise we should state that the instrument line shape (ILS) is implicitly included in these terms, as

$$L^M(\sigma) = L^M_{\text{TRUE}}(\sigma) * ILS(\sigma, \sigma_0)$$

Moreover, zero-mean noise is also present in this equation and its standard deviation is present to the NESR of the instrument.

Equation (3) expresses the linear relationship between the true spectral radiance L^M and the measured, uncalibrated spectrum $\overline{S}^M$. Two non-equivalent calibration observations made at a cold and hot temperatures are required in order to determine the two unknowns, that are the gain $\overline{G}$ and the offset radiance $\overline{O}$ as defined in Equation (3). The offset is the radiance which, if introduced at the input of the instrument, would give the same contribution as the actual emission from various parts of the optical train.

Equation (3) written for both the hot and cold blackbody can be solved to yield:

$$\overline{G} = \frac{\overline{S}^H - \overline{S}^C}{L^H - L^C} \qquad \text{[d.u./r.u.]} \tag{4}$$

$$\overline{O} = \frac{\overline{S}^C L^H - \overline{S}^H L^C}{\overline{S}^H - \overline{S}^C} \qquad \text{[r.u.]} \tag{5}$$

where L^C and L^H are the cold and hot calculated blackbody radiances, modeled by the theoretical spectral radiances of the observed blackbodies.

By inverting Equation (3), one can derive the calibration equation used to convert a spectrum from an unknown scene into calibrated data:

$$L^M = \frac{\overline{S}^M}{\overline{G}} - \overline{O} \tag{6}$$

If no error distorts the measurement, this expression for the calibrated radiance given in Equation (6) leads to a radiance L^M with no imaginary part. When non-linearity is present, a special correction must be applied on different interferograms coming from affected detectors.

3.3.2 MIPAS Specific Calibration Equation

For the MIPAS instrument, as the cold reference measurement obtained by looking at the deep space corresponds to an emission at a very low temperature ($T^C \approx 4$ K << T^M), one can safely make the approximation that the cold term has a negligible spectral radiance ($L^C \approx 0$). The calibration equation can now be expressed in the simplified form:

$$L^M = \left(\frac{\overline{S}^M - \overline{S}^C}{\overline{S}^H - \overline{S}^C} \right) L^H \tag{7}$$

With the purpose of simplifying the writing and to ease the numerical computation, we inverse the definition of the gain (given in the previous section), as a complex multiplication is easier to perform than a complex division. Using the calibration blackbody as the hot source, the deep space as the cold source and defining the radiometric gain as:

$$\overline{G}'(\sigma) = \frac{L^{bb}(\sigma)}{\overline{S}^{bb}(\sigma) - \overline{S}^{ds}(\sigma)} \tag{8}$$

The expression for radiometric calibration becomes

$$L^{M} = \overline{G}'(\sigma) \cdot \left(\overline{S}^{M}(\sigma) - \overline{S}^{ds}(\sigma)\right) \tag{9}$$

Section 3.4.2, Chapter 4, and Section 4.9.4 explain the non-linearity correction applied on the measured interferograms.

3.4 Special considerations

In this section, we will consider special aspects of the ground processing. The present topics are considered because of their inherent complexity or criticality.

3.4.1 Fringe count errors detection and correction

The basic ground processing for MIPAS contains no explicit phase correction or compensation. For a given interferometer sweep direction, it is assumed that the gain and offset calibrations and also the scene measurements have the same phase relationship, i.e. they are sampled at precisely the same intervals. This sampling is determined by a fringe counting system using a reference laser source within the interferometer subsystem, with the fringe counts forming a "clock" signal to the ADC in the on-board SPE. The fringes trigger the sampling of the IR interferogram. If, for any reason, a fringe is lost, then the phase of subsequent measurements will be affected and, if these are calibrated using a gain or offset measurement taken before the occurrence of the fringe loss, then errors will be introduced into the final spectrum. The ground processing scheme includes a method for detecting and correcting fringe losses by analyzing the residual phase of an interferogram following calibration. Hence there is no specific measurement required as part of calibration for this aspect.

In the following, we summarize the philosophy adopted for fringe count errors (FCE) detection and correction. The proposed approach assumes that fringe count errors occur at turn-around, i.e. between two measurements. Under this assumption, the effect of a fringe count error is to shift all measurements following the error by N points. The problem manifests itself at calibration because all the measurements involved do not have the same sampling positions, i.e. they do not have the same phase relationship.

An alternative method based on the APS position included in the ICU-provided auxiliary data is not accurate enough. The current accuracy only ties down the ZPD position to within the order of a hundred samples or so.

Fringe count errors occurrence within a measurement is believed much less probable. The effect of "in-sweep" fringe errors is twofold:

1– It shifts the last part of the interferogram in which the error occurs with respect to the first part of that interferogram.

2– It shifts all subsequent interferograms with respect to any previous (calibration) measurements.

The latter effect is the same as if the error would have been at the turn-around. Thus it will be covered by the above assumption. The first effect results in a distortion of the current measurement that is very difficult to recover, in particular for scene measurements). *At present, no correction is foreseen for that type of error*. They could possibly be detected as part of an observational validation process.

Fringe count errors can occur in all types of measurements done by the MIPAS instrument, except of course the LOS calibration measurements during which the sweeping mechanism is stopped. Depending on the type of measurement, the effect is not the same and therefore, the detection and correction approach will be different. Because the phase is not strictly the same for forward and reverse sweeps, the fringe count error detection and correction will be done independently for the two sweep directions. For all interferometric measurements, the fringe count reference interferogram of a given sweep direction will be the last gain interferogram of that sweep direction. The last gain interferogram can be either a deep space interferogram or a blackbody interferogram depending on the acquisition scenario requested.

With an un-filtered and un-decimated interferogram, the fringe count error detection could be done directly on the interferogram by looking at the position of the observed ZPD, i.e. the point of maximum amplitude. Since the detected signals are optically band limited, with bandwidth of 300 to 600 cm^{-1}, and since most observed targets will contain some sort of continuous background, we can expect the ZPD region of an un-filtered and un-decimated interferogram to contain a few tens of points. In that case, the maximum position could be easily determined and a shift of 1 to N points could be detected. When the interferogram is filtered and optimally decimated, the ZPD region is reduced to about one point. In addition, a shift by a number of points smaller than the decimation factor will produce only a small shift of the decimated interferogram. For example, the shift of a 20 times decimated interferogram will be 1/20 the effective sampling interval if the fringe error is one point. Therefore, the monitoring of the ZPD position of the decimated interferograms is not a sensitive approach to detect fringe count errors.

The approach selected for fringe count error detection consists in a coarse radiometric calibration of the actual measurement at very low resolution, followed by an analysis of the residual phase (consult [RD 16]). The radiometric calibration is done using the last available gain measurement. When the OPD axis definition of the actual measurement is the same as the gain used for radiometric calibration, then the residual phase should be zero. A shift will produce a phase error increasing linearly with wavenumber. This can be seen using the “shift theorem”.

Starting from Equation (1) relating the observed interferogram to the corresponding complex spectrum, we can re-write it for shifted signals in the following way using the shift theorem:

$$\bar{S}(\sigma)e^{-2\pi i\sigma a} = F\{I(x-a)\} \tag{10}$$

It can be demonstrated that if a radiometric calibration, consisting of a simple multiplication by a gain spectral vector, is applied on the Fourier transform of a shifted interferogram, then the residual phase of the calibrated spectrum will be the phase corresponding to the initial shift of the interferogram. Therefore, a linear regression on the residual phase of the calibrated spectrum will reveal the shift due to a fringe count error on the observed interferogram.

In summary, the approach for **fringe count error detection** will include the following steps

- Perform the Fourier transform of the ZPD region (very low resolution like e.g. 128 points) of the observed interferogram.
- Perform a spectral interpolation of the latest available gain (taken at the same low resolution) at the wavenumber values corresponding to the actual measurement.

- Multiply the observed spectrum by the interpolated gain
- Calculate the spectral phase of the calibrated spectrum
- Perform a linear regression of the phase versus wavenumber
- Calculate the OPD shift, averaged over the different channels.

Once the OPD shift is known, the correction of a shifted *un-decimated* interferogram is straightforward: you simply rotate on itself the interferogram back to its correct position. In order to do that, you simply remove a number of points equal to the shift on one end of the IGM and transfer these points to the other end of the interferogram. This ensues from the implicit periodicity in the Fourier domain. To do the phase correction, the cyclic rotation must done in the opposite side of the computed shift.

The correction of a shifted and *decimated* interferogram is more difficult. This is because the shift will not be normally an integer multiple of the decimation factor. Therefore, the decimated IGM would have to be shifted by a fractional number of points. This requires some sort of interpolation. The proposed approach is to perform a multiplication of the Fourier transformed of the shifted IGM by the phase function obtained in the detection procedure.

The method for **fringe count error correction** would proceed as follows:

- Perform the Fourier transform of the shifted IGM.
- Calculate the phase function necessary to correct the calculated shift, i.e. the phase function with the reverse shift, at the same wavenumbers as the observed spectrum.
- Perform the multiplication of the observed spectrum with the calculated phase function.
- Perform the inverse Fourier transform of the result.

$$I(x) = F^{-1}\left\{F\left\{I(x-a)\right\}e^{+2\pi i\sigma a}\right\} \tag{11}$$

With this method, no manipulation is done on the OPD axis of the interferogram but each data point is corrected to represent the value of its desired OPD position.

It should be mentioned that fringe count errors will affect interferograms of all bands. This characteristic will be used to improve accuracy of the detection and to, eventually, distinguish the fringe count errors from other types of errors. As a comparison, an error during data transmission to ground segment (a “bit error”) will affect only one band. Similarly, the spike that may be caused by a cosmic radiation will also be seen only in one detector or band.

The approach for fringe count error detection and correction will be the same for all types of measurements. However, the implementation will be somewhat different for the different types. This is discussed below. The fringe count error detection will be performed systematically on all incoming interferograms. However, the correction procedure will be applied only if a non-zero shift is detected.

3.4.1.1 FCE handling in offset measurements

Detection and correction are done with respect to the last available gain calibration. All the offsets corresponding to one orbit are aligned to the fringe count phase of this last gain. If one or more fringe count errors occur during the computation of one orbit, the ground processing will detect the same shift for all subsequent offset interferograms and will apply the same (always recalculated) correction on these offsets until the end of the processing of the orbit.

3.4.1.2 FCE handling in gain measurements

At the beginning of a gain measurement sequence, there is no reference against which we can check for fringe count errors. Since the last gain measurement, the interferometer has normally been stopped for LOS calibration, in principle just before the actual gain measurement. Thus, there is no relation between the actual measurement and the previous fringe counting reference. This is the main reason why we start with a new gain measurement.

Fringe count errors during gain calibration are checked by comparison with the first measurement of the sequence. As it was done for the offset measurements, it is again necessary to perform a standard radiometric calibration on the Fourier transformed ZPD region, because this calibration also performs the normal phase correction of the measurements.

Starting with the first measurement of the gain calibration sequence, typically a blackbody measurement (either forward or reverse), the first step will be to determine the OPD shift between that measurement and the *previous* gain. The same procedure as for normal error detection is followed

- Perform the Fourier transform of the ZPD region of the observed interferogram.
- If necessary, perform a spectral interpolation of the previous gain at the wavenumber values corresponding to the actual measurement
- Multiply the observed spectrum by the interpolated gain
- Calculate the spectral phase of the calibrated spectrum
- Perform a linear regression of the phase versus wavenumber
- Calculate the OPD shift

The second step is to correct the *previous* gain with respect to the actual measurement. The correction would proceed as follows.

- Calculate the phase function necessary to correct the calculated shift, i.e. the phase function with the reverse shift, at the same wavenumbers as the observed spectrum and at the very low resolution used to cover only the ZPD region.
- Multiply the previous gain the calculated phase function

This corrected gain will then be used for detection of fringe count errors on all subsequent interferograms. In principle, the calibrated spectra obtained with this corrected gain should show no additional phase until a fringe count error occurs. Then, all error-free measurements will be

coadded normally. Each time a fringe count error will be detected, a new coaddition group will be formed. When the complete calibration sequence is over, then all the coadded measurements are corrected with respect to the *last* measurement and the remaining processing of the radiometric calibration is performed normally. Correcting the gain with respect to the last measurement presents the advantage that all subsequent error-free measurements need no correction.

After processing the data corresponding to one orbit, if one or more FCE are detected, the current gain is shifted according to the last fringe count error measured. This is done in order to avoid correcting all the offsets and scenes in subsequent orbits.

3.4.1.3 FCE handling in scene measurements

When a scene is measured, its fringe count is checked against the last available gain calibration. All the scenes corresponding to one orbit are aligned to the fringe count phase of this last gain. If one or more fringe count errors occur during the computation of one orbit, the ground processing will detect the same shift for all subsequent scene interferograms and will apply the same (always recalculated) correction on these scenes until the end of the processing of the orbit.

More details on the implementation of the algorithm can be found in Section 4.9.3.

3.4.2 Non-linearity correction

The detectors from channels A1, A2, B1, and B2 corresponding to bands A, AB, and B are photoconductive (PC) detectors, subject to non-linearity depending on the total photon flux falling on them. Here, the non-linearity means that the response of the detector differs from a linear behavior as a function of the incoming flux. This phenomenon occurs at high fluxes and usually appears as a decrease of the responsivity. With the MIPAS detectors, the non-linearity can be a source of significant radiometric errors if it is not properly handled. As explained in [RD 2], the non-linearity produces a change in the effective responsivity as well as spectral artifacts, which will both be corrected for within the required radiometric accuracy.

The change of effective responsivity with DC photon flux will be taken into account in the radiometric calibration. The approach is the following:

A characterization will be performed first on ground, and then in space at specific intervals (TBD), at instrument level, of the total height of the unfiltered and undecimated interferogram (ADC_j^{Max} and ADC_j^{Min} values) with the on-board calibration blackbody at different pre-selected temperatures. These values will be used during the characterization phase for a computation of the non-linear responsivity coefficients. These values will be used to correct for the non-linearity of the detectors by means of a specific algorithm called the ASCM method

Although they are intended to be combined in a single band, the optical ranges of the detectors A1 and A2 are not the same. They will then exhibit a different behavior with respect to photon flux. As a result, they will require different non-linearity corrections. Because of this, the signals from these detectors are not equalized and combined on board the instrument in the SPE. This operation is instead performed by the ground processor following non-linearity correction. The

other two PC detectors, B1 and B2, are not combined in any case as they produce the bands AB and B. Other than the need to keep A1 and A2 separate in the baseline output set up at the SPE, the non-linearity measurements and correction has no impact upon the calibration scenario.

The effects of detector non-linearity have been analyzed and a corrective approach has been presented in [RD 2]. The results are summarized here.

The important effect of detector non-linearity is on the radiometric accuracy performance. The present radiometric error budget allocated to the non-linearity in the 685–1500 cm^{-1} (where the detectors are the most non-linear) shall be better than the sum of 2 $NESR_T$ and 5% of the source spectral radiance, using a blackbody with a maximum temperature of 230°K as source [RD 3].

Radiometric errors caused by non-linearity can be separated into:

- an error due to the change in effective responsivity with actual photon flux
- additional errors from spectral artifacts

A correction will be applied on the incoming interferograms at the appropriate step in the processing chain with the purpose of compensating for the global effects of responsivity. The non-linear responsivity of the detectors will be characterized on ground and calibration curves will be acquired during in-flight operation. For expected responsivity curves, it is anticipated that the correction of the non-linearity error due to the change of effective responsivity and from the cubic artifacts should lead to an accuracy within the allocated budget.

The non-linearity correction algorithm included in the ground processing described in this document is the “Adaptive Scaling Correction Method” (ASCM), as described in [RD 2]. More details on the implementation of the algorithm can be found in Section 4.9.4.

3.4.3 Spectral calibration

A study on spectral calibration was done in the frame of the MIPAS ground segment work [RD 4]. This study permits the definition of suitable algorithms for spectral calibration. Spectral calibration is performed using known features of standard scene measurements. It is necessary to choose appropriate scene measurements in order to obtain sufficiently accurate results.

In the definition and qualification of the approach for spectral calibration, the following issues need to be addressed.

- Number of scene measurements required for a calibration
- Equivalence of the different scene (e.g. different elevation) for the purpose of spectral calibration
- Necessity for calibration in the different bands

The following scenario is based on Section 5.3 of [RD 5]. Spectral calibration will be performed using standard measurements from the atmosphere. Particular spectral lines will be

retrieved in the observed spectrum and the known values of their wavenumbers will be used to establish the assignment of the wavenumber to the index of spectral data points. A spectral calibration will be used for the wavenumber assignment of all subsequent scene and gain measurements until a new spectral calibration is performed.

Because it is related to the same parameters, the spectral shift can be considered as a part of the instrument line shape. The disadvantage is that it is then necessary to perform a deconvolution of the ILS from an observed spectrum to get the proper wavenumber assignment. Here we will assume that the spectral shift is included in the spectral calibration, i.e. it is calibrated out by the spectral calibration procedure.

In summary, the spectral calibration is based on the following assumptions:

- The spectral calibration includes the spectral shift and is performed without any ILS deconvolution.
- A minimal number of scene measurement will be sufficient for a proper spectral calibration (TBD)
- All scene measurements will be equivalent with respect to spectral calibration, i.e. it will be possible to perform a spectral calibration using any scene measurement.
- The spectral calibration will be the same throughout the spectral range. It is assumed that the definition of the optical axis is common to all 4 detectors on the output ports, for both output ports. It is also assumed that the residual misalignment between the two output ports is low enough so that the difference in wavenumber is negligible.
- Appropriate spectral lines will be identified and the value of their wavenumber will be available for ground processing.

A spectral calibration will require specific data that is described in Section 5.3.3 of [RD 6] and in more details in Section 3 of [RD 4].

During ground processing of a spectrally calibrated spectrum, the wavenumber assignment of the spectral scale will be done using a derived calibration table. This is done via a spectral interpolation on a predefined spectral axis.

The processing for the generation of the spectral calibration table requires the following functional steps:

- Define the spectral window containing the reference spectral line. This is done using the current spectral calibration.
- Find the peak corresponding to the reference spectral line within the spectral window of the appropriate band.
- Define the new spectral axis (assignment of wavenumbers throughput a spectral band) for each band and each possible setting of resolution and decimation.

3.4.4 Complex numerical filtering

According to the present instrument (and particularly SPE) design, complex numerical filtering will be applied to the measurement data. The purpose of this Section is to provide some theoretical background on this topic.

Neglecting the dispersion phenomenon inducing a non-null phase, an observed interferogram is basically a real and symmetrical function. The symmetry is about ZPD and, by extension about every multiple of MPD. The Fourier transform of such an interferogram is a real and symmetrical spectrum with symmetry about every multiple of the sampling frequency[1] . In other words, the full spectrum will show on one half the true physical spectrum and on the other half the image of this spectrum. Depending on the convention, this second half may be displayed as negative frequencies or as frequencies above the sampling frequency divide by 2.

A numerical filter with *real coefficients* shows the same symmetry as described above. The passband defined by such a filter transmits both the desired physical band and its image. Undersampling this filtered spectrum is possible provided the following two conditions are met:

1– The decimation factor is not larger than $\sigma_s/2(\sigma_1-\sigma_0)$, where σ_s is the sampling frequency (or Nyquist frequency) and σ_0, σ_1 are the band limits.

2– There is no folding frequency within the passband.

A *complex numerical filter* can be defined such that it has no image passband, by defining its imaginary part antisymmetrical such that it produces a compensating negative image. After such a filtering, the only undersampling condition is:

1– The decimation factor is not larger than $\sigma_s/(\sigma_1-\sigma_0)$, where σ_s is the sampling frequency.

Thus, the decimation factor can be two times larger after complex filtering. On the other hand, two spectra are produced by the numerical filtering, one real and one imaginary.

Since the folding frequencies are not restricted to be out of the band of interest, there is not additional restriction on the decimation factor. It is then possible to better optimize the decimation factor. This is where a gain can be made with respect to data reduction.

Figure 3.4.4–1 summarizes the interferogram numerical acquisition process and Figure 3.4.4–2 summarizes the decimation and alias unfolding process. Another example of the effect aliasing of decimation after complex numerical filtering is provided in Figure 4.10.2-1. Further description of the unfolding method is given at Section 4.10. The processing needed for the proper recovery of the wavenumber axis for each spectrum is described in the ground segment document [RD 4]. This operation must be executed after each Fourier transform on decimated signals.

[1] We assume that the sampling frequency is chosen in order to meet the Nyquist criterion, i.e. there is no natural frequencies above the sampling frequency divided by 2.

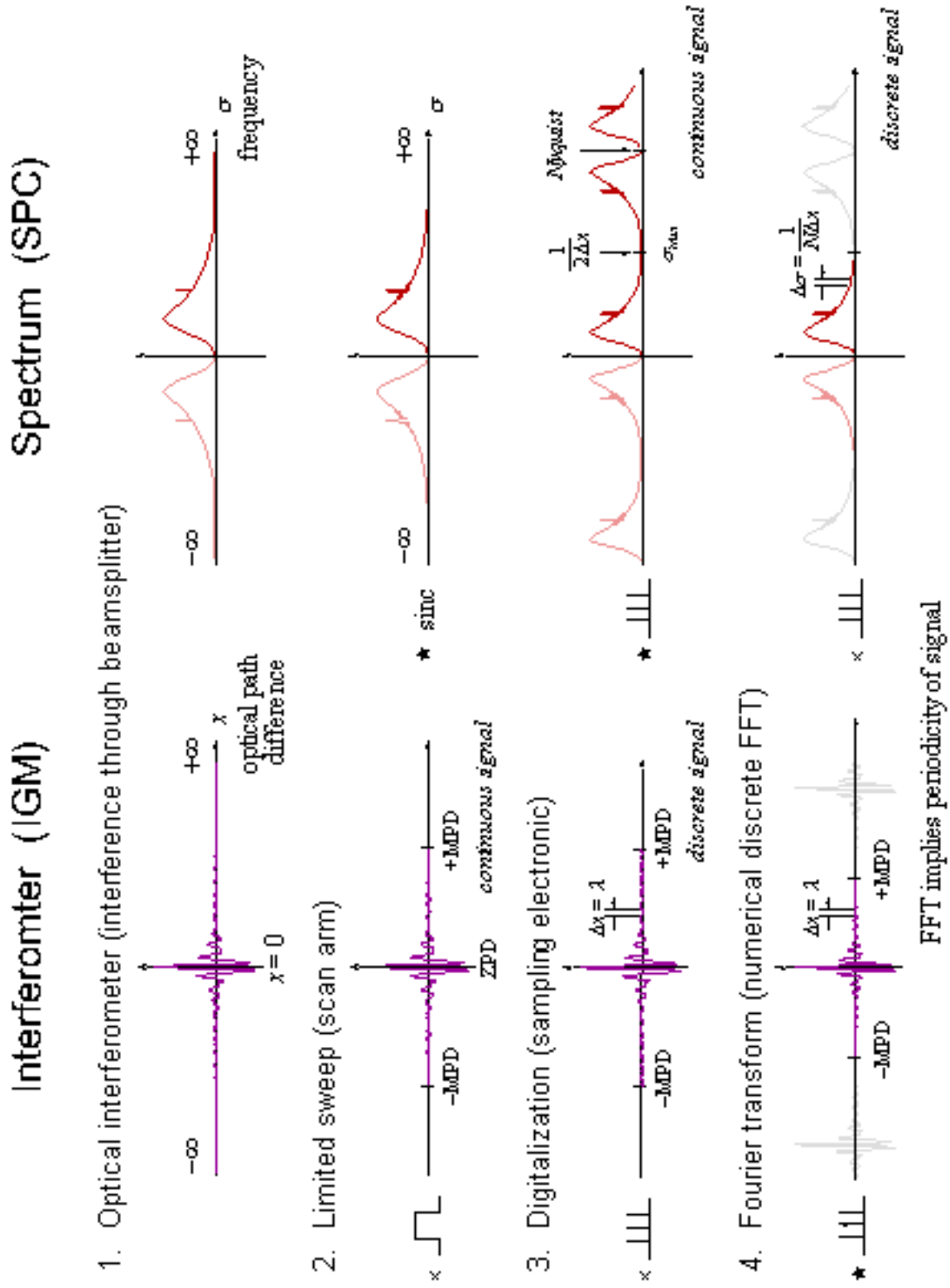

Figure 3.4.4 –1: Interferogram acquisition numerical process

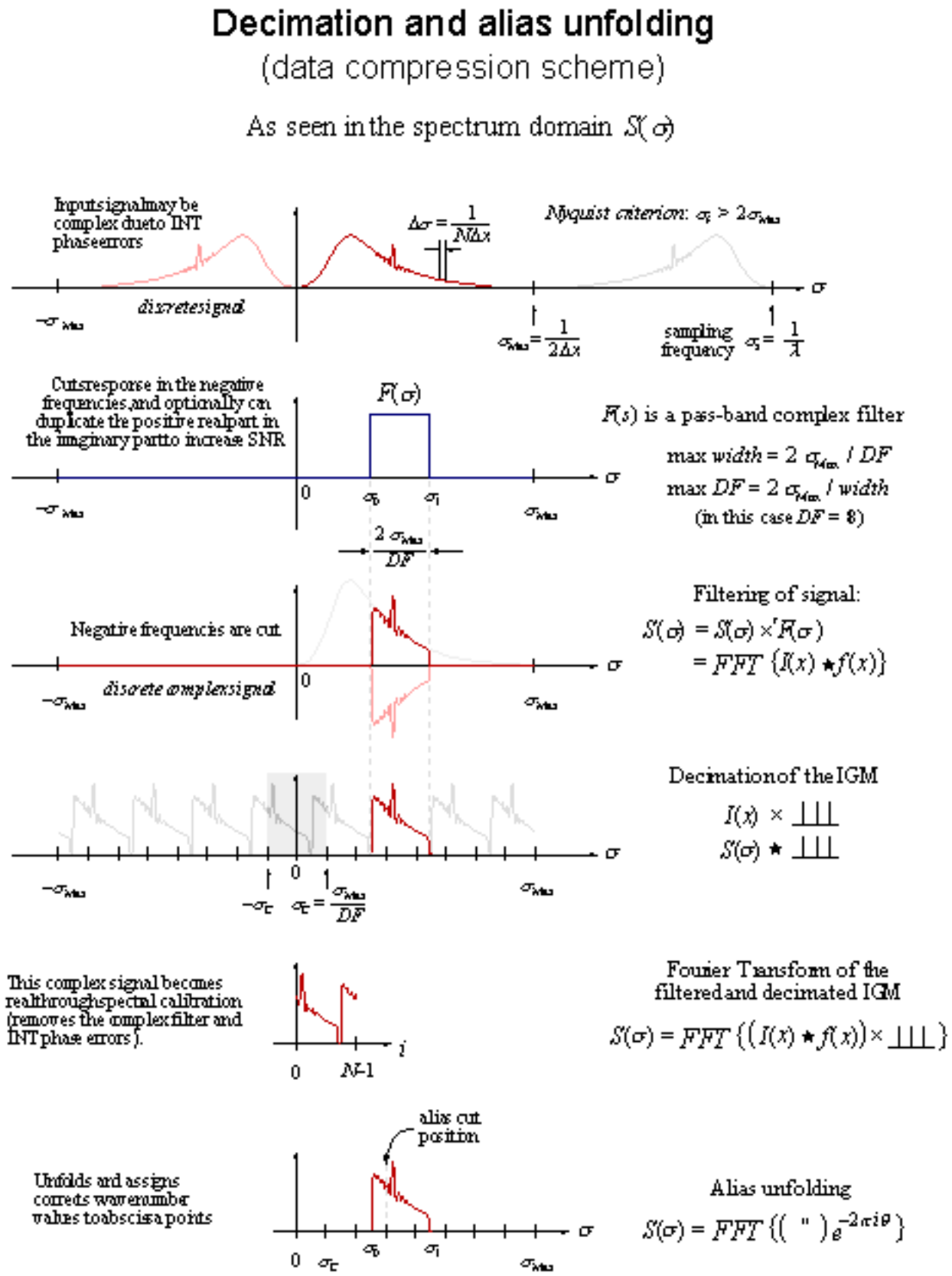

Figure 3.4.4 –2: Interferogram decimation and alias unfolding

3.4.5 SPE and PAW responsivity scaling

In practice, the three following scaling items need to be considered:

1) A scaling to account for a commanded gain change at the PAW.

The gains are predefined and are commanded by an 8-bit word sent via the ICU. Since different gains may be commanded, a data scaling in the ground segment to equalize performance must be foreseen. The commanded gain is available in the auxiliary data stream and so this is a simple scaling effect based on the extracted word. The PAW is the last amplifier stage of the overall Detector and Preamplifier Unit (DPU). This is the $k_{G,j}$ factor used in Chapter 4.

2) A temperature dependent scaling to account for changes in responsivity of the detectors (DTU) within the DPU.

The DTUs are specified to provide a stable response based upon assumed knowledge of their temperature (i.e. the responsivity may vary but it must be well characterized). For this reason, a correction of performance with time/temperature must be foreseen. This is made based on the measured temperature at the DTUs (available via thermistor values in the auxiliary data) and using characterization curves generated during DPU/DTU tests on ground. This is the k_R factor used in Chapter 4.

3) A temperature dependent scaling (gain & possibly phase) to account for the variations in the performance of the electronics of the PAW and the SPE round the orbit.

At present, it is not thought necessary to correct for these effects around the orbit as predictions show the variations will not cause the units to drift out of specification. The In-Flight Calibration Plan foresees to make around orbit measurements during Commissioning Phase to check whether there are any such variations. A particular manifestation of this item is the variation in the SPE performance during mode switching.

The baseline thus foresees scaling factors to cover points 1) and 2). Point 3) will be covered (if necessary) based on results from the Commissioning Phase. This means that the scaling factor k_R may be replaced by a vector which includes the DTU variations and the SPE/PAW variations. This is what is yet to be described in the updated In-Flight Calibration Plan.

Only two gain scalings are included in the baseline, although these can be modified to vector multiplications should this prove necessary.

3.5 Identification of the Ground Processing functions

The overall processing chain, divided into its high-level functions, will be processed in the following order:

1– *Load Data*
2– *Calculate Offset Calibration*
3– *Calculate Gain Calibration*
4– *Calculate Spectral Calibration*
5– *Calculate Radiance*
6– *Calculate ILS Retrieval*
7– *Calculate Pointing*
8– *Calculate Geolocation*
9– *Format Product*

Table 3.5-1 List of Ground Segment functions

The "*Load Data*" function extracts packets sequentially from on-board instrument data packages and constructs complete interferograms. These are then validated using auxiliary checking data before being sent to the proper function depending on the type of data. In addition, the Load Data function produces the pre-processed data output.

The "*Calculate Offset Calibration*" function generates the offset calibration data. Offset data is separated according to forward and reverse sweep. Then the data is validated and made available for the Radiance Calculation function.

The "*Calculate Gain Calibration*" function generates the gain calibration data. It performs the processing of all gain calibration measurements including every deep space and blackbody measurement of the gain calibration sequence.

The "*Calculate Spectral Calibration*" function performs the processing of some selected (radiometrically) calibrated scene measurements and generates the spectral calibration data.

The "*Calculate Radiance*" function performs the processing of the scene measurements and generates a radiometrically calibrated spectrum. It uses the currently available, i.e. the last measured, offset, gain and spectral calibration data.

The "*Calculate ILS Retrieval*" function performs the ILS retrieval from radiometrically and spectrally calibrated spectra. The result of this operation is made available to the output data products.

The "*Calculate Pointing*" function performs the LOS pointing calibration of the radiometrically and spectrally calibrated spectrum. The output is corrected LOS pointing angles.

The "*Calculate Geolocation*" function calculates the tangent point geolocation and related information.

The "*Format Product*" function performs the packaging of all the processed spectra, computed calibrations and diverse processings performed on the raw incoming data into the Level 1B product, as defined in document [RD 7].

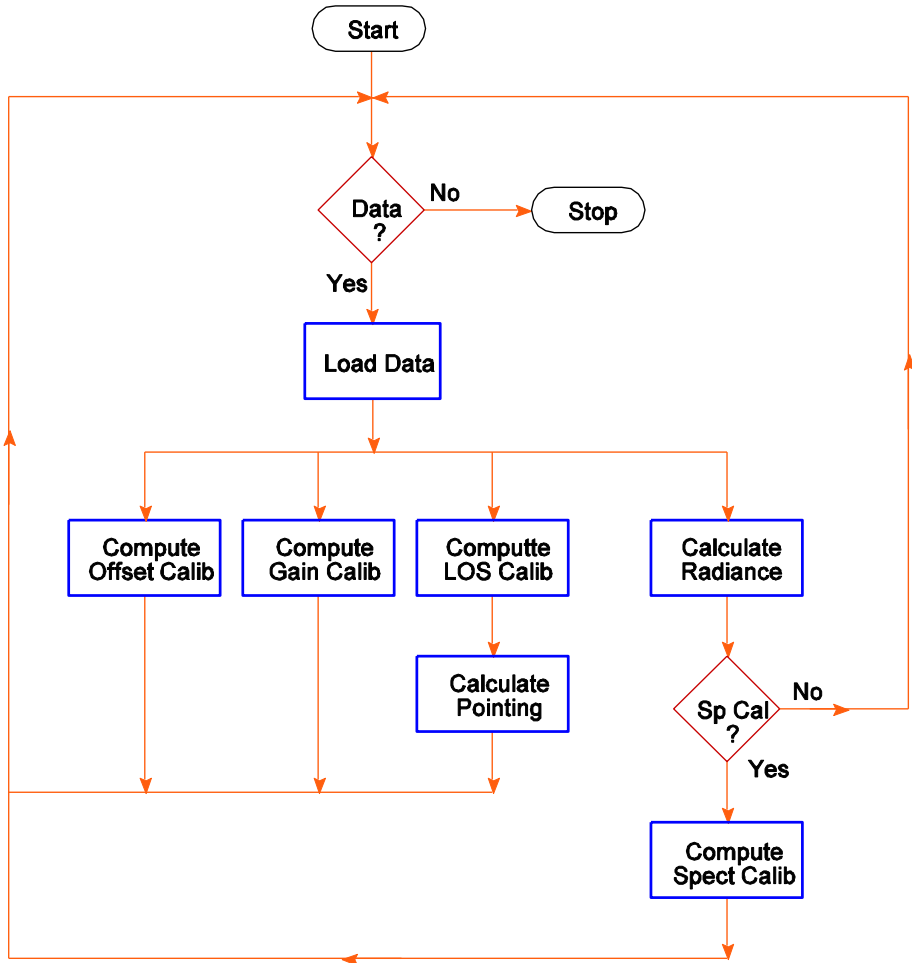

Figure 3.5-1: Ground Processing Control Flowchart

The conventions used in the following flowchart and all the ones in section 4 are described below.

Level 0 — Input/Output Products

Compute Offset Calib — Processing on Data

Scene Data — Auxiliary, Calibration or Intermediate Data

TEP → — Test Entry Point

Data flow (Different styles of lines are to distinguish between different paths)

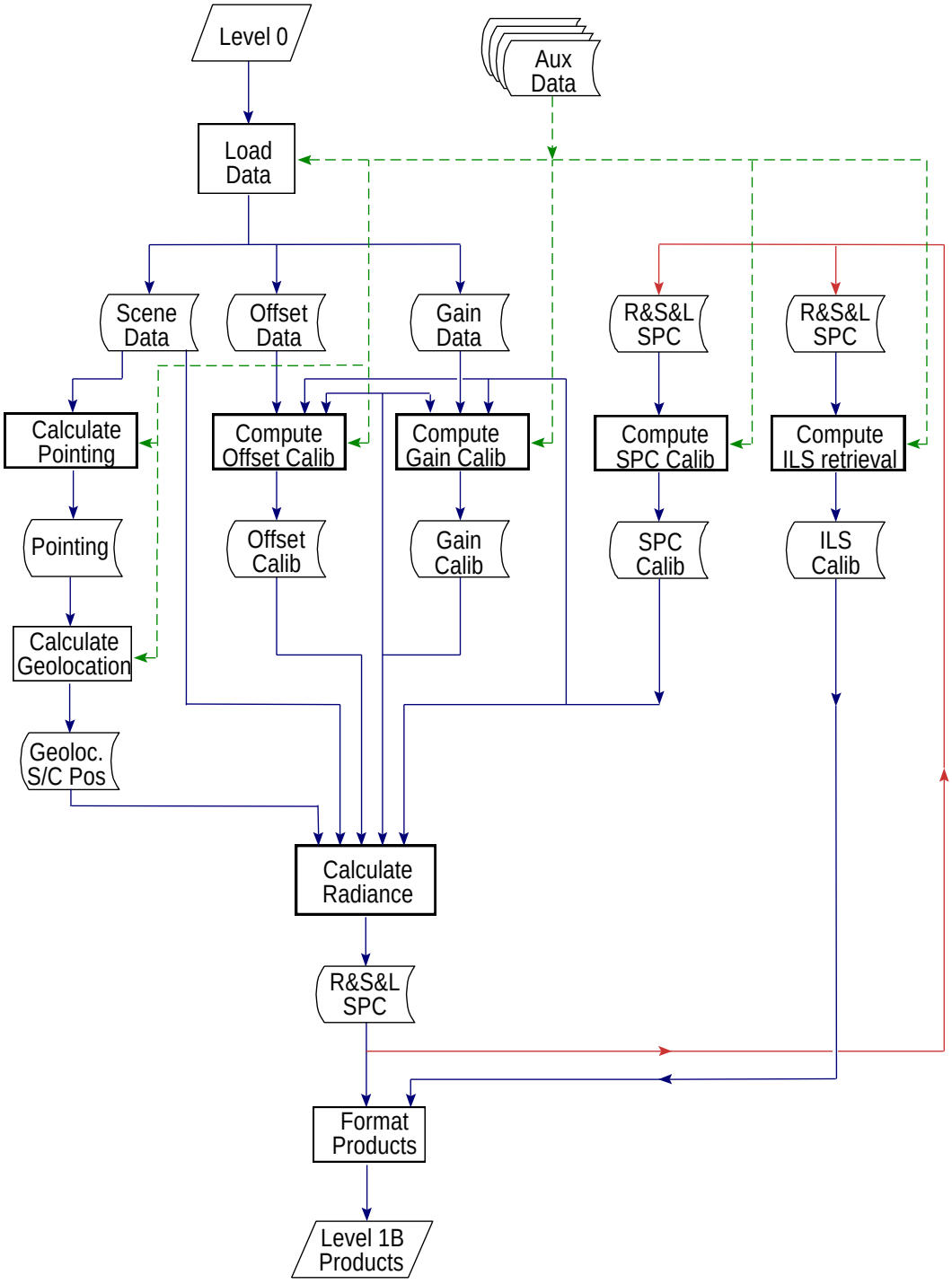

Figure 3.5-2 Ground Processing Data Flowchart

4. GROUND PROCESSING FUNCTIONS AND DESCRIPTION

In the following sections, each function defined in the overall structure (see Table 3.5-1) will be described in details. For each function, the description will cover the following aspects

- Objective
- Definition of variables
- Detailed structure and formulas
- Computational Sequence

In the tables for the definition of variables, the "**I/O**" (Input/Output) indication will follow the notation described below:

Notation	Description
I	Input to ground processing
i	Input to ground processing function (calculated by another function)
a	Specified in the auxiliary data
t	Temporary or intermediate variable
l	Loop or index variable
o	Output from ground processing (calculated by the actual function and made available for further processing)
O	Output from ground processing

Table 4-1 Notation used for the input/output indicators

Also in these tables, the "**Type**" indication will refer to the following notation:

Notation	Description
r	Real numbers
c	Complex numbers
i	Integer numbers
b	Binary numbers
t	Text or character data
m	Mixed, two or more of the above types

Table 4-2 Notation used for the type indications

Note: The type is not the data format used on the computer (long integer, double precision…). It gives the nature of the data. See section 5 for accuracy aspect on a computer.

Variable	Descriptive Name	I/O	Type
	Identifier indices		
j	Channel/band index number	l	i
d	Index for sweep direction	l	i
i	Index of group number in the gain calibration sequence	l	i
k	Index of IGM in a group of calibration IGMs	l	i
	Element indices		
n	Index of data point in a IGM	l	i
m	Index of data point in a SPC	l	i

Table 4-3 Description of various global identifiers

Note: on all equations, the *prime* identification (e.g. $I'^{ds}_{j,d}$) refers to a temporary corrected signal.

4.1 LOAD DATA

The present Section describes the *Load Data* function that performs the initial processing of all incoming instrument data. The data flowchart of this function is provided in Figure 4.1.4-1.

It is assumed that incoming data have been demultiplexed and time ordered. These operations are normally common to all instruments of the platform and they will not be covered in the present document.

4.1.1 Objective

The main objectives of the *Load Data* function is to convert data packets into single measurements properly identified and grouped.

Specific objectives of the function are

- Receive MIPAS data source packets from the on-board instrument
- Extract data packets and form single measurements
- Extract relevant auxiliary data
- Sort measurement data according to the type of measurement (i.e. scene, blackbody, or deep space)
- Stack the calibration measurements into the relevant groups
- Generate and deliver preprocessed data

The *Load Data* function is also important for the transfer of control because the processing following the *Load Data* function depends on the type of data received.

The actual MIPAS specification includes a constraint (Mission and System assumption) on the data transmission link quality. It is stated that the bit error rate of the data transmission link between platform and ground will be better than 10^{-8} [RD 3], which is low enough so that no error encoding method is required.

The detection of corrupted/missing ISP shall be done as follow:

- detection of missing ISP by checking continuity of block sequence number,
- detection of corrupted ISP by checking error counter different than 0 in FEP header.

In case of corrupted/missing ISPs for scene data only, if band B or C is not affected, all bands not affected shall be processed. Affected bands shall be filled with zeros and not used in further processing. Otherwise, if band B and C are affected all bands shall be filled with zeros. Band B and C are needed for FCE detection. In all cases for scene, if valid auxiliary data is present, time and geolocation information shall be reported in the Level 1B product. If the auxiliary data is missing for the last sweep, the scene data corresponding to this sweep is rejected because the scene data number of points cannot be determined and the end of scan is unknown.

In case of corrupted/missing ISPs for gain and offset data, the entire sweep shall not be used in further processing.

In addition, the number of raw data points in the auxiliary data packet should be verified. If the value is smaller than the number of taps M of the numerical filter, all channels should be marked as corrupted.

4.1.2 Definition of variables

Load Data

Variable	Descriptive Name	I/O	Type	Ranges / References / Remarks
$MIPAS^{in}$	Input MIPAS file	I	m	MIP_NL__0P
a_i	Resistance to temperature FEO coefficients	a	r	MIP_CA1_AX(4)
$b^{(j')}$	Resistance to temperature PRT(j') coefficients	a	r	MIP_CA1_AX(33)
$c^{(j')}$	Digital to resistance PRT(j') coefficients	a	r	MIP_CA1_AX(32)
σ_L	Nominal laser wavenumber	a	r	For the MIPAS instrument = 7606 cm^{-1} MIP_PS1_AX(4)
N^{ADC}	Number of sample data points in IGM before decimation	o	i	Extracted from MIPAS source packet
v^{nom}	Nominal optical speed	a	i	MIP_PS1_AX(65)
M	Number of points in complex filter	a	i	M = 256
to 4.2	*Calculate Offset Calibration*			
D_j	Decimation factor of band j	o	i	Extracted from auxiliary data of MIPAS source packet
N_j^{ds}	Number of data points in DS IGM	o	i	
Δx_j^{dec}	Sampling interval	o	r	D_j / σ_L
ADC_j^{Min} ADC_j^{Max}	Maximum and minimum values of the digitized IGM	o	i	Integer values as given by the ADC before filtering and decimation.
$I_{j,d,k}^{ds}(n)$	DS IGM measurement for offset calibration	o	c	
k_R	Responsivity scaling factor	o	r	function of temperature at the DTUs.
$k_{G,j}$	Gain scaling factor	o	r	defined by PAW gain switching.
to 4.3	*Calculate Gain Calibration*			
N_j^{gain}	Number of data points in a gain IGM	o	i	
N^{gg}	Number of groups in the calibration sequence	o	i	Extracted from MIPAS source packet (= 1 in baseline scenario)
N^{ig}	Number of measurements (IGMs) in a group	o	i	Extracted from MIPAS source packet (= 300 in baseline scenario)
Δx_j^{dec}	Sampling interval	o	r	D_j / σ_L
$I_{j,d,i,k}^{G}(n)$	Blackbody or DS measurement for gain calibration	o	c	

ADC_j^{Min} ADC_j^{Max}	Maximum and minimum values of the digitized IGM	o	i	Integer values as given by the ADC before filtering and decimation.
k_R	Responsivity scaling factor	o	r	function of temperature at the DTUs.
$k_{G,j}$	Gain scaling factor	o	r	defined by PAW gain switching.
$T_{PRT(j')}$	PRT temperatures	o	r	
$T_{AX\pm}$	Aft baffle temperatures	o	r	
T_{AH}	ASU housing temperature	o	r	
to 4.5	*Calculate Radiance*			
N_j^{sc}	Number of points in a scene IGM	o	i	
Δx_j^{dec}	Sampling interval	o	r	D_j / σ_L
$I_{j,d}^{sc}(n)$	IGM scene measurement	o	c	
ADC_j^{Min} ADC_j^{Max}	Maximum and minimum values of the digitized IGM	o	i	Integer values as given by the ADC before filtering and decimation.
k_R	Responsivity scaling factor	o	r	function of temperature at the DTUs.
$k_{G,j}$	Gain scaling factor	o	r	defined by PAW gain switching.
to 4.7	*Calculate Pointing*			
t^{scene}	Time of actual ZPD crossing	o	r	transformed from OBT to UTC
α^{meas}	Measured azimuth angle	o	r	α^{meas} = 270 - A , where A is the pointing angle reading
ε^{meas}	Measured elevation angle	o	r	ε^{meas} = A - 90 , where A is the pointing angle reading

Remark: The measurement variable includes both observational and auxiliary data. More specific data assignments are done at the subsequent functions.

4.1.3 Detailed structure and formulas

4.1.3.1 Extract packets from Level 0

This operation consists in loading, depacketizing and appending all the packets forming a given measurement. It also includes the extraction of auxiliary data, when they are present in a source packet.

No specific formulas are involved in the packet extraction. This sub-function is composed mainly of load and format operations. A file Level 0 contains instrument source packets corresponding to one orbit in nominal case with associated orbital information and PCD (Product Confidence Data) information. The format of file Level 0 is described in [RD 7]. The format of instrument source packets contain in the file is described in [RD 9]. From that, the algorithm for packet extraction has the following basic steps (for each packet).

- Extract source packet.
- Read instrument source packet header.
  - Extract API (Application Process Identifier) from which instrument and mode are determined and validated.
  - Check for presence of auxiliary data in header, extract it if present.
  - Extract latest scan gate start time from auxiliary data.
- From block information in header do for each block.
  - Determine channel and verify block sequence.
  - Extract block, perform bit expansion and concatenate to current channel signal.

Error encoding of instrument source packets is now assumed not necessary in the current baseline, hence no error decoding is perform at this level. However, PCD information from the FEP (demultiplexer) is checked and a warning flag is set for the sweep if transmission errors have occurred. The sweep is not set as corrupted but rather as possibly invalid.

4.1.3.2 Auxiliary data calibration

This is the calibration of the relevant auxiliary data. This subject is covered in more details in a separate document [RD 8]. In order to be used in subsequent processing, some information contained in the auxiliary data are calibrated.

The UTC time corresponding to the latest scan gate start time is calculated from orbital information using Envisat CFI software PPF_LIB [RD 18]. The time corresponds to the one at beginning of the sweep. To obtain the time at ZPD t^{scene}, simply add $\frac{N^{ADC}}{2 \cdot \sigma_L \cdot \nu^{nom}}$.

The CBB PRT readings are converted into temperature (Kelvin) using specific polynomials according to the procedure described in [RD 8]. The PRT read-outs in the data provided from the

CBA are actual ADC digital count values (12 bits,) which must first be converted into resistance values. Another polynomial is then used to relate resistance to temperature.

The number of points N_j^{ds}, N_j^{gain} or N_j^{sc} in the interferogram must be calculated since the SPE sends blocks of 512 (256 complex) points even if the last is not full. It is calculated as follow:

$$N_j^X = \text{Floor}\left[\frac{N^{ADC} - M}{D_j}\right] + 1 \qquad (1)$$

where M corresponds to the number of taps (256) in the SPE filter.

The minimum and maximum ADC values are checked for saturation and a PCD flag is set for each detector if the ADC values exceed the saturation level (<= -32768 or >= 32767).

4.1.3.3 Data sort

Raw data are only delivered as preprocessed data (i.e. stored appropriately). Nominal data are separated according to their type, i.e. scene data, offset data and gain data. They are delivered as preprocessed data and stored internally for further processing.

No specific formulas. Once reconstructed, signals are time ordered and store that way.

4.1.3.4 Generate Level 1A

This operation groups preprocessed data (Level 1A). The Level 1A product is composed of a set of reconstructed but uncalibrated measurements that can be either interferograms or LOS signals. This data is generated and stored at the processing facilities.

No specific formulas. Format of Level 1A file is described in appendix in [RD 7]. There is one Level 1A file produced for each Level 0 file.

4.1.4 Computational sequence

The execution of the *Load Data* function will start after reception of a data package from the instrument. The ground segment design will assume that a data package contains several measurements corresponding, e.g. to all measurements taken during one or several orbits. It will also assume that all measurements are complete and that they are time-ordered.

The data coming from the instrument will have the form of data packets. A single measurement will be formed of several data packets. The *Load Data* function will stack and structure all data packets until a complete measurement (of any type) is obtained. All calibration procedures require two or more successive measurements. Therefore, if calibration data is found, the *Load Data* function shall stack the individual measurements until all measurements are obtained. When this is done, this (scene) measurement, or stack of (calibration) measurements, is delivered at the output and the control is transferred to the appropriate function depending on the type of measurement.

- For scene measurements, the control is transferred to the *Calculate Radiance* function
- For offset measurements, the control is transferred to the *Calculate Offset Calibration* function
- For gain measurements, the control is transferred to the *Calculate Gain Calibration* function

If the measurement has been taken in the Raw Data mode, it is delivered at the output of the ground processor, as a Preprocessed Data, and the *Load Data* function resumes with the processing of another input data. There is no control transfer in that case.

Note: Since August 2004, MIPAS instrument is operating in a reduced resolution mode (namely measurements with *MPD* ~ 8.2 cm instead of the high resolution mode for scenes with MPD = 20 cm). All measurements (scenes, blackbody, deep space, offset) are done at the same resolution. This implies that the reduction of resolution by software of the calibration (gain and offset) interferograms is needed in order to meet error budget. The reduction of the resolution is done only when the quality flag for the interferogram is valid. To keep processing compatibility of already acquired data, reduction is not done when *MPD* ~ 20 cm. In addition to reduction of resolution by software of the calibration (gain and offset) interferograms, the scene measurements must also be reduced a little to avoid undersampling the spectrum at 8 cm. To keep compatibility with other S/W version, this reduction will be done only when the MPD value specified in the MIP-PS1 ADF is set to 8 cm.

The computational sequence of the *Load Data* function is illustrated by the flowchart of Figure 4.1.4-1.

It should be noted that in order to create a Level 1B type output, at least one scan together with the corresponding offset has to be processed.

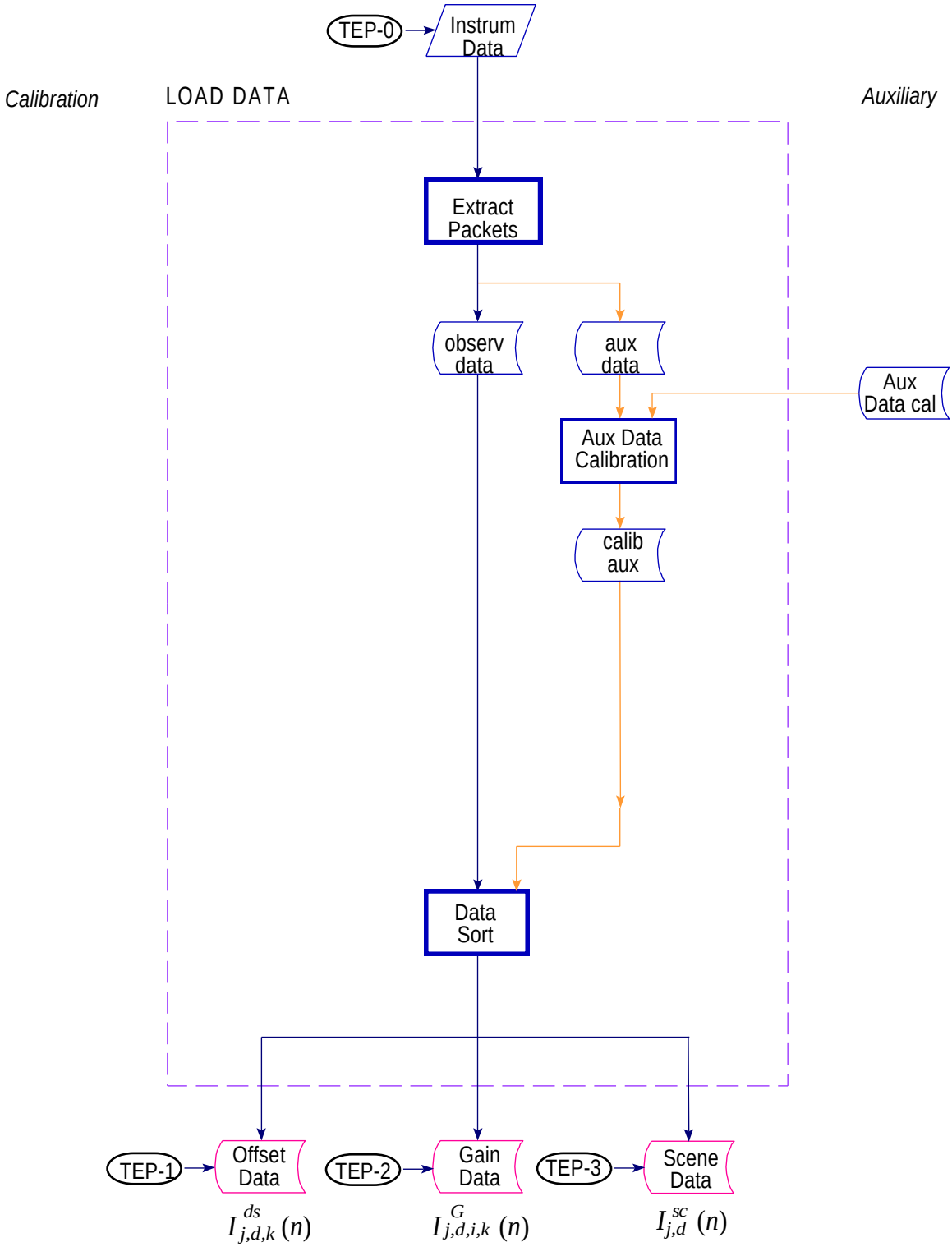

Figure 4.1.4-1 *Load Data* flowchart

4.2 CALCULATE OFFSET CALIBRATION

The present Section describes the *Calculate Offset Calibration* function that performs the processing of the offset calibration measurements including measurements in both sweep directions. The data flowchart of this function is provided in Figure 4.2.4-1.

This estimate of the instrument contribution is made by simply pointing the instrument to deep space (by moving the mirror of the ESU accordingly) and performing a measurement cycle as in the nominal case. For practical reasons, the deep space measurement is taken at a tangential height of around 150 km. Also, due to the potential difference in phase between different sweep directions of the instrument, a measurement is taken in each of the forward and reverse directions of the interferometer. In the ground segment, the latest offset measurement (in the correct sweep direction) is simply subtracted from each interferogram during processing.

The signals detected during offset measurements arise mainly from noise sources in detectors/ amplifiers and from thermal emission of the optical components within the interferometer. Even if the spectrum will be weak, it is believed that fringe count errors can be effectively determined. The scheme applied to scene and calibration measurements will most probably detect the occurrence of fringe errors, and the use of all interferograms (including offsets) maximizes the chance of detecting and correcting the errors as soon as possible after their occurrence.

The zero offset measurements will be subtracted from the relevant individual interferograms. Logically, these measurements should be made at the same spectral resolution as the scene measurements themselves, in order that the vectors are directly comparable. However, it is not expected that any high resolution features will be present in the offset spectra, which means that the measurements may be made at low resolution, with an interpolation on the ground segment. This has the advantage of reducing the duration of the offset measurement.

Simulations [RD 6] have shown that the consequence of using a single offset sweep at low resolution is that the overall NESR performance is degraded by around 5%, which is a too high degradation. If three forward or reverse sweeps are coadded, then the overall degradation in the NESR due to the offset estimate falls around 1.6%. Also, in order to lengthen the lifetime of the interferometer slides, offset measurement will now be made every *four* elevation scans instead of every two elevation scans.

In Full Resolution (FR) mode, the Offset Calibration will thus be performed every *four* scans, and use *six* sweeps at low resolution (three forward and three reverse), which must be combined to reduce the noise level to acceptable level. In Optimized Resolution (OR) mode, the Offset Calibration will use 12 sweeps at low resolution.

According to [RD 6] in FR mode, the total duration of the offset measurement is 16.15 seconds (including transition times), which is compliant with the new zero-offset requirement 3.10.2.2 in [RD 3]. Measurements will then be made every:

$$(4 \text{ scans} \times 16 \text{ sweeps/scan} \times 4.45 \text{ s/sweep}) - 0.45 \text{ s} + 16.15 \text{ s} = 300.5 \text{ s} \quad (1)$$

For an orbit of 100 minutes, assuming all measurements are performed with the same scan scenario, there will be about 20 offset measurements per orbit. By an examination of temperature variations, a worst case estimate of the rate of update to the offset contribution to the radiometric accuracy is one every 15.9 minutes, or roughly six times per orbit. This shows that the figure of 20 is well above the necessary minimum. This value will be revised during the Commissioning Phase of the instrument to see if the present scenario could not be relaxed to a lower number of offset measurements during one orbit.

Offset calibration will be performed when a new non-corrupted offset measurement becomes available. A 'closest in time strategy' shall be applied to select the calibrated offset that will be subtracted from the scene measurements, which means that a complete scan shall be calibrated with the closest calibrated offset. In case the closest calibrated offset is flagged as invalid by the "NESR Assessment and Offset Validation" function, it will be used anyway for the subtraction but a warning flag will be associated with the scene. If no offset at all is found in the input data, then the offset calibration data contained in the offset validation file shall be used but a warning flag will be associated with the scene.

The offset validation auxiliary data file is an input to the processor only. It shall contain a validation template (produced externally at the same frequency as the Gain ADF) and default offset calibration data.

4.2.1 Objective

The main objective of the *Calculate Offset Calibration* function is to deliver offset calibration measurement data in a form suitable for radiometric calibration of the spectra by the *Calculate Radiance* function.

Specific objectives of the function are

- Sort offset data according to the direction of interferometer sweep.
- Coadd all valid offset interferograms in each band and direction for the offset calibration group.
- Correct for detector non-linearity.
- Detect and correct fringe count errors in spectral bands B and C.
- Equalize and combine interferograms in band A.
- Assess NESR performance.

The offset calibration data shall be written to the Level 1B product annotated data set.

4.2.2 Definition of variables

Calculate Offset Calibration

Variable	Descriptive Name	I/O	Type	Ranges / References / Remarks
	Global variables & indices			
N_j^{ds}	Number of data points in DS IGM	i	i	input from *Load Data* function.
N_j^{zpd}	Number of points to define the *coarse* spectra	a	i	≈ 256 points retained in the ZPD region. MIP_PS1_AX(13)
j	Channel/band index number	l	i	
d	Index for sweep direction	l	i	0 = forward, 1 = reverse
Nb_d^{offcal}	Number of sweeps in given direction of a group of offset calibration	i	i	In FR mode, default value is 3 In OR mode, default value is 6
k	index of IGM in a group of offset calibration	l	i	The range of k is $k = 1,\ldots,3$
n^i	*input* IGM data point index	l	i	
n^c	*coarse* IGM data point index	l	i	$n^c = -N_j^{zpd}/2,\ldots,N_j^{zpd}/2-1$
m^c	*coarse* SPC data point index	l	i	$m^c = 0,\ldots,N_j^{zpd}-1$
$\Delta\sigma_j^{dscc}$	Wavenumber spacing in band j of calibrated coarse spectrum	t	r	calibrated with correction factor
σ_{0j}^{dscc}	Starting wavenumber in band j of calibrated coarse spectrum	t	r	calibrated with correction factor
σ_L	Nominal laser frequency	a	r	For the MIPAS instrument = 7606 cm^{-1} MIP_PS1_AX(4)
4.2.3.1	*Spikes detection*			
$I_{j,d,k}^{ds}(n^i)$	DS IGM	i	c	input from *Load Data*
4.2.3.3	*Interferogram coaddition*			
$I_{j,d}^{ds}(n^i)$	Coadded DS IGMs	t	c	Coaddition of 6 IGMs: 3 forward and 3 reverse.
4.2.3.4	*Gain spectral interpolation*			
m^r	*requested* SPC data point index	l	i	$m^r = 0,\ldots,N_j^{req}-1$
$G_{j,d}(m^r)$	Previous gain	i	c	input from *Calculate Gain Calibration* function
$G_{j,d}^I(m^c)$	Previous gain, interpolated	t	c	
4.2.3.5	*Calculate coarse spectra*			
$S_{j,d,k}^{dsc}(m^c)$	Coarse DS SPC	t	c	
$\Delta\sigma_j^{dsc}$	Wavenumber spacing in band j of coarse spectrum	t	r	computed from the coarse IGM by the unscrambling method
σ_{0j}^{dsc}	Starting wavenumber in band j of coarse spectrum	t	r	computed from the coarse IGM by the unscrambling method

Variable	Descriptive Name	I/O	Type	Ranges / References / Remarks
k_{SC}	Spectral calibration correction factor	i	r	computed in *Calculate Spectral Calibration* function MIP_CS1_AX(4.3)
4.2.3.6	*Calculate calibrated spectra*			
$S^{dscc}_{j,d,k}(m^c)$	Coarse calibrated DS SPC	t	c	
4.2.3.7	*Fringe count error detection*			
N^{ADC}	Number of sample data points in IGM before decimation	i	i	Extracted from MIPAS source packet
D_j	Decimation factor of band *j*	i	i	Extracted from auxiliary data of MIPAS source packet
h^{sys}_j	Systematic OPD shift of a DS IGM	t	i	$h^{sys}_j = \left(N^{ADC}/2 - 128\right) \bmod D_j$ if $\left(\left(N^{ADC} - 256\right)/D_j + 1\right) \bmod 2 = 0$ then $h^{sys}_j = h^{sys}_j - D_j$
$h^{ds}_{d,k}$	OPD shift of a DS IGM	t	i	
Δx	Nominal sampling interval	t	r	$1/\sigma_L$
4.2.3.8	*Fringe count error correction*			
4.2.3.9	*Responsivity scaling*			
k_R	Responsivity scaling factor	i	r	function of temperature at the DTUs. From *Load Data* function
$k_{G,j}$	Gain scaling factor	i	r	defined by PAW gain switching. From *Load Data* function
4.2.3.10	*Non-linearity correction*			
$ADC^{Min}_{j,d,k}$ $ADC^{Max}_{j,d,k}$	Maximum and minimum values of the digitized IGM	i	i	input from *Load Data* function. Integer values as given by the ADC before filtering and decimation.
$c_{q,j,d}$	Responsivity polynomial fit coefficients corresponding to a given non-linear detector	a	r	Polynomial order is 4 *j* covers only the index of non-linear detectors, A1, A2, AB and B MIP_CA1_AX(13)
4.2.3.11	*Equalization and combination*			
$I^{ds}_{j,d}(n^i)$	Final DS IGM	o	c	output from *Calculate Offset Calibration*
4.2.3.12	*NESR Assessment*			
N^{dsmx}_j	Number of points in band *j* for the *actual* DS	i	i	
m^{imx}	*actual* SPC data point index	l	i	$m^{imx} = 0,\ldots,N^{dsmx}_j - 1$
$\Delta\sigma^{dsmx}_j$	Wavenumber spacing in band *j* for the actual DS	t	r	
$\sigma_{0\,j}{}^{dsmx}$	Starting wavenumber in band *j* for the actual DS	t	r	
$S^{NESR}_{j,d}(m^{imx})$	Uncalibrated spectrum of residual error	t	c	

Variable	Descriptive Name	I/O	Type	Ranges / References / Remarks
u	Template reduction factor	a	i	$u \geq 1$. MIP_PS1_AX(18)
m^u	*reduced* SPC data point index	l	i	$m^u = 0,\ldots,\mathrm{Floor}\left\{N_j^{req}/u\right\}-1$
$N_{j,d}(m^u)$	DS spectrum residual noise radiance	t	r	
ℓ^{prev}	Previous sequential index of the deep space offset reading	i	i	MIP_CO1_AX(3) MDS 2
$\langle N_{j,d}^{prev}(m^u)\rangle$	Previous mean of noise	i	r	MIP_CO1_AX(9) MDS 2
$NESR_{j,d}^{prev}(m^u)$	Previous standard deviation of noise	i	r	Also called NESR of instrument. MIP_CO1_AX(10) MDS 2
$IPRV_{j,d}^{ds}(n^i)$	Previous valid interferogram offsets			MIP_CO1_AX(8, 13, 18, 23, 28) MDS 1
$LSModMean_{j,d}$	Least square mean of uncalibrated offset power spectrum	i	r	MIP_CO1_AX(3.1) MDS 1
$LSModStd_{j,d}$	Least square standard deviation of uncalibrated offset power spectrum	i	r	MIP_CO1_AX(3.2) MDS 1
ℓ	Sequential index of the deep space offset reading	o	i	$\ell = \ell^{prev} + 1$
$\langle N_{j,d}(m^u)\rangle$	Mean of noise	o	r	
$NESR_{j,d}(m^u)$	Standard deviation of noise	o	r	
$s_{NESR}^{\mathrm{thres}}$	Standard deviation threshold	a	r	value should be between 1 and 10. MIP_PS1_AX(16)
t_{NESR}	Threshold of rejection expressed as a percentage	a	r	$0 \leq t_{NESR} \leq 100$. MIP_PS1_AX(17)

4.2.3 Detailed structure and formulas

4.2.3.1 Spikes detection

This subfunction has the purpose of detecting spurious spikes in an offset interferogram. The presence of spikes in an interferogram can be caused by cosmic radiation or transmission errors. The affected interferogram is discarded in order to avoid contamination of the coadded offset.

The detection of spikes (no correction here) is computed on the input interferogram, according to the procedure described in Section 4.9.1.2:

$$I'^{ds}_{j,d,k}(n^i) = \text{CorrectSpikes}\left\{ I^{ds}_{j,d,k}(n^i),\, N^{ds}_j \right\} \tag{1}$$

with

$$n^i = \begin{cases} -\dfrac{N^{ds}_j}{2},\ldots,+\dfrac{N^{ds}_j}{2}-1, & \text{if } N^{ds}_j \text{ is even} \\ -\dfrac{N^{ds}_j-1}{2},\ldots,+\dfrac{N^{ds}_j-1}{2}, & \text{if } N^{ds}_j \text{ is odd} \end{cases}$$

4.2.3.2 Data sorting

This subfunction consists in the separation of the offset data according to the direction of the interferometer sweep. Six offset calibration measurements are expected at each four elevation scans. Three in the forward direction and three in the reverse direction.

No specific formula is applicable. This subfunction requires only read/write and compare operations.

4.2.3.3 Interferogram coaddition

The coaddition is performed on each deep space interferograms. If a fringe count error is detected, the offset is first corrected for fringe count error and then coadded. There is a separate coaddition for each sweep direction:

$$I^{ds}_{j,d}(n^i) = \frac{1}{Nb^{offcal}_d} \sum_{k=1}^{Nb^{offcal}_d} I^{ds}_{j,d,k}(n^i) \tag{1}$$

Note that the coaddition will exclude the offsets containing detected spikes or corrupted offsets having transmission errors. In this case, the average will be done on a smaller number than Nb^{offcal}_d.

4.2.3.4 Gain spectral interpolation

This subfunction performs a spectral interpolation of the actual calibrated gain unto a coarse spectral axis definition.

Note that as the gain to be interpolated is a smooth function, small N^{si} and N^{psi} parameters could be used to speed up the computation, or a simple linear interpolation between points could also be used instead. See Section 4.9.2 and 4.10.5 for more details about the *Linear Interpolation Method*.

For *j* limited to band B and C, we do an interpolation of the actual gain to a coarser resolution by the operation:

$$G^{I}_{j,d}(m^c) = \text{Interpolate}\left\{ G_{j,d}(m^r);\ \Delta\sigma_j^{req}, \sigma_{0j}^{req}, N_j^{req} \rightarrow \Delta\sigma_j^{dscc}, \sigma_{0j}^{dscc}, N_j^{zpd} \right\} \quad (3)$$

The range of data points index of the input gain is defined by the *requested* spectral calibration:

$$m^r = 0,\ldots,N_j^{req} - 1$$

The computed range of data points index is defined by the actual spectral calibration, but at coarse resolution:

$$m^c = 0,\ldots,N_j^{zpd} - 1$$

4.2.3.5 Calculate coarse spectra

This subfunction computes a coarse spectrum by performing the Fourier transform of a small portion around the ZPD of each incoming deep space interferogram (corresponding to a at very low resolution). This operation is followed by the computation of the corresponding spectral axis. This axis is then calibrated by a multiplication by the current spectral calibration correction factor. Unscrambling is finally performed with the purpose of re-ordering spectra computed from decimated interferograms.

The purpose of this subfunction is to provide coarse spectra for fringe count error detection. Thus it is applied only to band B and C interferograms.

$$S^{dsc}_{j,d,k}(m^c) = \text{FFT}\left\{ I^{ds}_{j,d,k}(n^c) \right\} \quad (1)$$

The range of data points index defined by the *coarse* spectral calibration is:

$$n^c = -\frac{N_j^{zpd}}{2},\ldots,+\frac{N_j^{zpd}}{2} - 1$$

where N_j^{zpd} is an integer power of 2, and j is limited to the B and C bands. For a given scene measurement, the sweep direction may be either forward or reverse.

The radiometric vector is then unscrambled following the method described in Section 4.10.2. The corresponding spectral axis vector $\sigma_j^{dsc}(m^c)$ is computed according to equation (4) of that same section. This spectral vector is then calibrated by a multiplication by the current spectral calibration correction factor k_{SC}. If no spectral calibration is available yet, this scaling is taken as unity.

$$\begin{aligned}\Delta\sigma_j^{dscc} &= \Delta\sigma_j^{dsc} \cdot k_{SC} \\ \sigma_{0j}^{dscc} &= \sigma_{0j}^{dsc} \cdot k_{SC}\end{aligned} \tag{2}$$

In addition to this stretching of the spectral axis, an inverse stretching must be applied on the radiometric scale to ensure the conservation of energy in the signal. This compensation can be applied with the following spectral calibration.

4.2.3.6 Calculate calibrated spectra

This subfunction performs a crude radiometric calibration of the coarse spectra by a simple multiplication by the previously interpolated coarse gain.

For j = B and C, the coarse calibrated deep space spectrum is obtained with:

$$S_{j,d,k}^{dscc}(m^c) = S_{j,d,k}^{dsc}(m^c) \cdot G_{j,d}^{I}(m^c) \big/ k_{SC} \tag{1}$$

4.2.3.7 Fringe count error detection

This subfunction analyses the phase of the coarse spectrum to establish if there was a fringe count error. It is necessary to detect fringe count errors before the actual interferogram is coadded with the previous interferograms of the same type. Thus, the detection procedure interacts with the coaddition procedure. In case a fringe count error is detected, the currently on-going coaddition is stopped and a new one is started.

Detection is done only in band B and C. Two bands were selected to increase the chance of detecting a fringe count error. Fringe count error detection should be done independently for the forward and reverse sweep direction.

The fringe count error detection can be computed from this calibrated spectrum, according to the procedure described in Section 4.9.3.2 for j = B and C:

$$h_{d,k}^{ds} = \text{FCE Detect}\left\{S_{j,d,k}^{dscc}(m^c), \sigma_j^{dscc}(m^c), \Delta x, h_j^{sys}\right\} \tag{1}$$

4.2.3.8 Fringe count error correction

In the case where a fringe count error was detected, that is if a non-zero OPD shift $\left(h_{d,k}^{ds} - h_j^{sys}\right)$ is calculated, this subfunction corrects the full deep space interferogram measurement. The correction is applied to all detectors or bands.

The fringe count error correction is applied on the current coaddition sequence of deep space interferograms at the input resolution, according to the procedure described in Section 4.9.3.3:

$$I'^{ds}_{j,d,k}(n^i) = \text{FCE Correct}\left\{I^{ds}_{j,d,k}(n^i), \left(h^{ds}_{d,k} - h^{sys}_j\right), \Delta x\right\} \quad (1)$$

The correction is applied to all detectors/bands so:

j = A1, A2, AB, B, C and D

4.2.3.9 Responsivity scaling

Based on the temperature measured at the DTUs, each individual interferogram must be scaled to account for the current DPU detector absolute responsivity at time of measurement. This responsivity is a function of temperature and varies over the orbit.

Also, there may be an additional vector multiplication to account for the current gain setting at the PAW on various channels, in the event of gain switching during orbit. In the case that the DPU gain is switched one or more times per orbit on one or more channels, the data has to be correctly scaled based on the selected gain factors (and using a characterization table giving the actual gain values corresponding to the selected settings).

These two corrections are still TBC. See Section 5.2.2.4 of [RD 6] for more details.

It is assume that k_R and $k_{G,j}$ are constant wrt to d and k. The correction is a simple scalar multiplication per vector:

$$I'^{ds}_{j,d}(n^i) = I^{ds}_{j,d}(n^i) \cdot k_R \cdot k_{G,j} \quad (1)$$

4.2.3.10 Non-linearity correction

The non-linearity correction is applicable on the non-linear detectors of channels A1, A2, B1, and B2 only. There is a different correction for each non-linear detector. Correction is performed on each incoming interferograms after responsivity scaling.

The non-linearity correction is derived from characterization data and based on an indicator of the DC total photon flux φ_{DC} of the actual measurement, i.e. the minimum and maximum values of the digitized IGM by the ADC before filtering and decimation given as input with the incoming interferogram. The characterization data contains non-linear responsivity polynomial coefficients

for each affected detectors. These coefficients are previously computed from readings of calibration blackbodies, according to the procedure described in [RD 2].

Since all measurements within a calibration group are equivalent, and therefore should be subject to the same non-linearity, the correction is performed on the coadded interferograms.

Knowing the minimum and maximum values of the digitized IGM by the ADC before filtering and decimation ($ADC_{j,d}^{Min} = \frac{1}{3}\sum_k ADC_{j,d,k}^{Min}$ and $ADC_{j,d}^{Max} = \frac{1}{3}\sum_k ADC_{j,d,k}^{Max}$) for the current coadded measure, and the responsivity coefficients for the detector under consideration ($c_{q,j,d}$), the non-linearity correction can be computed directly on the interferogram, according to the procedure described in Section 4.9.4 for j = A1, A2, AB and B:

$$I'^{ds}_{j,d}(n^i) = \text{CorrectNL}\left\{I^{ds}_{j,d}(n^i), ADC^{Min}_{j,d}, ADC^{Max}_{j,d}, c_{q,j,d}\right\} \quad (1)$$

4.2.3.11 Equalization and combination

For channels A1 and A2, the equalization must be performed since it was omitted on board because of the non-linearity problem. Combination allows an improvement of the signal-to-noise ratio.

The equalization is done only on one of the two detectors to be combined, using a convolution with proper coefficients. The combination is obtained by subtracting the A2 interferogram from the A1 interferogram.

The equalization and combination is computed on the deep space interferogram, according to the procedure described in Section 4.9.5.2:

$$I'^{ds}_{j,d}(n^i) = \text{EqualizeCombine}\left\{I^{ds}_{j,d}(n^i)\right\} \quad (1)$$

4.2.3.12 NESR Assessment and Offset Validation

In the purpose of accumulating the NESR vector, the values obtained by the deep space offset observation are used.

The first step is to compute the equivalent offset spectrum according to the procedure described in Section 4.2.4.5. A Fourier transform is done at the input resolution, followed by an unscrambling and an appropriate calibration of the spectral and radiometric axes for j = A, AB, B, C and D. Note that the result of the subtraction is zero-filled to N_j^{dsmx} (next power of 2 of N_j^{ds}) points before the FFT is done.

$$S^{NESR}_{j,d}(m^{imx}) = \text{FFT}\left\{I^{ds}_{j,d}(n^i) - I^{ds\,\text{prev}}_{j,d}(n^i)\right\} \quad (1)$$

where the notation "prev" indicates the value refers to the previous valid calibrated offset interferogram, i.e. the value of $I_{j,d}^{ds}(n^i)$ obtained during previous offset calibration. The range of data points index of the *input* spectral calibration is:

$$m^{imx} = 0,\ldots, N_j^{dsmx} - 1$$

Note : the fringe count of $I_{j,d}^{ds\,\mathrm{prev}}$ must be 0 wrt to the current gain as $I_{j,d}^{ds}$ before subtraction, i.e., detect FCE and correct FCE (if needed) must be applied on $I_{j,d}^{ds\,\mathrm{prev}}$. Note that for $I_{j,d}^{ds\,\mathrm{prev}}$, the systematic OPD shift must be set to 0 because it is already apply.

This uncalibrated spectrum is then interpolated (according to the Section 4.9.2 *Sinc Interpolation Method*) on a reduced grid of the requested spectral axis. One point out of every *u* points is kept, where *u* is the template reduction factor.

$$S_{j,d}^{NESR}(m^u) = \mathrm{Interpolate}\left\{S_{j,d}^{NESR}(m^{imx});\ \Delta\sigma_j^{dsmx}, \sigma_{0\,j}^{\ dsmx}, N_j^{dsmx} \rightarrow u\,\Delta\sigma_j^{req}, \sigma_{0\,j}^{\ req}, N_j^{req}/u\right\} \qquad (2)$$

The deep space noise radiance is given by the following definition, taking one point out of every *u* in the gain sampled on the requested axis:

$$N_{j,d}(m^u) = \mathrm{Re}\left\{S_{j,d}^{NESR}(m^u)\cdot G_{j,d}(m^u \cdot u)\right\} \qquad (3)$$

For each deep space reading (numbered ℓ = 1, 2, ...), two vectors $\langle N_{j,d}(m^u)\rangle$ and $NESR_{j,d}(m^u)$ are accumulated. The mean and the standard deviation can be recursively computed in a way to avoid storing all intermediate values in memory (that could lead to a huge table).

The mean computed can be expressed as a function of the previous mean, in the following way (for any value of ℓ):

$$\langle N_{j,d}(m^u)\rangle = \frac{(\ell-1)\,\langle N_{j,d}^{prev}(m^u)\rangle + N_{j,d}}{\ell} \qquad (4)$$

The standard deviation computed can be expressed as a function of the previous mean and the previous standard deviation, in the following way:

if ℓ = 1:

$$NESR_{j,d}(m^u) = 0 \qquad (5)$$

else

$$NESR_{j,d}(m^u) = \sqrt{\frac{\left(N_{j,d}(m^u)\right)^2 + (\ell-2)\left(NESR_{j,d}^{prev}(m^u)\right)^2 + (\ell-1)\langle N_{j,d}^{prev}(m^u)\rangle^2 - \ell\langle N_{j,d}(m^u)\rangle^2}{\ell-1}} \qquad (6)$$

Before inserting the value of $N_{j,d}(m^u)$ in the running mean $\langle N_{j,d}(m^u)\rangle$ and into the $NESR_{j,d}(m^u)$ vector, its validity must be first checked the following way:

Calculate the normalized modulus offset spectrum over all offset measurements in the L0 product and calculate the normalized modulus offset spectrum of previous reference valid offset. The interferograms are zero-filled to the next power of 2 and a Fast-Fourier Transform performed following the method described in Section 4.10.1.

$$S^{ds}_{j,d,k}(m^{imx}) = \mathrm{FFT}\left\{I^{ds}_{j,d,k}(n^i)\right\} \tag{7}$$

$$SPRV^{ds}_{j,d}(m^{imx}) = \mathrm{FFT}\left\{IPRV^{ds}_{j,d}(n^i)\right\} \tag{8}$$

The radiometric vectors $S^{ds}_{j,d,k}$ and $SPRV^{ds}_{j,d}$ are then unscrambled following the method described in Section 4.10.2 and the spectral grid interpolated according to Section 4.9.2.

$$SAbsNormOff_{j,d,k}(m^{imx}) = \frac{N_j^{dsmx}}{\sum_{m^{imx}=0}^{m^{imx}=N_j^{dsmx}-1} abs\left\{S^{ds}_{j,d,k}(m^{imx})\right\}} * abs\left\{S^{ds}_{j,d,k}(m^{imx})\right\} \tag{9}$$

$$SAbsNormPRVOff_{j,d}(m^{imx}) = \frac{N_j^{dsmx}}{\sum_{m^{imx}=0}^{m^{imx}=N_j^{dsmx}-1} abs\left\{SPRV^{ds}_{j,d}(m^{imx})\right\}} * abs\left\{SPRV^{ds}_{j,d}(m^{imx})\right\} \tag{9a}$$

Calculate the least square for the modulus of each offset measurement

$$LSMod_{j,d,k} = \sum_{m=0}^{m=N_j^{dsmx}-1} (SAbsNormOff_{j,d,k}(m)) - SAbsNormPRVOff_{j,d}(m))^2 \tag{10}$$

Compare the least square of modulus with previous LSModMean and LSModStd contained in MIP_CO1_AX ADF. Note that if LSModStd = 0, the comparison is not done and the offset is considered valid.

$$\text{if} \left| LSMod_{j,d,k} - LSModMean_{j,d} \right| > s^{\text{thres}}_{NESR} \cdot LSModStd_{j,d} \tag{11}$$

then there is a chance that $N_{j,d}(m^u)$ comes from erroneous data.

else $\langle N_{j,d}(m^u)\rangle$ and $NESR_{j,d}(m^u)$ are updated as described previously.

s^{thres}_{NESR} is a standard deviation threshold previously defined.

The flag is provided in the data product. $\langle N_{j,d}(m^u)\rangle$ and $NESR_{j,d}(m^u)$ are kept with calibrated data and referred in the data product.

The mean $LSModMean_{j,d}$ and the standard deviation $LSModStd_{j,d}$ stored in MIP_CO1_AX ADFs are calculated once a week over all the offsets of a complete orbit by MICAL S/W using the following equations.

$$LSModMean_{j,d} = mean(LSMod_{j,d,k}) \tag{12}$$

$$LSModStd_{j,d} = \sqrt{Variance(LSMod_{j,d,k})} \tag{13}$$

4.2.4 Computational sequence

The *Calculate Offset Calibration* function receives control from the *Load Data* function when offset data have been found. It then processes this data and sends control back to the *Load Data* function.

The output, i.e. an offset calibration, is generated only when the measurements for forward and reverse sweeps have been processed. The new offset calibration file replaces the old one. The old file is delivered as an output of the ground processing.

The computational sequence of the *Calculate Offset Calibration* function is illustrated by the flowchart of Figure 4.2.4-1.

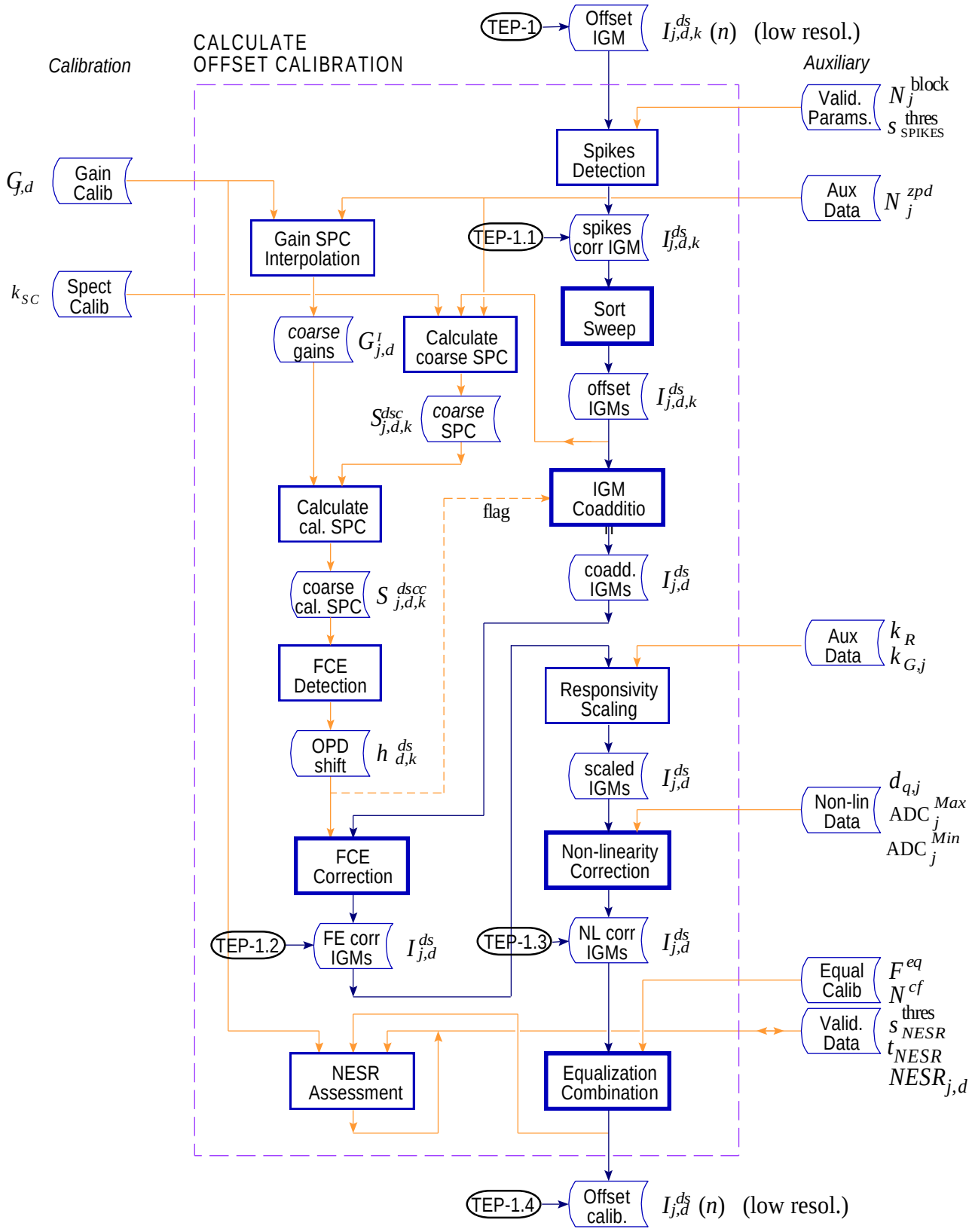

Figure 4.2.4-1 *Calculate Offset Calibration* flowchart

4.3 CALCULATE GAIN CALIBRATION

The present Section describes the *Calculate Gain Calibration* function that performs the processing of gain calibration measurements including all deep space and blackbody measurements of the gain calibration sequence. The data flowchart for gain calibration processing is provided in Figure 4.3.4-1.

The radiometric gain calibration requires blackbody measurements. Since in this case the instrument is again contributing to the observed signal, it is also necessary to perform deep space measurements before the blackbody measurements in order to subtract the appropriate instrument offset. (In this instance, the term "Deep Space Radiometric Calibration" is used to distinguish the measurements from the regular Offset Calibration made with the scan sequences. The Deep Space Radiometric Calibrations are used only to correct the CBB measurements and must be explicitly commanded as described in [RD 10]). In fact, several measurements of each kind will be needed. This is because the signal to noise ratio of a single, offset-corrected, blackbody measurement is not high enough, particularly in band D, to achieve the required radiometric accuracy. Therefore a single gain calibration implies several successive measurements.

It is expected that there will be no high frequency features in either the CBB spectrum or in the instrument contribution (as assumed also for the offset calibration). These assumptions will be verified on the ground during instrument AIT, but the assumption is reasonable. Therefore, each CBB or Deep Space sweep of the instrument will be made at low-spectral resolution, i.e. with a duration of 0.4 seconds. The baseline scenario uses 300 sweeps at low resolution in both forward and reverse directions for both CBB and Deep Space measurements. The reduced resolution scenario uses 200 sweeps at low resolution in both forward and reverse directions.

Radiometric gain calibration will be performed after the instrument slides have been stopped in order to re-establish a phase reference. The gain sequence will therefore be commanded as the first operation in any nominal measurement sequence. Radiometric Deep Space Calibration measurements precede those made looking towards the CBB to cover the worst case condition of the instrument entering measurement mode directly after the boost heater phase of the CBB.

The radiometric gain calibration has two commanded sequences, each of 600 low resolution sweeps. In addition to the duration of the sweep sequences themselves, there will be two commanded transitions, followed by an automatic transition. According to [RD 6], each commanded sequence has a duration of 520.6 seconds. The total duration of the radiometric gain sequence (DS and CBB) is:

$$(2 \times 520.6 \text{ s}) = 1041.2 \text{ s, or } 17.35 \text{ min} \quad (1)$$

With this duration required once par week, the baseline radiometric calibration easily satisfies the requirement 3.10.2.3 in [RD 3].

A special consideration is given to the South Atlantic Anomaly (SAA) and its potential effects upon instrument performance (e.g. detector spikes). At present, it is proposed to monitor the effect of the SAA by a simple gain check performed once per orbit as soon as possible after the passage through the SAA [RD 6]. The purpose of the check is simply to give an indication whether the

gain/phase performance of the instrument has been affected in any way. It is currently assumed that there will be no effect, and hence the baseline uses a simple measurement which comprises of 6 sweeps (3 forward, 3 reverse) for DS and CBB measurements. These gain vectors should be analyzed and compared to the current gain vector being applied in the processing to detect any significant differences in amplitude profile (e.g. spikes).

The gain auxiliary product shall be produced by the Level 1B processor if gain data are found in the input Level 0 product (a flag shall indicate if the gain data are valid or not). The gain data shall be processed at the beginning before scene data. The produced gain calibration data shall NOT be used to process scene data in the current input data. An initial gain product will be given as input to the processor at all processing stations and shall be used until a next gain will be made available. During processing, the gain file shall not be modified by the processor.

4.3.1 Objective

The main objective of the *Calculate Gain Calibration* function is to deliver a file representing the radiometric gain of the instrument, computed using gain calibration measurements, in a form suitable for radiometric calibration of the spectra by the *Calculate Radiance* function.

Specific objectives of the function are:

- Sort the gain calibration measurements according to types of measurement and sweep direction, i.e. deep space or blackbody measurements, and forward or reverse sweep.
- Coadd interferograms to increase SNR.
- Detect and correct fringe count errors in spectral bands B and C.
- Correct DS and BB measurements for non-linearity of each affected detector.
- Subtract offset due to contribution of the instrument.
- Equalize and combine interferograms in band A.
- Compute spectra using a FFT algorithm applied on the interferograms.
- Interpolate gain spectral vectors to provide the gain on a predefined spectral axis.
- Calculate expected blackbody radiance from temperature readings corresponding to blackbody measurements.
- Calculate the complex ratio of theoretical to calculated spectrum.
- Check for radiometric accuracy of the incoming data.

These objectives have been followed in the detailed design of the function.

NOTE: in the following, the "*G"* superscript stands for "*gain measurement"* and means that the measurement can be either a deep space (*ds*) or a blackbody (*bb*) measurement.

e.g.: $S^{Gc}_{j,d,i,k}(m)$ stands for $S^{dsgc}_{j,d,i,k}(m)$ and $S^{bbc}_{j,d,i,k}(m)$

e.g.: $$I^{G}_{j,d,i}(n) = \frac{1}{N^{ig}} \sum_{k=1}^{N^{ig}} I^{G}_{j,d,i,k}(n)$$

means $$I^{dsg}_{j,d,i}(n) = \frac{1}{N^{ig}} \sum_{k=1}^{N^{ig}} I^{dsg}_{j,d,i,k}(n)$$

and $$I^{bb}_{j,d,i}(n) = \frac{1}{N^{ig}} \sum_{k=1}^{N^{ig}} I^{bb}_{j,d,i,k}(n)$$

4.3.2 Definition of variables

Calculate Gain Calibration

Variable	Descriptive Name	I/O	Type	Ranges / References / Remarks
	Global variables & indices			
N_j^{gain}	Number of data points in a gain IGM (DS or BB)	i	i	Input from *Load Data* function. IGMs at low resolution
N^{gg}	Number of groups in the calibration sequence	i	i	Input from *Load Data* function. 1 group
N^{ig}	Number of measurements (IGMs) in a group	i	i	Input from *Load Data* function. 300 sweeps in both directions and both types
$N_j^{G\max}$	Number of points in band *j* for the *actual* gain	t	i	Computed from number of input points (next power of 2)
N_j^{zpd}	Number of points retained in the ZPD region to define the *coarse* spectra	a	i	The choice of the number of points depends on the assumption that can be done on the maximum shift due to a FCE (power of 2) MIP_PS1_AX(13)
N_j^{req}	Number of points in band *j* for the requested spectral axis	a	i	MIP_PS1_AX(7)
j	Channel or band index number	l	i	j = A1, A2, A, AB, B, C, D
d	Index for sweep direction	l	i	0 = forward, 1 = reverse
i	Index of group number in the calibration sequence	l	i	The range of i is $i = 1,\ldots,N^{gg}$
k	Index of an IGM in a group of calibration IGMs	l	i	The range of k is $k = 1,\ldots,N^{ig}$
n^i	*input* IGM data point index	l	i	
m^r	*requested* SPC data point index	l	i	$m^r = 0,\ldots,N_j^{req}-1$
n^a	*actual* IGM data point index	l	i	$n^a = -N_j^{G\max}/2,\ldots,N_j^{G\max}/2-1$
m^a	*actual* SPC data point index	l	i	$m^a = 0,\ldots,N_j^{G\max}-1$
n^c	*coarse* IGM data point index	l	i	$n^c = -N_j^{zpd}/2,\ldots,N_j^{zpd}/2-1$
m^c	*coarse* SPC data point index	l	i	$m^c = 0,\ldots,N_j^{zpd}-1$
$\Delta\sigma_j^{Gcc}$	Wavenumber spacing in band *j* of calibrated coarse spectrum	t	r	calibrated with correction factor
$\sigma_{0_j}^{Gcc}$	Starting wavenumber in band *j* of calibrated coarse spectrum	t	r	calibrated with correction factor
σ_L	Nominal laser wavenumber	a	r	For the MIPAS instrument = 7606 cm^{-1} MIP_PS1_AX(4)

Variable	Descriptive Name	I/O	Type	Ranges / References / Remarks
4.3.3.1	*Spikes detection*			
$I^{G}_{j,d,i,k}(n^{i})$	Single gain IGM measurement, either DS or BB	i	c	input from *Load Data* function
4.3.3.3	*Interferogram coaddition*			
$I^{G}_{j,d,i}(n^{i})$	Coadded DS or BB IGM	t	c	
4.3.3.4	*Gain spectral interpolation*			
$\Delta\sigma^{req}_{j}$	Wavenumber spacing in band *j* for the requested spectral axis	t	r	Computed with MIP_PS1_AX(7, 8, 9)
$\sigma_{0\,j}^{req}$	Starting wavenumber in band *j* for the requested spectral axis	a	r	MIP_PS1_AX(8)
$G^{prev}_{j,d}(m^{r})$	Previous gain	i	c	input from *Calculate Gain Calibration* function
$G^{I}_{j,d}(m^{c})$	Previous gain, interpolated	t	c	
4.3.3.5	*Calculate coarse spectra*			
$S^{Gc}_{j,d,i,k}(m^{c})$	Coarse gain SPCs, either DS or BB	t	c	
$\Delta\sigma^{Gc}_{j}$	Wavenumber spacing in band *j* of coarse spectrum	t	r	computed from the coarse IGM by the unscrambling method
$\sigma_{0\,j}^{Gc}$	Starting wavenumber in band *j* of coarse spectrum	t	r	computed from the coarse IGM by the unscrambling method
k_{SC}	Spectral calibration correction factor	i	r	computed in *Calculate Spectral Calibration* function
4.3.3.6	*Gain shift correction*			
$S^{Gcc}_{j,d,i,k}(m^{c})$	Coarse calibrated gain SPCs, either DS or BB	t	c	
Δx	Nominal sampling interval	t	r	$1/\sigma_{L}$
$\sigma^{G}_{j}(m^{c})$	*coarse* wavenumber vector	i	r	Defines band *j*, according to the coarse spectral axis definition
$C^{G}_{j,d}(m^{c})$	Phase correction spectral function for a gain SPC	t	c	
$G^{I*}_{j,d}(m^{c})$	Previous gain, interpolated and shifted	t	c	
4.3.3.7	*Calculate calibrated spectra*			
4.3.3.8	*Fringe count error detection*			
N^{ADC}	Number of sample data points in IGM before decimation	i	i	Extracted from MIPAS source packet
D_{j}	Decimation factor of band *j*	i	i	Extracted from auxiliary data of MIPAS source packet
h^{sys}_{j}	Systematic OPD shift of a DS or BB measurement	t	i	$h^{sys}_{j} = \left(N^{ADC}/2 - 128\right) \bmod D_{j}$ if $\left(\left(N^{ADC} - 256\right)/D_{j} + 1\right) \bmod 2 = 0$ then $h^{sys}_{j} = h^{sys}_{j} - D_{j}$
$h^{G}_{d,i,k}$	OPD shift for a DS or BB measurement	t	r	
4.3.3.9	*Fringe count error correction*			

Variable	Descriptive Name	I/O	Type	Ranges / References / Remarks
4.3.3.10	*Responsivity scaling*			
k_R	Responsivity scaling factor	i	r	function of temperature at the DTUs. From *Load Data* function
$k_{G,j}$	Gain scaling factor	i	r	defined by PAW gain switching. From *Load Data* function
4.3.3.11	*Non-linearity correction*			
$ADC^{Min}_{j,d,i,k}$ $ADC^{Max}_{j,d,i,k}$	Maximum and minimum values of the digitized IGM	i	i	input from *Load Data* function. Integer values as given by the ADC before filtering and decimation.
$c_{q,j,d}$	Responsivity polynomial fit coefficients corresponding to a given non-linear detector	a	r	Polynomial order is 4 *j* covers only the index of non-linear detectors A1, A2, AB and B MIP_CA1_AX(13)
4.3.3.12	*Offset subtraction*			
$I^{gain}_{j,d,i}(n^i)$	Coadded and offset corrected gain IGM	t	c	
4.3.3.13	*Equalization and combination*			
4.3.3.14	*Zero-filling of interferogram*			
$I^{zf}_{j,d,i}(n^a)$	Zero-filled (and coadded) gain IGM.	t	c	
4.3.3.15	*Calculate spect. cal. spectra*			
$\Delta\sigma_j^{G\max}$	Wavenumber spacing in band *j* for the actual gain	t	r	
$\sigma_{0\,j}^{G\max}$	Starting wavenumber in band *j* for the actual gain	t	r	
Δx_j^{dec}	Sampling interval	i	r	current value of the IGM sampling input from *Load Data* function
$S^{gain}_{j,d,i}(m^a)$	Coadded gain spectra	t	c	
4.3.3.16	*Spectral interpolation*			
$S^{gain}_{j,d,i}(m^r)$	Interpolated gain spectra	t	c	
4.3.3.17	*BB radiance calculation*			
$L_{j,d,i}(m^r)$	Theoretical spectral radiance of the calibration BB.	t	r	The range of m^r corresponds to the requested spectral axis definition
$\sigma_j(m^r)$	Vector of wavenumber values.	t	r	Defines band *j*, according to the requested spectral axis definition
$R_{BB}(\sigma)$	Blackbody radiance function	t	r	
$\varepsilon_{eff}(\sigma)$	Blackbody effective emissivity	a	r	MIP_CA1_AX(30)
$\varepsilon_{surf}(\sigma)$	Blackbody surface emissivity	a	r	MIP_CA1_AX(29)
$F_{b\pm S}$	View factors	a	r	MIP_CA1_AX(25)
$x_{i'}$	Base area element locations	a	r	MIP_CA1_AX(23)
$l_{j'}$	Base area PRT locations	a	r	MIP_CA1_AX(24)
$T_{PRT(j')}$	Base area PRT temperatures	i	r	Output of *Load Data* function
$T_{\pm S}$	Wall temperatures	i	r	Output of *Load Data* function
$T_{AX\pm}$	Aft baffle temperatures	i	r	Output of *Load Data* function
T_{AH}	ASU housing temperature	i	r	Output of *Load Data* function

Variable	Descriptive Name	I/O	Type	Ranges / References / Remarks
4.3.3.18	*Radiometric accuracy*			
u	Template reduction factor	a	i	$u \geq 1$. MIP_PS1_AX(23)
m^u	*reduced* SPC data point index	l	i	$m^u = 0,\ldots,\mathrm{Floor}\left\{N_j^{req}/u\right\}-1$
$A_{j,d}(m^u)$	Gain spectrum residual noise radiance	t	r	
ℓ^{prev}	Previous sequential index of the gain reading	i	i	MIP_CG1_AX(3) MDS 2
$\langle A_{j,d}^{prev}(m^u)\rangle$	Previous mean of radiometric accuracy	i	r	MIP_CG1_AX(9) MDS 2
$NRMS_{j,d}^{prev}(m^u)$	Previous standard deviation of accuracy	i	r	MIP_CG1_AX(10) MDS 2
ℓ	Sequential index of the gain reading	o	i	$\ell = \ell^{prev}+1$ MIP_CG1_AX(3) MDS 2
$\langle A_{j,d}(m^u)\rangle$	Mean of radiometric accuracy	o	r	MIP_CG1_AX(9) MDS 2
$NRMS_{j,d}(m^u)$	Standard deviation of accuracy	o	r	MIP_CG1_AX(10) MDS 2
s_{RACC}^{thres}	Standard deviation threshold	a	r	value should be between 1 and 10 MIP_PS1_AX(21)
t_{RACC}	Threshold of rejection expressed as a percentage	a	r	$0 \leq t_{RACC} \leq 100$ MIP_PS1_AX(22)
4.3.3.19	*Ratio*			
$G_{j,d,i}(m^r)$	Radiometric gain for group *i*, sweep direction *d* and band *j*	t	c	
4.3.3.20	*Gain coaddition*			
$G_{j,d}(m^r)$	Radiometric gain for band *j* and sweep direction *d*	o	c	output from *Calculate Gain Calibration* MIP_CG1_AX(22) MDS 1

4.3.3 Detailed structure and formulas

4.3.3.1 Spikes detection

This subfunction has the purpose of detecting spurious spikes in the interferogram of a deep space or a blackbody reading. The presence of spikes in an interferogram can be caused by cosmic radiation or transmission errors. The affected interferogram is discarded in order to avoid contamination of the coadded offset.

The detection of spikes (no correction here) is computed on the input interferogram, according to the procedure described in Section 4.9.1.2:

$$I'^{G}_{j,d,i,k}(n^i) = \text{CorrectSpikes}\left\{ I^{G}_{j,d,i,k}(n^i),\, N_j^{gain} \right\} \tag{1}$$

with

$$n^i = \begin{cases} -\dfrac{N_j^{gain}}{2},\ldots,+\dfrac{N_j^{gain}}{2}-1, & \text{if } N_j^{gain} \text{ is even} \\ -\dfrac{N_j^{gain}-1}{2},\ldots,+\dfrac{N_j^{gain}-1}{2}, & \text{if } N_j^{gain} \text{ is odd} \end{cases}$$

4.3.3.2 Data sorting

Because of the different types of calibration measurements, it is necessary to perform several sorting operations.

- Sorting according to the type of data: offset data and blackbody data
- Sorting according to sweep direction: onward sweep and reverse sweep
- Sorting according to sweep groups: depending on the radiometric calibration scenario, the measurements may be grouped into sets of successive measurements of deep space and blackbody.

No specific formula is applicable. This subfunction requires only read/write and compare operations.

4.3.3.3 Interferogram coaddition

In order to improve the signal to noise ratio, several successive blackbody and deep space measurements are accomplished. Gain interferograms means here blackbody interferograms and deep space interferograms.

The coaddition procedure must account for the groups defined by the calibration scenario as well as for the groups that may be defined because of fringe count errors.

Coaddition is a simple point-by-point addition divided by the number of measurements.

The coaddition is performed separately on blackbody and deep space interferograms. For each type, there is a separate coaddition for each sweep direction:

$$I^G_{j,d,i}(n^i) = \frac{1}{N^{ig}} \sum_{k=1}^{N^{ig}} I^G_{j,d,i,k}(n^i) \qquad (1)$$

If a fringe count error is detected, the coaddition sequence is stopped, the coadded interferograms are stored separately and a new coaddition sequence is started.

4.3.3.4 Gain spectral interpolation

This subfunction performs a spectral interpolation of the previous gain according to the actual spectral calibration.

Note that as the gain to be interpolated is a smooth function, small N^{si} and N^{psi} parameters could be used to speed up the computation, or a simple linear interpolation between points could also be used instead. See Section 4.9.2 and 4.10.5 for more details about the *Linear Interpolation Method*..

For *j* limited to bands B and C, we interpolate the *previous* gain at wavenumber values corresponding to the coarse spectrum:

$$G^I_{j,d}(m^c) = \text{Interpolate}\left\{ G^{prev}_{j,d}(m^r);\ \Delta\sigma^{req}_j, \sigma^{req}_{0_j}, N^{req}_j \rightarrow \Delta\sigma^{Gcc}_j, \sigma^{Gcc}_{0_j}, N^{zpd}_j \right\} \qquad (1)$$

The range of data points index of the input gain is defined by the *requested* spectral calibration:

$$m^r = 0, \ldots, N^{req}_j - 1$$

The computed range of data points index is defined by the *actual* spectral calibration:

$$m^c = 0, \ldots, N^{zpd}_j - 1$$

4.3.3.5 Calculate coarse spectra

This subfunction computes a coarse spectrum by performing the Fourier transform of a small portion around the ZPD of each incoming interferogram (corresponding to a very low resolution). This operation is followed by the computation of the corresponding spectral axis. This axis is then calibrated by a multiplication by the current spectral calibration correction factor. Unscrambling is finally performed with the purpose of re-ordering spectra computed from decimated interferograms.

The purpose of this subfunction is to provide coarse spectra for previous gain shift correction (first SPC) and fringe count error detection. Thus it is applied only to band B and C interferograms. A coarse spectrum is calculated for each measurement of the gain calibration sequence (not on coadded interferograms).

A Fourier transform is done at very low resolution for both the deep space and the blackbody measurements:

$$S^{Gc}_{j,d,i,k}(m^c) = \mathrm{FFT}\left\{ I^{G}_{j,d,i,k}(n^c) \right\} \tag{1}$$

The range of data points index defined by the *coarse* spectral calibration is:

$$n^c = -\frac{N_j^{zpd}}{2},\ldots,+\frac{N_j^{zpd}}{2} - 1$$

and

$$m^c = 0,\ldots,N_j^{zpd} - 1$$

where N_j^{zpd} is an integer power of 2, and j is limited to the B and C bands. For a given scene measurement, the sweep direction may be either forward or reverse.

The radiometric vector is then unscrambled following the method described in Section 4.10.2. The corresponding spectral axis vector $\sigma_j^{Gc}(m^c)$ is computed according to equation (4) of that same section. This vector is then calibrated by a multiplication by the current spectral calibration correction factor k_{SC}. If no spectral calibration is available yet, this factor is taken as unity.

$$\begin{aligned} \Delta\sigma_j^{Gcc} &= \Delta\sigma_j^{Gc} \cdot k_{SC} \\ \sigma_{0j}^{Gcc} &= \sigma_{0j}^{Gc} \cdot k_{SC} \end{aligned} \tag{2}$$

4.3.3.6 Gain shift correction

The purpose of this subfunction is to correct the OPD shift between the *last* gain measurement and the *actual* gain measurement. This shift is due to the fact that the interferometer sweep mechanism has been stopped between these two calibrations. The correction is applied on the last gain measurement. It is based only on the first measurement of the actual gain measurement sequence.

Since we want to produce a gain according to the last fringe count reference, we first have to correct the previous gain OPD shift with respect to the last reference. This correction uses only the very last (one for each directions) measurements of the complete gain calibration sequence. The procedure is basically the same as for fringe count errors detection and correction except that here the correction is applied to the previous coarse gain.

The coarse calibrated gain spectrum of the last reading is obtained with:

$$S^{Gcc}_{j,d,N^{gg},N^{ig}}(m^c) = S^{Gc}_{j,d,N^{gg},N^{ig}}(m^c) \cdot G^{I}_{j,d}\left(m^c\right) \Big/ k_{SC} \tag{1}$$

The second step is to establish the OPD shift according to the procedure described in Section 4.9.3.2:

$$h^{G}_{d,N^{gg},N^{ig}} = \text{FCE Detect}\left\{S^{Gcc}_{j,d,N^{gg},N^{ig}}(m^c), \sigma^{Gcc}_{j}(m^c), \Delta x, h^{sys}_{j}\right\} \tag{2}$$

The third step is the correction of the observed OPD shift. This correction stage is similar to the FCE correction function described in Section 4.9.3.3. We start by calculating the phase correction spectral function.

$$C^{G}_{j,d}(m^c) = \exp(-2\pi i \cdot \sigma^{G}_{j}(m^c) \cdot (h^{G}_{d,N^{gg},N^{ig}} - h^{sys}_{j}) \cdot \Delta x) \tag{3}$$

with

$$\sigma^{G}_{j}(m^c) = \sigma^{Gcc}_{0_j} + m^c \, \Delta\sigma^{Gcc}_{j} \tag{4}$$

Then we multiply the previous coarse gain by the phase function:

$$G^{I*}_{j,d}(m^c) = G^{I}_{j,d}(m^c) \cdot C^{G}_{j,d}(m^c) \tag{5}$$

for both sweep directions and for bands j = B and C.

This new gain function will be used in the fringe count errors detection for all subsequent interferograms of the gain calibration sequence.

4.3.3.7 Calculate calibrated spectra

This subfunction performs a crude radiometric calibration of the coarse spectra by a simple multiplication by the previously interpolated coarse gain.

Since the non-linearity correction will only be done on the coadded interferograms, here we are only looking at the fringe count errors. So, the j index only covers the bands B and C. Spectral interpolation of the previous gain is not necessary anymore since it was done with the first gain measurement.

The coarse calibrated deep space and blackbody spectra is obtained with:

$$S^{Gcc}_{j,d,i,k}(m^c) = S^{Gc}_{j,d,i,k}(m^c) \cdot G^{I*}_{j,d}\left(m^c\right) \Big/ k_{SC} \tag{1}$$

The index in the gains *G*, at positions corresponding to the coordinates *m* in spectra is not guaranteed to fall inside the valid requested gain range: the exceeding points at the extremities have to be neglected to avoid contamination of the following linear regression in the operation of fringe count error detection.

4.3.3.8 Fringe count error detection

This subfunction analyses the phase of the coarse spectrum to establish if there was a fringe count error. It is necessary to detect fringe count errors before the actual interferogram is coadded with the previous interferograms of the same type. Thus, the detection procedure interacts with the coaddition procedure. In case a fringe count error is detected, the currently on-going coaddition is stopped and a new one is started

Detection is done only in band B and C. However, it should be done independently for the forward and reverse sweep direction. Two bands were selected to increase the chance of detecting a fringe count error. Detection is performed for each measurement of the gain calibration sequence.

The same procedure is followed for the deep space and for the blackbody measurements. The fringe count error detection can be computed from this coarse calibrated spectrum, according to the procedure described in Section 4.9.3.2 for *j* = B and C:

$$h^{G}_{d,i,k} = \text{FCE Detect}\left\{S^{Gcc}_{j,d,i,k}(m^{c}), \sigma^{Gcc}_{j}(m^{c}), \Delta x, h^{sys}_{j}\right\} \quad (1)$$

4.3.3.9 Fringe count error correction

In the case where a fringe count error was detected, that is if a non-zero spectral shift $\left(h^{G}_{d,i,k} - h^{sys}_{j}\right)$ is calculated, this subfunction corrects the full deep space or blackbody coadded interferograms measurements. The correction is applied to all detectors or bands.

The fringe count error correction is applied on the current coaddition sequence of deep space or blackbody interferogram at the input resolution, according to the procedure described in Section 4.9.3.3:

$$I'^{G}_{j,d,i,k}(n^{i}) = \text{FCE Correct}\left\{I^{G}_{j,d,i,k}(n^{i}), (h^{G}_{d,i,k} - h^{sys}_{j}), \Delta x\right\} \quad (1)$$

where the correction is applied to all detectors/bands so:

j = A1, A2, AB, B, C and D

4.3.3.10 Responsivity scaling

Based on the temperature measured at the DTUs, each individual interferogram must be scaled to account for the current DPU detector absolute responsivity at time of measurement. This responsivity is a function of temperature and varies over the orbit.

Also, there may be an additional vector multiplication to account for the current gain setting at the PAW on various channels, in the event of gain switching during orbit. In the case that the DPU gain is switched once or more times per orbit on one or more channels, the data has to be correctly scaled based on the selected gain factors (and using a characterization table giving the actual gain values corresponding to the selected settings).

These two corrections are still TBC. See Section 5.2.2.4 of [RD 6] for more details.

It is assume that k_R and $k_{G,j}$ are constant wrt to *d*, *k* and *i*. The correction is a simple scalar multiplication per vector:

$$I'^{G}_{j,d,i}(n^i) = I^{G}_{j,d,i}(n^i) \cdot k_R \cdot k_{G,j} \tag{1}$$

4.3.3.11 Non-linearity correction

The non-linearity correction is applicable on the non-linear detectors of channels A1, A2, B1, and B2 only. There is a different correction for each non-linear detector. Correction is performed on each incoming interferograms after responsivity scaling.

The non-linearity correction is derived from characterization data and based on an indicator of the DC total photon flux φ_{DC} of the actual measurement, i.e. the minimum and maximum values of the digitized IGM by the ADC before filtering and decimation given as input with the incoming interferogram. The characterization data contains non-linear responsivity polynomial coefficients for each affected detectors. These coefficients are previously computed from readings of calibration blackbodies, according to the procedure described in [RD 2].

Since all measurements within a calibration group are equivalent, and therefore should be subject to the same non-linearity, the correction is performed on the coadded interferograms.

Knowing the minimum and maximum values of the digitized IGM by the ADC before filtering and decimation ($ADC^{Min}_{j,d,i} = \frac{1}{N^{ig}} \sum_k ADC^{Min}_{j,d,i,k}$ and $ADC^{Max}_{j,d,i} = \frac{1}{N^{ig}} \sum_k ADC^{Max}_{j,d,i,k}$) for the current measure, and the responsivity coefficients for the detector under consideration ($c_{q,j,d}$), the non-linearity correction can be computed directly on the interferogram, according to the procedure described in Section 4.9.4 for *j* = A1, A2, AB and B:

$$I'^{G}_{j,d,i}(n^i) = \mathrm{CorrectNL}\left\{I^{G}_{j,d,i}(n^i), ADC^{Min}_{j,d,i}, ADC^{Max}_{j,d,i}, c_{q,j,d}\right\} \tag{1}$$

4.3.3.12 Offset subtraction

Offset subtraction is also performed during gain determination in order to remove the contribution from the instrument. During gain determination, deep space and blackbody measurements are taken at the same resolution and the SPE makes sure that the points retained in undersampling are the same in both cases.

Offset subtraction is a simple point-by-point subtraction:

$$I_{j,d,i}^{gain}(n^i) = I_{j,d,i}^{bb}(n^i) - I_{j,d,i}^{dsg}(n^i) \quad (1)$$

4.3.3.13 Equalization and combination

For channel A1 and A2, the equalization must be performed since it was omitted on board because of the non-linearity problem. Combination allows an improvement of the signal-to-noise ratio.

The equalization is done only on one of the two detectors to be combined, using a convolution with proper coefficients. The combination is obtained by subtracting the A2 interferogram from the A1 interferogram.

The equalization and combination is computed on the gain interferogram, according to the procedure described in Section 4.9.5.2:

$$I'^{gain}_{j,d,i}(n^i) = \text{EqualizeCombine}\left\{ I_{j,d,i}^{gain}(n^i) \right\} \quad (1)$$

4.3.3.14 Zero-filling of interferogram

This subfunction performs the zero-filling of the interferograms in order to get a number of points corresponding to the smallest power of two greater than the initial number of points in the gain interferogram.

First, the number of points is computed as follows:

$$N_j^{G\max} = 2^{\text{Ceil}\left\{\log_2\left(N_j^{gain}\right)\right\}} \quad (1)$$

The new range of indices for the zero-filled gain interferograms is extended to:

$$n^a = -\frac{N_j^{G\max}}{2}, \ldots, \frac{N_j^{G\max}}{2} - 1$$

If N_j^{gain} is even then the interferogram becomes

$$I_{j,d,i}^{zf}(n^a) = \begin{cases} 0, & -N_j^{G\max}/2 \le n^a < -N_j^{gain}/2 \\ I_{j,d,i}^{gain}(n^a), & -N_j^{gain}/2 \le n^a < N_j^{gain}/2 \\ 0, & -N_j^{gain}/2 \le n^a < N_j^{G\max}/2 \end{cases} \quad (2)$$

and if N_j^{gain} is odd then it becomes

$$I_{j,d,i}^{zf}(n^a) = \begin{cases} 0, & -N_j^{G\max}/2 \le n^a < -\left(N_j^{gain}-1\right)/2 \\ I_{j,d,i}^{gain}(n^a), & -\left(N_j^{gain}-1\right)/2 \le n^a \le \left(N_j^{gain}-1\right)/2 \\ 0, & -\left(N_j^{gain}-1\right)/2 < n^a < N_j^{G\max}/2 \end{cases} \quad (3)$$

4.3.3.15 Calculate spectrally calibrated spectra

This subfunction performs the Fourier transform of the processed zero-filled interferograms. See Section 4.10.1 for more details about the numerical Fourier transform.

$$S_{j,d,i}^{gain}(m^a) = \mathrm{FFT}\left\{I_{j,d,i}^{zf}(n^a)\right\} \quad (1)$$

The radiometric vector is then unscrambled following the method described in Section 4.10.2. This operation is followed by the computation of the corresponding spectral axis. The corresponding spectral axis vector inferior limit $\sigma_{0j}^{G\max}$ is computed according to equation (4) of that same section. The definition of the spectral axis spacing can be expressed as:

$$\Delta\sigma_j^{G\max} = \frac{1}{N_j^{G\max}\Delta x_j^{dec}} \quad (2)$$

The spectral axis is then calibrated by a multiplication by the current spectral calibration correction factor k_{SC}. If no spectral calibration is available yet, this correction factor is taken as unity.

$$\Delta\sigma_j^{G\max} = \Delta\sigma_j^{G\max} \times k_{SC} \quad (3)$$

$$\sigma_{0j}^{G\max} = \sigma_{0j}^{G\max} \times k_{SC} \quad (4)$$

Unscrambling is finally performed with the purpose of re-ordering spectra computed from decimated interferograms. In addition to this stretching of the spectral axis, an inverse stretching must be applied on the radiometric scale to ensure the conservation of energy in the signal:

$$S'^{gain}_{j,d,i}(m^a) = S_{j,d,i}^{gain}(m^a)/k_{SC} \quad (5)$$

4.3.3.16 Spectral interpolation

Interpolation of the gain spectral vector is required for two reasons. First, the resolution setting for gain measurements may be different than that used for scene measurements. Second, the spectral axis corresponding to the actual gain measurement shall be as defined by the latest spectral calibration. However, because of the specification on the spectral stability, this spectral calibration may vary significantly until the next scene measurement. So, interpolation is also needed to have the spectral axis of the gain matching the one of the scene.

On the other hand, it will likely be necessary to produce the final calibrated spectra with some pre-defined (requested by the user) spectral axis. Thus we will choose to always interpolate the gain to this user-defined spectral axis. The scene spectra will also be interpolated to the same spectral axis.

Note that as the gain to be interpolated is a smooth function, small N^{si} and N^{psi} parameters could be used to speed up the computation, or a simple linear interpolation between points could also be used instead. See Section 4.9.2 and 4.10.5 for more details about interpolation.

The spectral calibration valid for the *actual* scene measurement is described by $\Delta\sigma_j^{G\max}$, $\sigma_{0j}^{G\max}$, and $N_j^{G\max}$, while the *requested* spectral axis definition is defined by $\Delta\sigma_j^{req}$, σ_{0j}^{req}, and N_j^{req} (see Section 4.3.4.1).

We want to interpolate the calculated spectra according to the *requested* spectral axis definition:

$$S'^{gain}_{j,d,i}(m^r) = \text{Interpolate}\left\{S^{gain}_{j,d,i}(m^a);\ \Delta\sigma_j^{G\max}, \sigma_{0_j}^{G\max}, N_j^{G\max} \rightarrow \Delta\sigma_j^{req}, \sigma_{0_j}^{req}, N_j^{req}\right\} \qquad (1)$$

with the procedure described at Section 4.9.2 according to the *Sinc Interpolation Method*.

The range of data points index is defined by the requested spectral parameters.

4.3.3.17 Blackbody radiance calculation

This operation is the evaluation, at all relevant wavenumbers, of the on-board blackbody spectral radiance corresponding to its temperature readings. It should be pointed out that it is necessary to use a spectral calibration with enough accuracy to avoid the introduction of radiometric error.

The spectral radiance of an ideal blackbody is defined by the Plank function. However, the spectral radiance of a realistic blackbody is complicated by the fact that emissivity will be lower than one and will exhibit a spectral behavior. Furthermore, non-uniformity of the cavity introduces an additional dependence on the actual throughput seen by the instrument. For these reasons, the blackbody radiance will be characterized as a function of temperature readings and wavenumber. Consult Section 6.2 of [RD 8] for more details about blackbody radiance calculation.

The spectral radiance of the blackbody is given by:

$$L_{j,d,i}(m^r) = R_{BB}(\sigma_j(m^r)) \quad (1)$$

The blackbody radiance R_{BB} is function of environment temperature and on individual CBB element temperatures. Each temperature is given by polynomial expansions derived from PRT calibrations. The equations to convert the PRT values from ADC counts into actual temperatures [K] can be found in load data section.

The environmental temperature, T_{env}, will be calculated from a weighted combination of FEO temperature measurements. Analysis has established that the temperature of the CBA environment is strongly influenced by three sources: the Aft Baffle, the ASU housing & the shield. The auxiliary data contains a set of thermistor values, of which several are placed within the FEO, including two on the Aft Baffle (+X and -X faces) and one on the ASU housing. No thermistor is placed upon the shield, but thermal analysis shows that the mean shield temperature can be approximated by simply using the value measured by the ASU housing thermistor (as the temperatures of these two items are within five degrees of each other even in the worst case).

4.3.3.18 Radiometric accuracy

This subfunction allow a radiometric data validation based on accumulated statistics. These statistics are computed with incoming readings from the internal reference blackbody and also from readings from the deep space.

The radiometric accuracy *A* vector is computed (on a reduced grid) as the difference between the assigned spectral radiance and the true spectral radiance on single gain measurements (see [RD 11]), sequentially summed on each group in the following manner:

$$A_{j,d}(m^u) = \frac{1}{N^{gg}} \sum_{i=1}^{i=N^{gg}} \mathrm{Re}\left\{ S^{gain}_{j,d,i}(m^u \cdot u) \cdot G^{prev}_{j,d}(m^u \cdot u) \right\} - L_{j,d,i}(m^u \cdot u) \quad (1)$$

where the notation "*prev*" indicates the value refers to the previous gain, i.e. the value $G_{j,d}$ obtained during previous gain calibration pass.

The $G^{prev}_{j,d,i}$ must be corrected to match the same fringe count than the current coadded gain $S^{gain}_{j,d,i}$, with a procedure similar to the one presented in Section 4.2.3.8.

For each gain calibration pass (numbered ℓ = 1, 2, 3, ...), two vectors $\langle A_{j,d}(m^u) \rangle$ and $NRMS_{j,d}(m^u)$ are accumulated. The mean and the standard deviation can be recursively computed in a way to avoid storing all intermediate values in memory (this could lead to a huge table).

The mean computed can be expressed as a function of the previous mean, in the following way (for any value of ℓ):

$$\langle A_{j,d}(m^u)\rangle = \frac{(\ell-1)\langle A_{j,d}^{prev}(m^u)\rangle + A_{j,d}(m^u)}{\ell} \quad (2)$$

The standard deviation computed can be expressed as a function of the previous mean and the previous standard deviation, in the following way:

$$\text{if } \ell = 1: \qquad NRMS_{j,d}(m^u) = 0 \quad (3)$$

else

$$NRMS_{j,d}(m^u) = \sqrt{\frac{\left(A_{j,d}(m^u)\right)^2 + (\ell-2)\left(NRMS_{j,d}^{prev}(m^u)\right)^2 + (\ell-1)\langle A_{j,d}^{prev}(m^u)\rangle^2 - \ell\langle A_{j,d}(m^u)\rangle^2}{\ell-1}} \quad (4)$$

Before inserting the value of $A_{j,d}(m^u)$ in the running mean $\langle A_{j,d}(m^u)\rangle$ and into the $NRMS_{j,d}(m^u)$ vector, its validity must be first checked the following way:

$$\text{if} \quad \left| A_{j,d}(m^u) - \langle A_{j,d}^{prev}(m^u)\rangle \right| > s_{RACC}^{\text{thres}} \cdot NRMS_{j,d}^{prev}(m^u) \quad (5)$$

then there is a chance that $A_{j,d}(m^r)$ comes from erroneous data.

else $\langle A_{j,d}(m^u)\rangle$ and $NRMS_{j,d}(m^u)$ are updated as described previously.

s_{RACC}^{thres} is a standard deviation threshold previously defined.

The particular value $A_{j,d}(m^u)$ may be outside the pre-defined limits (fixed by s_{RACC}^{thres}), but still be statistically valid. To avoid biasing results by systematically removing larger deviations, a rejection should be based on the whole vector $A_{j,d}$. This way, if more than t_{RACC}% of the values of $A_{j,d}$ exceed the pre-defined deviation s_{RACC}^{thres}, a flag is raised indicating a probable error or invalidity of the currently processed data. On the other hand, if less than t_{RACC}% of the vector is suspect, the processing could resume its normal way, taking the deviation as statistically correct.

It will be needed to consider the possibility to interrupt the accumulation of statistics and to reset both vectors to zero. Indeed, because of the expected inherent drifts of the noise, it would be preferable to perform periodic resets of statistics at appropriate time intervals.

The flag is provided in the data product. $\langle A_{j,d}(m^u)\rangle$ and $NRMS_{j,d}(m^u)$ are kept with calibrated data and referred in the data product.

4.3.3.19 Ratio

The ratio subfunction consists in a straightforward division, for each spectral data point, of two complex numbers: the theoretical blackbody radiance and the calculated spectrum. The two spectral vectors share the same spectral axis definition, namely the one requested for the output spectra.

The radiometric gain is obtained by the ratio of the spectral power to the observed spectrum

$$G_{j,d,i}(m^r) = \frac{L_{j,d,i}(m^r)}{S^{gain}_{j,d,i}(m^r)} \quad (1)$$

4.3.3.20 Gain coaddition

It is a simple coaddition of spectral vectors done independently for each sweep direction.

Coaddition of gain from different groups is done according to:

$$G_{j,d}(m^r) = \frac{1}{N^{gg}} \sum_{i=1}^{N^{gg}} G_{j,d,i}(m^r) \quad (1)$$

As it is apparent from the indices, we get one gain vector for each band and for each sweep direction, defined on wavenumber values corresponding to the requested spectral axis. The current baseline is N^{gg} = 1 of N^{ig} = 300 bb interferograms. In case of more than one group with different number of bb interferograms, weighting should be done.

4.3.4 Computational sequence

The *Calculate Gain Calibration* function receives control from the Load Data function when gain calibration data have been found. The *Calculate Gain Calibration* function processes this data and sends control back to the Load Data function.

The output, i.e. a gain calibration, is generated only when all measurements of deep space and blackbody for forward and reverse sweeps for all groups of the gain calibration sequence have been processed. The new gain calibration file replaces the old one. The old file is delivered as an output of the ground processing.

The computational sequence is illustrated by the flowchart of Figure 4.3.4-1 (extending on the following pages).

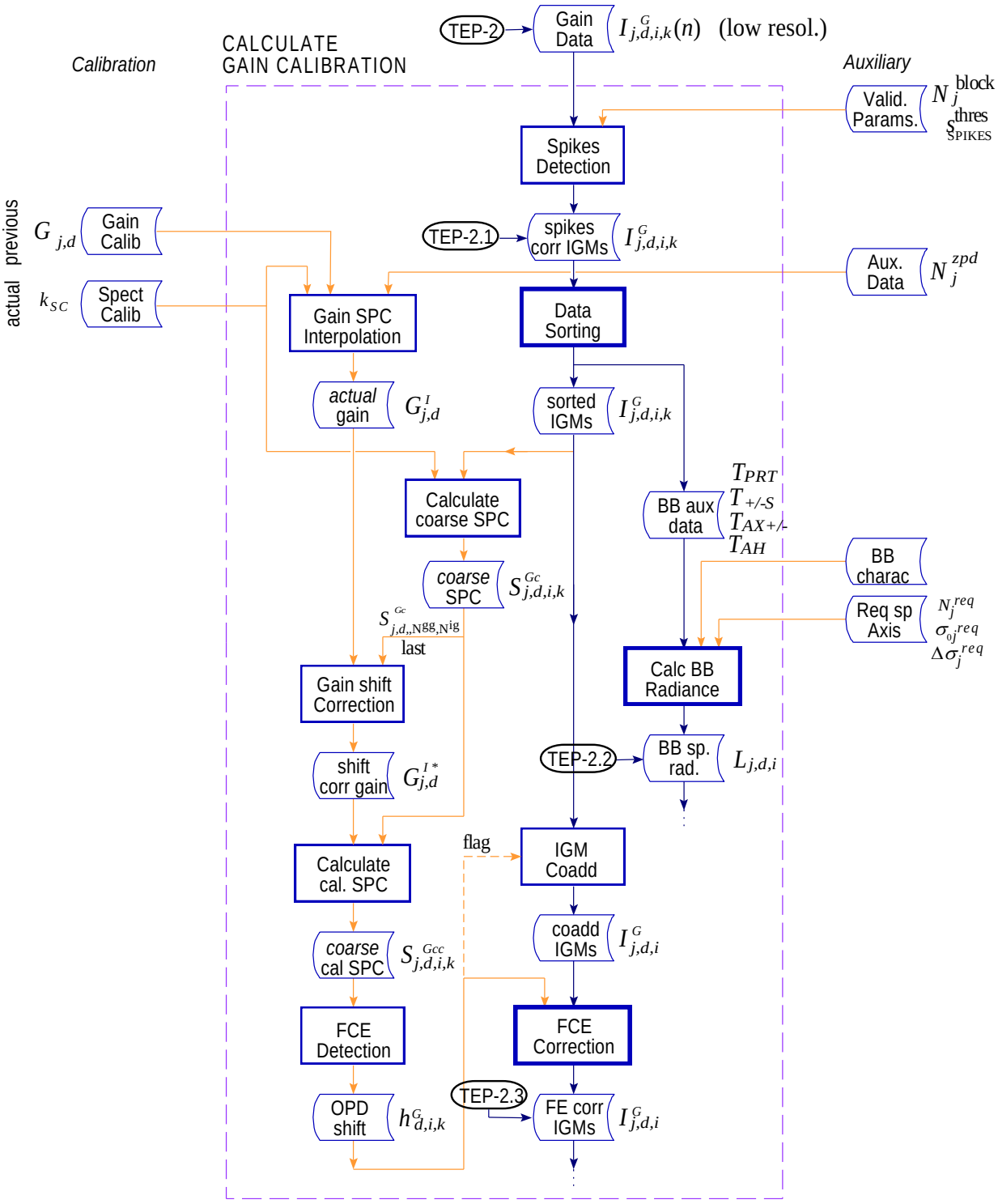

Figure 4.3.4-1 *Calculate Gain Calibration* flowchart (*first part*)

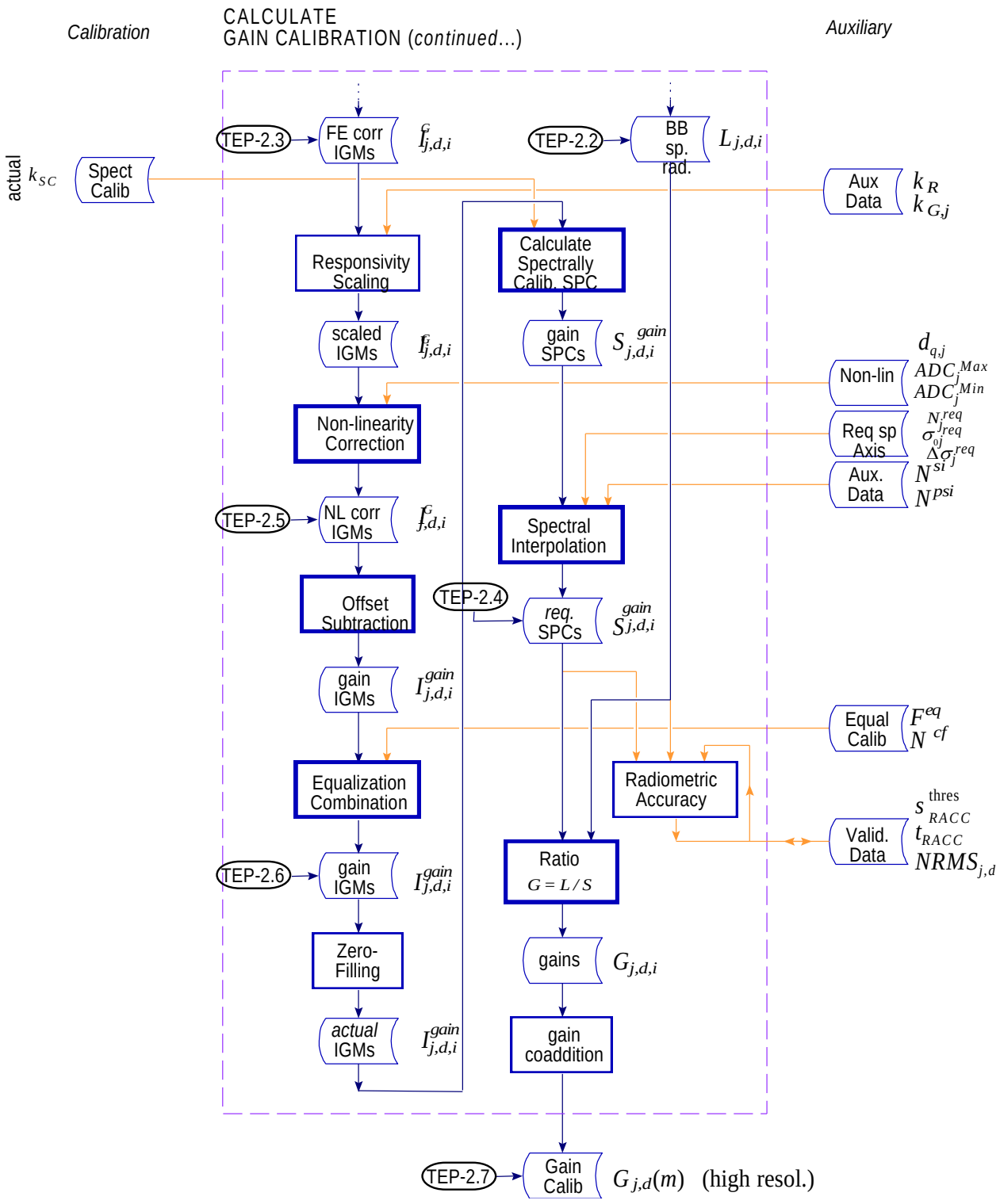

Figure 4.3.4-1 *Calculate Gain Calibration* flowchart (*second part*)

4.4 CALCULATE SPECTRAL CALIBRATION

This Section describes the *Calculate Spectral Calibration* function that performs the necessary processing of spectra that have been radiometrically calibrated previously, in order to generate a spectral calibration, i.e. a definition of the spectral axis corresponding to actual measurements. See Section 3.5 from the present document for more details about the spectral calibration scenario. The data flowchart of this function is provided in Figure 4.4.4-1.

Spectral calibration has been studied extensively in the technical note [RD 4]. The principle is to locate one or several known spectral lines in each band of the experimental spectrum (already corrected for the Doppler effect by the *Calculate Radiance* function) and assign the corresponding exact theoretical wavenumbers to their positions.

Two algorithms have been proposed and studied: the *Peak Finding Method* (PFM) and the *Cross-Correlation Method* (CCM). The feasibility of both these methods have been demonstrated in the technical note, and both algorithms have demonstrated strengths and weaknesses. The PFM have shown to be a little simpler to implement and faster to execute, but the CCM presents the advantage of giving information related to the precision of a given fit. Both algorithms are presented here, but the baseline is taken as the PFM algorithm.

Appropriate peaks for spectral calibration that represent known features of standard scene measurements have been identified and studied in the document [RD 4]. The present algorithm is supposed to work on such or equivalent spectral lines. The precision of the peak identification algorithm is proportional to the number of equivalent scenes that are coadded, as the noise affecting the signal decreases when multiple readings are superposed. This number will probably vary between 1 and 5 (to attain stability and a precision equal or less than 0.001 cm^{-1} [RD 12]), and will be defined in auxiliary data. We suppose for the present algorithm that two scenes per peak are used for each spectral calibration.

Topics of the frequency at which the instrument calibration shall be done and the necessity for calibration in the different bands are not addressed here.

Spectral calibration will be performed such that the latest available valid spectral measurement is used until a new valid spectral measurement becomes available. If in the middle of the input stream invalid spectral calibration are calculated, then a 'previous closest in time strategy' shall be applied, which means that complete scans shall be calibrated with the previous valid spectral calibration. If no valid spectral calibration at all is available, then the spectral calibration data contained in the current ILS and spectral calibration file shall be used. Spectral calibration data shall be written to auxiliary file simultaneously with ILS retrieved data (see section 4.6). Otherwise the file shall not be modified by the processor.

4.4.1 Objective

The main objectives of the *Calculate Spectral Calibration* function are

- Analyze several typical scene spectra to locate individual reference peaks of well defined wavenumber.
- Find the position of the peaks.
- Define and assign spectral axis parameters for each band.

It is important to mention first the assumptions on the format of the spectral calibration that are used in the definition of the other function of the present document. These assumptions are:

- The spectral calibration for a given measurement consists in the suitable definition of the spectral axis for each band.

- The spectral axis of a given band is defined by the following parameters

  $\Delta\sigma_j$ the spacing between spectral data points in the band
  σ_{0j} the starting wavenumber of the band
  N_j^{req} the number of points in the band
  k_{SC} the spectral calibration correction factor

  With these parameters and the index of points *m*, the numerical vector can be generated according to the following formula:

$$\sigma = \sigma_{0j} + m \cdot \Delta\sigma_j \tag{1}$$

- If the CCM method is used, the number of points must be a power of two because of the FFTs involved; otherwise there is no restriction on the number of points in the spectral axis definition or the PFM method.

4.4.2 Definition of variables

Calculate Spectral Calibration

Variable	Descriptive Name	I/O	Type	Ranges / References / Remarks
	Global variables & indices			
N_j^{req}	Number of points in band *j* for the requested spectral axis	a	i	MIP_PS1_AX(7)
m^r	Numerical index of points in vector	l	i	$m^r = 0,\ldots,N_j^{req}-1$
$N^{\mu w}$	Number of points in the μw	t	r	= 1024
m^w	Numerical index data points in the μw	l	i	$m^w = 0,\ldots,N^{\mu w}-1$
n	Index of line	l	i	$n = 1,\ldots,N^{\text{lines}}$
$\Delta\sigma_j^{req}$	Spacing between spectral data points in the band	t	r	Computed with MIP_PS1_AX(7, 8, 9)
σ_{0j}^{req}	Starting wavenumber of the band	a	r	MIP_PS1_AX(8)
$\Delta\sigma_n^{\mu w}$	Spacing between spectral data points in the μw	t	r	
$\sigma_{l_n}^{\mu w}$	Starting wavenumber of the μw containing line *n*	a	r	MIP_MW1_AX(8)
$\sigma_{r_n}^{\mu w}$	Ending wavenumber of the μw containing line *n*	a	r	MIP_MW1_AX(9)
CM	Calibration method, PFM or CCM	a	r	MIP_PS1_AX(43)
4.4.3.1	*Selection of microwindows*			
s	Index of elevation scans	l	i	$s = 1,\ldots,N_n^{coadd}$
N^{lines}	Number of spectral lines to be identified Number fitted	a o	i	Equal to number of μw to be used during spectral calibration in file MIP_MW1_AX MIP_CS1_AX(4.6)
N_n^{coadd}	Number of equivalent scenes that must be coadded for line *n* Number coadded	a o	i	Practical values are $1 \le N_n^{coadd} \le 10$ MIP_PS1_AX(39.8) MIP_CS1_AX(4.12)
$S_{j,s}^{cal}(m^r)$	Radiometrically and spectrally calibrated input spectrum band *j* and elevation *s*	i	r	Input from *Calculate Radiance* function
$S_j^{coadd}(m^r)$	Coadded spectrum band *j*	t	r	
$S_n^{\mu w}(m^w)$	Working spectral μw for line *n*	t	r	
4.4.3.2	*Fit Peak*			
$E_{n,k}$	Sum of square residuals	t	r	local to Simplex routine
$g_D(\sigma)$	Gaussian profile model	t	r	

Variable	Descriptive Name	I/O	Type	Ranges / References / Remarks
$g_L(\sigma)$	Lorentzian profile model	t	r	
$g_S(\sigma)$	Sinc profile model	t	r	
Simp^{tol}	Simplex convergence tolerance	a	r	Set to about 1×10^{-6} to 1×10^{-8} MIP_PS1_AX(40)
$\text{Simp}^{\text{itermax}}$	Maximum number of iterations for the simplex	a	i	Set to about 1000 MIP_PS1_AX(41)
k	Simplex iteration index	l	i	$k = 0,\ldots, N_n^{\text{iter}}$
N_n^{iter}	Number of Simplex iterations done to reach convergence tolerance for line *n*	t	i	typically $N^{\text{iter}} < 1000$
σ_n^c	Final peak center computed position for line *n*	t	r	
R_n^2	Coefficient of correlation for the fit for line *n*	o	r	computed value: $R_n^2 \le 1$ MIP_CS1_AX(4.11)
R_{min}^2	Threshold of validity for R_n^2	a	r	Set to about 0.5 MIP_MW1_AX(15)
$P(n)$	Computed positions for each reference peaks	t	r	Dimension of table is N^{lines} elements
4.4.3.3	*Generation of reference SPC*			
$S_j^T(m^w)$	Theoretical spectral μw	t	r	
4.4.3.4	*Cross-correlation*			
$C(m^w)$	Cross-correlation vector	t	r	
4.4.3.5	*Spectral axis definition*			
k_{SC}^{i-1}	Previous spectral calibration correction factor	i	r	MIP_CS1_AX(4.3)
σ_n^{ref}	Reference known position of theoretical line	a o	r	MIP_MW1_AX(7) MIP_CS1_AX(4.9)
k_{SC}^i	Spectral calibration correction factor	o	r	Final output of *Compute Spectral Calibration* MIP_CS1_AX(4.3)
s_{SC}^i	Standard deviation indicator	o	r	MIP_CS1_AX(4.4)
$\sigma_n^{ref} - \sigma_n^c$	Detected frequency shift	o	r	MIP_CS1_AX(4.10)
$s_{StdRatio}^{\text{thres}}$	Standard deviation threshold	a	r	MIP_PS1_AX(42)
A_{SC}^i	Spectral calibration correction factor 1st quadratic term	o	r	MIP_CS1_AX(4.5)
B_{SC}^i	Spectral calibration correction factor 2nd quadratic term	o	r	MIP_CS1_AX(4.5)
C_{SC}^i	Spectral calibration correction factor 3rd quadratic term	o	r	MIP_CS1_AX(4.5)

4.4.3 Detailed structure and formulas

4.4.3.1 Selection of microwindows

This subfunction extracts one (or more) spectral line(s) located in portions of the observed spectrum, defined on a pre-calibrated spectral scale, according to the extremities of specific microwindows listed in a reference lines database. This subfunction also performs the coaddition of equivalent scene measurements before sending the result to the *Find peak* subfunction.

This subfunction selects pre-defined portions of the observed pre-calibrated spectrum that contain reference lines, as defined in an auxiliary database (see Table 4.4.3-1). If no line can be identified, because no one correspond to the current altitude for example, the subfunction gives back control to the main processing flow and waits for another pass.

In the database are stored N^{lines} reference lines with their natural characteristics and the associated microwindow details. An example corresponding to a given line would be following this structure:

Microwindow ID :	"17-Ozone O_3"
Peak position [cm^{-1}] :	1884.563300
Peak height [r.u.] :	6×10^{-8}
Peak width [cm^{-1}] :	0.025
Microwindow left position [cm^{-1}] :	1884.0
Microwindow right position [cm^{-1}] :	1885.0
Measurement altitude [km] :	50
Mathematical model [1–3] :	1
Number of necessary coadditions :	5
Validity threshold [0–1] :	0.9

Table 4.4.3-1 Structure for the identification of reference lines

Microwindow ID identifies the line number and the name of the gas. Peak position gives the exact known theoretical position of the line and the peak height gives the expected strength of the line in radiance units. The peak width gives the approximate half width at half maximum of the natural line *widened by the ILS*, as it would be seen by the instrument. Microwindow left and right positions specify the lower and upper wavenumber between which the line is centered (the width is about one cm^{-1}). Measurement altitude specify the height at which the line can be used (± 3 km). The appropriate mathematical profile defines the equation best suited to fit the line. The number of coadditions indicates the number of scene coadditions necessary to perform before sending the observed line to the peak fitting subfunction. Finally, a validity threshold defines the minimal value of the correlation coefficient that would lead to a valid fit. Some of those previous values can be taken from atmospheric databases, like the HITRAN one used for this example.

The minimal case would consist of only one reference peak present in any one of the bands covered by the MIPAS detectors (N^{lines}=1). But the more reference lines can be identified, more precise the method will be. A practical case would consist of at least one reference peak in each band. The exact number of reference lines required in each band is still TBD, but it can be taken as one for the current baseline.

In order to reduce noise, N_n^{coadd} equivalent scenes are coadded, i.e., scenes with altitude included in the range (MIP_PS1_AX(39.6)) for the last number of elevation scans (MIP_PS1_AX(39.4)) specified in the processing parameter file. The band *j* is the one that contains the microwindow *n*.

$$S_j^{coadd}(m^r) = \frac{1}{N_n^{coadd}} \sum_{s=1}^{N_n^{coadd}} S_{j,s}^{cal}(m^r) \tag{1}$$

The extraction of microwindows from the spectrum is done according to the extremities of the microwindow defined in the database. The spectral points that are microwindow members are transferred in a working spectral vector $S_n^{\mu w}(m^w)$.

$$S_n^{\mu w}(m^w) = \text{ Interpolate } \left\{ S_j^{coadd}(m^r); \Delta\sigma_j^{req}, \sigma_{0j}^{req}, N_j^{req} \rightarrow \Delta\sigma_n^{\mu w}, \sigma_{l_n}^{\mu w}, N^{\mu w} \right\} \tag{2}$$

with the procedure described at Section 4.9.2 according to the *Sinc Interpolation Method*.

The range of data points index of the microwindow is defined by:

$$m^w = 0, \ldots, N^{\mu w} - 1$$

The spacing between spectral data points is equal to:

$$\Delta\sigma_n^{\mu w} = \frac{\sigma_{r_n}^{\mu w} - \sigma_{l_n}^{\mu w}}{N^{\mu w} - 1}$$

And, the total number of points $N^{\mu w}$ is fixed (1024) and is a power of two. Finally, this vector is sent to the next processing step.

4.4.3.2 Fit peak

This subfunction consists in the determination of the position of the incoming selected spectral line. The peak fitting algorithm proceeds by the minimization of the sum of square residuals between a parametric mathematical function and the actual spectrum data. Initial guesses are supplied to the mathematical function and a Simplex algorithm iterates on these parameters until a minimum is reached. Note that initial guesses must be different than 0. The final peak position is given by the horizontal position parameter *b*. A more detailed description of the Simplex algorithm and its implementation can be found in appendix A.

The error function to be minimized by the Simplex is:

$$E_{n,k} \leftarrow \sum_{m^w=0}^{N^{\mu w}-1} \left[f(\sigma(m^w),\, params_k) - S_n^{\mu w}(m^w) \right]^2 \tag{1}$$

$$\text{with} \qquad \sigma(m^w) = \sigma_{l_n}^{\mu w} + m^w \cdot \Delta\sigma_n^{\mu w}$$

and where $params_k$ are a set of input parameters that characterize the theoretical model at Simplex iteration k. These parameters must be initialized with approximate values computed from initial spectral line.

The initial guesses can be found with the help of the fit peak subfunction described in Section 4.9.6:

$$params_0 = a_0, b_0, c_0, d_0 \leftarrow \text{FitPeak}\left\{ S_n^{\mu w}(m^w),\, \sigma_{l_n}^{\mu w},\, \Delta\sigma_n^{\mu w},\, N^{\mu w} \right\} \tag{2}$$

The three different mathematical models $f(\sigma, params = a, b, c, d)$ used for the fitting are given below, numbered 1 to 3. For each of these models, a represents the radiance, b the spectral position, c the HWHM of the central peak, and d the DC offset of the signal:

1) The *Gaussian profile*:
$$g_D(\sigma) = a\, e^{-\left(\frac{\sigma - b}{c}\right)^2 \ln(2)} + d \tag{3}$$

2) The *Lorentzian profile*:
$$g_L(\sigma) = \frac{a}{\left(\frac{\sigma - b}{c}\right)^2 + 1} + d \tag{4}$$

3) The *Sinc profile*:
$$g_S(\sigma) = a\,\text{sinc}\left(\frac{\sigma - b}{c\,\gamma}\right) + d \quad (\gamma = 0.52756688184) \tag{5}$$

The Simplex algorithm is performed until a predefined tolerance Simp^{tol} is reached on the residual values. If a maximum number of iterations is reached, expressed as:

$$N_n^{\text{iter}} > \text{Simp}^{\text{itermax}}$$

then the algorithm is stopped and an error is dispatched.

The result of the *Fit Peak* is the value of parameter b_k at final simplex iteration $k = N^{\text{iter}}$, that gives the sought wavenumber position σ_n^c of the peak.

$$\sigma_n^c = b_{N_n^{\text{iter}}} \tag{6}$$

After a fit has been computed, a statistical test can be performed to check for the validity of the operation. The coefficient of correlation that characterizes the goodness of the fit is defined as follows:

$$R_n^2 = 1 - \frac{E_{n,N_n^{\text{iter}}}}{\sum_{m^w=0}^{N^{\mu w}-1} \left(S_n^{\mu w}(m^w)\right)^2} \tag{7}$$

This number indicates a perfect fit when $R_n^2 = 1$, while $R_n^2 = 0$ means that the data is completely uncorrelated (negative values indicate an anti-correlation trend but should never occur). For an appropriate fit, the value of R_n^2 shall be higher than $R_{\min}^2$ (set at about 0.5). If the value computed is less than $R_{\min}^2$, the fit should be rejected.

Finally, a vector $P(n)$ is accumulated with the numerically found positions σ_n^c corresponding to each identified peak. The index n covers to reference lines corresponding in each row of Table 4.4.4-1.

$$n = 1, \ldots, N^{\text{lines}} \tag{8}$$

Note: The exact values of Simp^{tol}, $\text{Simp}^{\text{itermax}}$, $R_{\min}^2$, will have to be fine tuned based on actual operating spectra given by the instrument. The initial values suggested in the table of Section 4.4.2 may be subject to adjustments.

4.4.3.3 Generation of reference SPC

This subfunction is used by the CCM to generate a theoretical spectrum simulation of the same spectral line(s) as the ones(s) present in the measured spectrum and adjust resolution and width of window to be numerically compatible.

The exact procedure for the generation of a reference spectrum is TBC. The closest the theoretical spectrum will be with respect to the actual scene, the more precise will be the determination of the peak position. The simplest approach is to build a theoretical spectrum containing only the reference line defined according to the different parameters contained in Table 4.4.3-1 and the mathematical equations for the different types of lines ($g_D(\sigma)$, or $g_L(\sigma)$, or $g_S(\sigma)$ given previously).

$$S_n^T(m^w) = g_{D/L/S}(\sigma_{l_n}^{\mu w} + m^w \cdot \Delta\sigma_n^{\mu w}) \tag{1}$$

4.4.3.4 Cross-correlation

This subfunction is used by the CCM to cross-correlate the theoretical spectrum with the experimental one. The cross-correlation is performed by means of FFTs on real data (a factor of two in computing time can be saved by taking this fact into account). A reversal of one of the two vectors must be performed in order to calculate a correlation instead of a convolution.

$$C(m^w) = \mathrm{IFFT}\{\ \mathrm{FFT}\{S_n^{\mu w}(m^w)\} \cdot \mathrm{FFT}\{\mathrm{Reverse}\{S_n^T(m^w)\}\}\ \} \tag{1}$$

After the computation of the cross-correlation, the peak finding algorithm (or another equivalent algorithm) is performed on the resulting distribution with the same steps as described before.

4.4.3.5 Spectral axis definition

This subfunction calculates the basic parameters defining the spectral axis for each band, based on the computed peaks position. The basic parameters are the lower wavenumber, the spectral spacing between data points, and the number of data points. The scaling factor computed is also given as one of the spectral calibration parameters.

Once the position of a selected experimental peak is known up to a given precision σ_n^c, the ratio k_{SC} between the reference and the computed position is computed, with a mean taken over each considered reference lines (with valid fit):

$$k_{SC}^i = \frac{k_{SC}^{i-1}}{N^{\mathrm{lines}}} \sum_{n=1}^{N^{\mathrm{lines}}} \frac{\sigma_n^{\mathrm{ref}}}{\sigma_n^c} \tag{1}$$

The reference position σ_n^{ref} is known from the first column of Table 4.4.3-1 at line *n*.

The operation of taking the mean for each peak shift is based on the assumption that the shift is linear as a function of wavenumber (this has been shown to be the case; see Section 6.3.3.3 of [RD 13]). This way, the extrapolated origin of the experimental spectrum is correct (at 0 cm^{-1}), so that a simple linear correction by the multiplication of a constant can be applied.

If the distribution appears to be non-linear, a quadratic polynomial fit (with zero origin) could be performed in order to correctly evaluate the amount of stretch of the spectral axis as a function of the wavenumber.

$$y_n = A_{SC}^i + B_{SC}^i \times x_n + C_{SC}^i \times x_n^2 \tag{1a}$$

where

$$y_n = \sigma_n^{\mathrm{ref}} \times k_{SC}^{i-1} \tag{1b}$$

and

$$x_n = \sigma_n^{\mathrm{c}} \tag{1c}$$

$$A_{SC}^{i}, B_{SC}^{i}, C_{SC}^{i} \leftarrow \mathrm{PolyFit}\left\{y_n, x_n, N^{\mathrm{lines}}, 2\right\} \tag{1d}$$

Finally, global spectral correction can be applied to all bands according to the following relation:

$$\sigma'_{0j} = \sigma_{0j} \times k_{SC}^{i} \tag{2}$$

$$\Delta\sigma'_{j} = \Delta\sigma_{j} \times k_{SC}^{i} \tag{3}$$

In order to have a quality indicator of the estimated spectral correction factor k_{SC}^{i}, its standard deviation is computed.

$$s_{SC}^{i} = \sqrt{\frac{1}{N^{\mathrm{lines}} - 1} \sum_{n=1}^{N^{\mathrm{lines}}} \left(\frac{k_{SC}^{i-1} \cdot \sigma_n^{\mathrm{ref}}}{\sigma_n^{c}} - k_{SC}^{i} \right)^2} \tag{4}$$

The validity of the estimated spectral correction factor is checked the following way:

$$\text{if} \quad s_{SC}^{i} > s_{StdRatio}^{\mathrm{thres}} \tag{5}$$

then there is a chance that k_{SC}^{i} comes from erroneous data.

else k_{SC}^{i} becomes the new spectral correction factor.

$s_{StdRatio}^{\mathrm{thres}}$ is a standard deviation threshold previously defined.

4.4.4 Computational sequence

The *Calculate Spectral Calibration* function receives control from the main program when it is appropriate to update the spectral calibration. It will use a certain number of radiometrically calibrated scene spectra.

The *Calculate Spectral Calibration* function processes these spectra and generate a new spectral calibration. The new calibration replaces the old one. The old spectral calibration is delivered as an output of the ground processing.

The computational sequence is illustrated by the flowchart of Figure 4.4.4-1. The present baseline for spectral calibration is to use the PFM method. The CCM is drawn in parallel to identify the other optional algorithm.

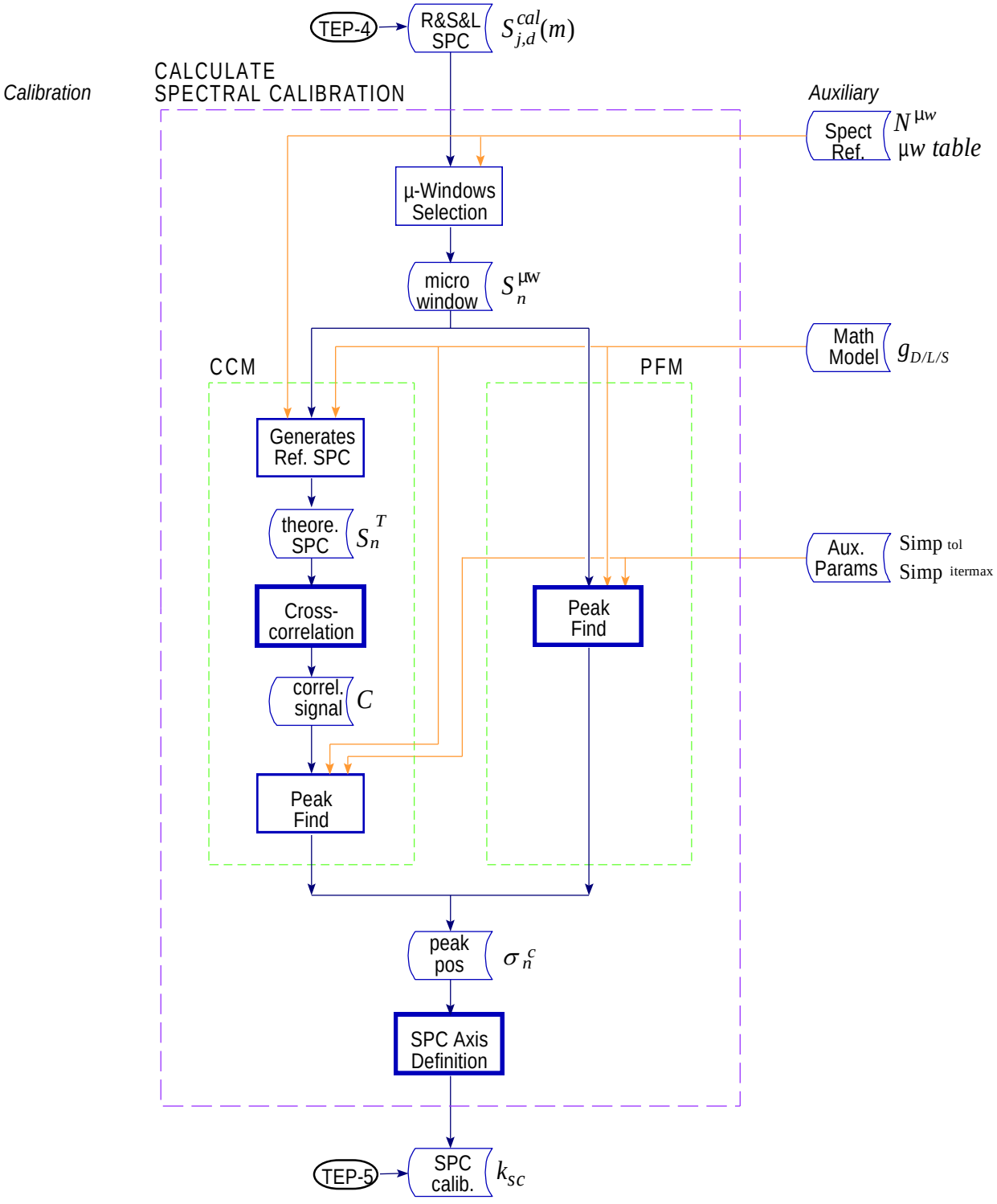

Figure 4.4.4-1 *Calculate Spectral Calibration* flowchart

4.5 CALCULATE RADIANCE

This Section describes the *Calculate Radiance* function that performs the processing of the scene measurements in order to generate a radiometrically calibrated spectrum. The data flowchart of this function is provided in Figure 4.5.4-1.

4.5.1 Objective

The main objective of the *Calculate Radiance* function is to transform each scene measurement into a radiometrically calibrated spectrum.

Specific objectives of the function are:

- Detect fringe count errors in spectral bands B and C, and in the case of misalignment adjust the phase of the gain and offset according to the current fringe count.
- Correct scene measurements for non-linearity of each affected detector.
- Equalize and combine interferograms in band A.
- Subtract offset due to contribution of the instrument.
- Compute spectra using a FFT algorithm applied on the interferograms.
- Correct spectral axis for Doppler shift and perform spectral interpolation onto a predefined uniform spectral axis.
- Radiometric calibration by a complex multiplication of the actual scene spectrum with the actual gain.
- Perform scene measurement quality verification.

4.5.2 Definition of variables

Calculate Radiance

Variable	Descriptive Name	I/O	Type	Ranges / References / Remarks
	Global variables & indices			
N_j^{sc}	Number of points in a scene interferogram	i	i	input from *Load Data* function.
$N_j^{\max}$	Number of points in band *j* for the spectral calibration of the actual scene measurement	t	i	Computed from number of input points (next power of 2)
N_j^{zpd}	Number of points in the ZPD region of band *j*	a	i	MIP_PS1_AX(13)
N_j^{req}	Number of points in band *j* for the requested spectral axis	a	i	MIP_PS1_AX(7)
j	Channel/band index number	l	i	*j* = A1, A2, A, AB, B, C, D
d	Index for sweep direction	l	i	0 = forward, 1 = reverse
n^i	*input* IGM data point index	l	i	
m^r	*requested* SPC data point index	l	i	$m^r = 0,\ldots,N_j^{req}-1$
n^c	*coarse* IGM data point index	l	i	$n^c = -N_j^{zpd}/2,...,N_j^{zpd}/2-1$
m^c	*coarse* SPC data point index	l	i	$m^c = 0,\ldots,N_j^{zpd}-1$
n^a	*actual* IGM data point index	l	i	$n^a = -N_j^{\max}/2,...,N_j^{\max}/2-1$
m^a	*actual* SPC data point index	l	i	$m^a = 0,\ldots,N_j^{\max}-1$
$\Delta\sigma_j^{sccc}$	Wavenumber spacing in band *j* of calibrated coarse spectrum	t	r	calibrated with correction factor
σ_{0j}^{sccc}	Starting wavenumber in band *j* of calibrated coarse spectrum	t	r	calibrated with correction factor
σ_L	Nominal laser wavenumber	a	r	For the MIPAS instrument = 7606 cm^{-1} MIP_PS1_AX(4)
4.5.3.1	*Spikes detection*			
$I_{j,d}^{sc}(n^i)$	IGM scene measurement	i	c	input from *Load Data* function
4.5.3.2	*Gain spectral interpolation*			
$\Delta\sigma_j^{req}$	Wavenumber spacing in band *j* for the requested spectral axis	a	r	Computed with MIP_PS1_AX(7,8,9)
σ_{0j}^{req}	Starting wavenumber in band *j* for the requested spectral axis	a	r	MIP_PS1_AX(8)
$G_{j,d}(m^r)$	Previous gain	i	c	input from *Calculate Gain Calibration* function
$G_{j,d}^I(m^c)$	Previous gain, interpolated	t	c	
4.5.3.3	*Calculate coarse spectra*			
$S_{j,d}^{scc}(m^c)$	Coarse scene SPCs	t	c	

Variable	Descriptive Name	I/O	Type	Ranges / References / Remarks
$\Delta\sigma_j^{scc}$	Wavenumber spacing in band *j* at coarse resolution	t	r	computed from the IGM by the unscrambling method
$\sigma_{0\,j}^{scc}$	Starting wavenumber in band *j* at coarse resolution	t	r	computed from the IGM by the unscrambling method
k_{SC}	Spectral calibration correction factor	i	r	computed in *Calculate Spectral Calibration* function MIP_CS1_AX(4.3)
4.5.3.4	*Calculate calibrated spectra*			
$S_{j,d}^{sccc}(m^c)$	Coarse calibrated scene SPCs	t	c	
4.5.3.5	*Fringe count error detection*			
N^{ADC}	Number of sample data points in IGM before decimation	i	i	Extracted from MIPAS source packet
D_j	Decimation factor of band *j*	i	i	Extracted from auxiliary data of MIPAS source packet
h_j^{sys}	Systematic OPD shift of a scene IGM	t	i	$h_j^{sys} = \left(N^{ADC}/2 - 128\right) \bmod D_j$ if $\left(\left(N^{ADC} - 256\right)/D_j + 1\right) \bmod 2 = 0$ then $h_j^{sys} = h_j^{sys} - D_j$
h_d^{sc}	OPD shift of a scene IGM	t	i	
Δx	Nominal sampling interval	t	r	$1/\sigma_L$
4.5.3.6	*Fringe count error correction*			
4.5.3.7	*Responsivity scaling*			
k_R	Responsivity scaling factor	i	r	function of temperature at the DTUs. From *Load Data* function
$k_{G,j}$	Gain scaling factor	i	r	defined by PAW gain switching. From *Load Data* function
4.5.3.8	*Non-linearity correction*			
$ADC_{j,d}^{Max}$ $ADC_{j,d}^{Min}$	Maximum and minimum values of the digitized IGM	i	i	input from *Load Data* function. Integer values as given by the ADC before filtering and decimation.
$c_{q,j,d}$	Responsivity polynomial fit coefficients corresponding to a given non-linear detector	a	r	Polynomial order is 4 *j* covers only the index of non-linear detectors, A1, A2, AB and B MIP_CA1_AX(13)
4.5.3.10	*Offset subtraction*			
N_j^{ds}	Number of data points in calibrated DS IGM	i	i	coming from *Calculate Offset Calibration* function
n^d	Calibrated DS IGM data point index	l	i	
$I_{j,d}^{ds}(n^d)$	Calibrated DS IGM	i	c	coming from *Calculate Offset Calibration* function
$I_{j,d}^{sub}(n^i)$	Offset corrected scene IGM	t	c	

Variable	Descriptive Name	I/O	Type	Ranges / References / Remarks
4.5.3.11	*Zero-filling of interferogram*			
$I_{j,d}^{zf}(n^a)$	Zero-filled offset corrected scene IGM	t	c	
4.5.3.12	*Calculate spect. cal. spectra*			
Δx_j^{dec}	Sampling interval	i	r	input from *Load Data* function
$\Delta\sigma_j^{\max}$	Wavenumber spacing in band j for actual scene measurement	t	r	
$\sigma_{0j}^{\max}$	Starting wavenumber in band j for actual scene measurement	t	r	
$S_{j,d}^{sc}(m^a)$	Scene SPC (uncalibrated)	t	c	
4.5.3.13	*Spectral interpolation*			
v	Earth-fixed target to satellite range-rate	i	r	From *Geolocation* function
$\Delta\sigma_D$	Doppler shift in cm^{-1}	t	r	
D_c	Doppler correction factor	t	r	
$\Delta\sigma_j^{D\max}$	Wavenumber spacing in band j for the Doppler corrected scene	t	r	
$\sigma_{0j}^{D\max}$	Starting wavenumber in band j for the Doppler corrected scene	t	r	
$N_j^{D\max}$	Number of points in band j for the Doppler corrected scene	t	i	
$S_{j,d}^{sc}(m^r)$	Spectrally interpolated scene SPC (uncalibrated)	t	c	
4.5.3.14	*Radiometric calibration*			
$S_j^{cal}(m^r)$	Radiometrically calibrated scene SPC	O	r	The range of m^r corresponds to the requested spectral axis definition MIP_NL__1P(26-30) MDS 1
4.5.3.15	*Scene quality verification*			
$S_j^{\text{qual}}(m^r)$	Imaginary part of $S_j^{cal}(m^r)$	t	r	
$\langle S_j^{\text{qual}} \rangle$	Mean of imaginary part	t	r	
S_j^{rms}	Standard deviation of imaginary part	t	r	
s_{SVAL}^{thres}	Standard deviation threshold for scene validity evaluation	a	r	s_{SVAL}^{thres} should be between 1 and 10 MIP_PS1_AX(26)
t_{SVAL}	Threshold of rejection, expressed as a percentage	a	r	$0 \le t_{SVAL} \le 100$ MIP_PS1_AX(27)
4.5.3.16	*Reporting NESR*			
u	Template reduction factor	a	i	$u \ge 1$. MIP_PS1_AX(28)
$\Delta\sigma^{NESR}$	NESR wavenumber spacing	t	r	Used to calculate MIP_NL__1P(22-24) SPH
σ_0^{NESR}	NESR starting wavenumber	t	r	

Variable	Descriptive Name	I/O	Type	Ranges / References / Remarks
N^{NESR}	NESR number of points	t	i	
m^N	NESR data point index	l	i	$m^N = 0,\ldots,N^{NESR}-1$
$S^{NESR}(m^N)$	NESR	O	r	MIP_NL__1P(14) Scan Information ADS

4.5.3 Detailed structure and formulas

4.5.3.1 Spikes detection

This subfunction has the purpose of detecting spurious spikes in the interferogram of a scene data reading. The presence of spikes in an interferogram can be caused by cosmic radiation or transmission errors. The affected points in the scene interferogram are corrected by taking the mean between immediate non affected points.

The detection and correction of spikes is computed on the input interferogram, according to the procedure described in Section 4.9.1.2:

$$I'^{sc}_{j,d}(n^i) = \text{CorrectSpikes}\left\{ I^{sc}_{j,d}(n^i),\, N^{sc}_j \right\} \tag{1}$$

with

$$n^i = \begin{cases} -\dfrac{N^{sc}_j}{2},\ldots,+\dfrac{N^{sc}_j}{2}-1, & \text{if } N^{sc}_j \text{ is even} \\ -\dfrac{N^{sc}_j-1}{2},\ldots,+\dfrac{N^{sc}_j-1}{2}, & \text{if } N^{sc}_j \text{ is odd} \end{cases}$$

4.5.3.2 Gain spectral interpolation

This subfunction performs a spectral interpolation of the previous gain on a spectral axis corresponding to the actual gain calibration, but at a coarse resolution.

Note that as the gain to be interpolated is a smooth function, small N^{si} and N^{psi} parameters could be used to speed up the computation, or a simple linear interpolation between points could also be used instead. See Section 4.9.2 and 4.10.5 for more details about interpolation.

For *j* limited to band B and C, we do an interpolation of the actual gain to a coarser resolution by the operation:

$$G^I_{j,d}(m^c) = \text{Interpolate}\left\{ G_{j,d}(m^r);\ \Delta\sigma^{req}_j, \sigma^{req}_{0\,j}, N^{req}_j \rightarrow \Delta\sigma^{sccc}_j, \sigma^{sccc}_{0\,j}, N^{zpd}_j \right\} \tag{3}$$

with the procedure described at Section 4.10.5 according to the *Linear Interpolation Method*.

The range of data points index of the input gain is defined by the *requested* spectral calibration:

$$m^r = 0,\ldots,N^{req}_j - 1$$

The computed range of data points index is defined by the *coarse* spectral calibration:

$$m^c = 0,\ldots,N^{zpd}_j - 1$$

4.5.3.3 Calculate coarse spectra

This subfunction computes a coarse spectrum by performing the Fourier transform of a small portion around the ZPD of the incoming interferograms (corresponding to a at very low resolution). This operation is followed by the computation of the corresponding spectral axis. This axis is then calibrated by a multiplication by the current spectral calibration correction factor. Unscrambling is finally performed with the purpose of re-ordering spectra computed from decimated interferograms.

The purpose of this subfunction is to provide coarse spectra for fringe count error detection. Thus it is applied only to band B and C interferograms. A coarse spectrum is calculated for each measurement of the gain calibration sequence.

A Fourier transform is done at very low resolution for the scene measurement:

$$S_{j,d}^{scc}(m^c) = \mathrm{FFT}\left\{ I_{j,d}^{sc}(n^c) \right\} \tag{1}$$

The range of data points index defined by the *coarse* spectral calibration is:

$$n^c = -\frac{N_j^{zpd}}{2},\ldots,+\frac{N_j^{zpd}}{2} - 1$$

where N_j^{zpd} is an integer power of 2, and j is limited to the B and C bands. For a given scene measurement, the sweep direction may be either forward or reverse.

The radiometric vector is then unscrambled following the method described in Section 4.10.2. The corresponding spectral axis vector $\sigma_j^{scc}(m^c)$ is computed according to equation (4) of that same section. This vector is then calibrated by a multiplication by the current spectral calibration correction factor k_{SC}. If no spectral calibration is available yet, this correction factor is taken as unity.

$$\begin{aligned} \Delta\sigma_j^{sccc} &= \Delta\sigma_j^{scc} \cdot k_{SC} \\ \sigma_{0j}^{sccc} &= \sigma_{0j}^{scc} \cdot k_{SC} \end{aligned} \tag{2}$$

In addition to this stretching of the spectral axis, an inverse stretching must be applied on the radiometric scale to ensure the conservation of energy in the signal. This compensation can be applied with the following spectral calibration.

4.5.3.4 Calculate calibrated spectra

This subfunction performs a crude radiometric calibration of the coarse spectra by a simple multiplication by the previously interpolated coarse gain.

The coarse calibrated scene spectrum is obtained with:

$$S_{j,d}^{sccc}(m^c) = S_{j,d}^{scc}(m^c) \cdot G_{j,d}^{I}(m^c) / k_{SC} \quad (1)$$

4.5.3.5 Fringe count error detection

This subfunction analyses the phase of the coarse spectrum to establish if there was a fringe count error. Detection is done only in band B and C. However, it should be done independently for the forward and reverse sweep direction. Two bands were selected to increase the chance of detecting a fringe count error.

The fringe count error detection is computed from the calibrated spectrum, according to the procedure described in Section 4.9.3.2:

$$h_d^{sc} = \text{FCE Detect}\left\{S_{j,d}^{sccc}(m^c), \sigma_j^{sccc}(m^c), \Delta x, h_j^{sys}\right\} \quad (1)$$

4.5.3.6 Fringe count error correction

In the case where a fringe count error was detected, if a non-zero OPD shift $(h_d^{sc} - h_j^{sys})$ is calculated, this subfunction corrects the full resolution scene interferogram accordingly. The correction is applied to all detectors or bands.

The fringe count error correction is applied on complete scene interferogram at the input resolution, according to the procedure described in Section 4.9.3.3:

$$I'^{sc}_{j,d}(n^i) = \text{FCE Correct}\left\{I^{sc}_{j,d}(n^i), (h_d^{sc} - h_j^{sys}), \Delta x\right\} \quad (1)$$

The correction is applied to all detectors/bands so:

j = A1, A2, AB, B, C and D

4.5.3.7 Responsivity scaling

Based on the temperature measured at the DTUs, each individual interferogram must be scaled to account for the current DPU detector absolute responsivity at time of measurement. This responsivity is a function of temperature and varies over the orbit.

Also, there may be an additional vector multiplication to account for the current gain setting at the PAW on various channels, in the event of gain switching during orbit. In the case that the DPU gain is switched once or more times per orbit on one or more channels, the data has to be correctly scaled based on the selected gain factors (and using a characterization table giving the actual gain values corresponding to the selected settings).

These two corrections are still TBC. See Section 5.2.2.4 of [RD 6] for more details.

It is assume that k_R and $k_{G,j}$ are constant wrt to *d*, *k* and *i*. The correction is a simple scalar multiplication per vector:

$$I'^{sc}_{j,d}(n^i) = I^{sc}_{j,d}(n^i) \cdot k_R \cdot k_{G,j} \quad (1)$$

4.5.3.8 Non-linearity correction

The non-linearity correction is applicable on the non-linear detectors of channels A1, A2, B1, and B2 only. There is a different correction for each non-linear detector. Correction is performed on each incoming interferograms after responsivity scaling.

The non-linearity correction is derived from characterization data and based on an indicator of the DC total photon flux φ_{DC} of the actual measurement, i.e. the minimum and maximum values of the digitized IGM by the ADC before filtering and decimation given as input with the incoming interferogram. The characterization data contains non-linear responsivity polynomial coefficients for each affected detectors. These coefficients are previously computed from readings of calibration blackbodies, according to the procedure described in [RD 2].

Since all measurements within a calibration group are equivalent, and therefore should be subject to the same non-linearity, the correction is performed on the coadded interferograms.

Knowing the minimum and maximum values of the digitized IGM by the ADC before filtering and decimation ($ADC^{Min}_{j,d}$ and $ADC^{Max}_{j,d}$) for the current measure, and the responsivity coefficients for the detector under consideration ($c_{q,j,d}$), the non-linearity correction can be computed directly on the interferogram, according to the procedure described in Section 4.9.4 for *j* = A1, A2, AB and B:

$$I'^{sc}_{j,d}(n^i) = \mathrm{CorrectNL}\left\{I^{sc}_{j,d}(n^i), ADC^{Min}_{j,d}, ADC^{Max}_{j,d}, c_{q,j,d}\right\} \quad (1)$$

4.5.3.9 Equalization and combination

For channel A1 and A2, the equalization must be performed since it was omitted on board because of the non-linearity problem. Combination allows an improvement of the signal-to-noise ratio.

The equalization is done only on one of the two detectors to be combined, using a convolution with proper coefficients. The combination is obtained by subtracting the A2 interferogram from the A1 interferogram.

At the opposite of the Offset Calculation and the Gain calculation, equalization and combination must be done *before* Offset Subtraction because the offset calibration data is already equalized and combined. Otherwise, it would be necessary to separate offsets in band A1 and A2, and individually subtract them to spectra in equivalent bands before performing equalization and combination, that would be a more complicated approach.

The equalization and combination is computed on the scene interferogram, according to the procedure described in Section 4.9.5.2:

$$I'^{sc}_{j,d}(n^i) = \text{EqualizeCombine}\left\{I^{sc}_{j,d}(n^i)\right\} \quad (1)$$

4.5.3.10 Offset subtraction

Offset subtraction is performed to remove the contribution from the instrument. In this subfunction, the following aspects are considered:

- It is implicitly assumed that the spectral shift between the scene and the offset is small and that it introduces no significant errors.
- Subtraction is done only on points corresponding to low-resolution, in the case where offset calibration is done at a lower resolution than the scene. The result is a vector with the same number of points than the scene.
- When taking the offset measurement at a lower resolution, we implicitly assume that there are no high-resolution features in the offset spectrum (i.e. no feature at a resolution higher than the resolution selected).

The subtraction is done on the interferograms, before the Fourier Transform, in order to reduce the amount of calculations. In case the offset measurement is taken at low resolution, the subtraction is performed on the points corresponding to low-resolution only, i.e. at the center of the interferogram (lateral points are taken as zero). This corresponds to an interpolation of the scene offset with a zero filling in the spatial domain.

Offset subtraction is a simple point-by-point subtraction.

$$I^{sub}_{j,d}(n^i) = I^{sc}_{j,d}(n^i) - I^{ds}_{j,d}(n^d) \quad (1)$$

The result is a vector with the same number of points than the scene that is assumed greater than or equal to the range of the calibrated offset interferogram.

4.5.3.11 Zero-filling of interferogram

This subfunction performs the zero-filling of the interferograms in order to get a number of points corresponding to the smallest power of two greater than the initial number of points in the scene interferogram.

First, the number of points is computed as follows:

$$N^{\max}_j = 2^{\text{Ceil}\left\{\log_2\left(N^{sc}_j\right)\right\}} \quad (1)$$

The new range of indices for the zero-filled gain interferograms is extended to:

$$n^a = -\frac{N_j^{\max}}{2}, \ldots, \frac{N_j^{\max}}{2} - 1$$

with $$m^a = 0, \ldots, N_j^{\max} - 1$$

If N_j^{sc} is even then the interferogram becomes

$$I_{j,d}^{zf}(n^a) = \begin{cases} 0, & -N_j^{\max}/2 \le n^a < -N_j^{sc}/2 \\ I_{j,d}^{sub}(n^a), & -N_j^{sc}/2 \le n^a < N_j^{sc}/2 \\ 0, & -N_j^{sc}/2 \le n^a < N_j^{\max}/2 \end{cases} \quad (2)$$

and if N_j^{sc} is odd then it becomes

$$I_{j,d}^{zf}(n^a) = \begin{cases} 0, & -N_j^{\max}/2 \le n^a < -\left(N_j^{sc}-1\right)/2 \\ I_{j,d}^{sub}(n^a), & -\left(N_j^{sc}-1\right)/2 \le n^a \le \left(N_j^{sc}-1\right)/2 \\ 0, & -\left(N_j^{sc}-1\right)/2 < n^a < N_j^{\max}/2 \end{cases} \quad (3)$$

4.5.3.12 Calculate spectrally calibrated spectra

This subfunction performs the Fourier transform of the processed interferograms. See Section 4.10.1 for more details about the numerical Fourier transform.

$$S_{j,d}^{sc}(m^a) = \mathrm{FFT}\left\{I_{j,d}^{zf}(n^a)\right\} \quad (1)$$

The radiometric vector is then unscrambled following the method described in Section 4.10.2. This operation is followed by the computation of the corresponding spectral axis. The corresponding spectral axis vector inferior limit $\sigma_{0j}^{\max}$ is computed according to equation (4) of that same section. The definition of the spectral axis spacing can be expressed as:

$$\Delta\sigma_j^{\max} = \frac{1}{N_j^{\max}\Delta x_j^{dec}} \quad (2)$$

The spectral axis is then calibrated by a multiplication by the current spectral calibration correction factor k_{SC}. If no spectral calibration is available yet, this correction factor is taken as unity.

$$\Delta\sigma_j^{\max} = \Delta\sigma_j^{\max} \times k_{SC} \quad (3)$$

$$\sigma_{0j}^{\max} = \sigma_{0j}^{\max} \times k_{SC} \quad (4)$$

Unscrambling is finally performed with the purpose of re-ordering spectra computed from decimated interferograms. In addition to this stretching of the spectral axis, an inverse stretching must be applied on the radiometric scale to ensure the conservation of energy in the signal:

$$S'^{sc}_{j,d}(m^a) = S^{sc}_{j,d}(m^a) / k_{SC} \quad (5)$$

4.5.3.13 Spectral interpolation

The incoming spectra are stretched by the Doppler shift and therefore every scene must be corrected for this effect. The correction transforms the axis with linearly spaced points into a more closely spaced distribution. The spectral axis corresponding to the actual measurement shall be as defined by the latest spectral calibration. However, because of the specification on the spectral stability, this spectral calibration may be significantly different than the one effective during the last gain measurement. This is the reason why it is necessary to interpolate the actual scene spectrum. Since we have already chosen to interpolate the gain to the spectral axis requested (user defined), we will here have to interpolate to the same spectral axis.

The spectral calibration valid for the *actual* scene measurement is described by $\Delta\sigma_j^{\max}$, $\sigma_{0j}^{\max}$, and $N_j^{\max}$, while the *requested* spectral axis definition is defined by $\Delta\sigma_j^{req}$, σ_{0j}^{req}, and N_j^{req} (see Section 4.5.4.2).

We now interpolate the actual scene measurement onto the requested spectral axis. But before, the Doppler shift correction first has to be taken into account in the incoming spectral axis in order to compensate for the motion between the platform with respect to the current observed scene. Doppler (line) broadening due to the translational motion of the molecules and distortions induced by the presence of other molecules is not part of the correction.

The computed correction factor uses Earth-fixed target to satellite range-rate. The range-rate computation is based on the geolocation parameters (defined at ZPD time) computed from the orbital data and with help from dedicated software from ESA. The range-rate is expressed in Earth-fixed reference system [RD 14].

$$\Delta\sigma_D(\sigma) \approx \frac{v}{c}\sigma \quad (1)$$

(v/c has the order of magnitude of 2.5×10^{-5})

Then, each wavenumber σ will be modified in the following way:

$$\sigma' = \sigma - \Delta\sigma = \frac{\sigma}{D_c} \quad (2)$$

with $$D_c = \frac{1}{1 - \frac{v}{c}} \qquad (3)$$

This shows that the grid is simply modified by a global shrinking factor D_c leading to the corrected definition of the *actual* spectral axis:

$\Delta\sigma_j^{D\max} = \Delta\sigma_j^{\max} \times D_c$ Doppler corrected wavenumber spacing between spectral data points

$\sigma_{0j}^{D\max} = \sigma_{0j}^{\max} \times D_c$ the starting wavenumber of the band *j*

$N_j^{D\max} = N_j^{\max}$ the number of points in band *j* (stays the same)

In addition to this stretching of the spectral axis, an inverse stretching must be applied on the radiometric scale to ensure the conservation of energy in the signal:

$$S'^{sc}_{j,d}(m^a) = S^{sc}_{j,d}(m^a) \big/ D_c \qquad (4)$$

This new spectral axis distribution, with a different grid spacing, finally has to be interpolated according to the *requested* spectral axis definition.

$$S'^{sc}_{j,d}(m^r) = \text{Interpolate}\left\{ S^{sc}_{j,d}(m^a);\ \Delta\sigma_j^{D\max}, \sigma_{0j}^{D\max}, N_j^{D\max} \rightarrow \Delta\sigma_j^{req}, \sigma_{0j}^{req}, N_j^{req} \right\} \qquad (5)$$

with the procedure described at Section 4.9.2 according to the *Sinc Interpolation Method*.

The range of data points index is defined by the requested spectral parameters.

4.5.3.14 Radiometric calibration

Radiometric calibration is essentially a multiplication of the scene spectrum by the overall gain. This is a straightforward point-by-point complex multiplication. The result is a complex spectrum where the imaginary part is in principle zero.

Gain corrections based on characterization measurements are no longer needed, since correction for different electrical gain adjustment between scene and calibration is assumed not necessary, and since correction for pointing direction considering the azimuth angle for the actual scene measurement is also assumed not necessary (see Section 5.2.2.4.6 of [RD 6]).

Radiometric calibration includes correction for the radiometric calibration gain. The correction for the azimuth mirror gain no longer exists [RD 6]. Since the radiometric gain is already interpolated to the requested spectral axis, the radiometric calibration is a point-by-point complex multiplication. The result is a complex spectrum where the imaginary part is in principle zero.

$$S_j^{complex}(m^r) = S_{j,d}^{sc}(m^r) \cdot G_{j,d}(m^r) \tag{1}$$

Finally, only the real part is return as

$$S_j^{\mathrm{cal}}(m^r) = \mathrm{Re}\left\{ S_j^{complex}(m^r) \right\} \tag{2}$$

As it is apparent from the indices, we get a scene vector for each band defined on wavenumber values corresponding to the requested spectral axis.

4.5.3.15 Scene quality verification

The scene quality verification is based on the imaginary part of the calibrated scene measurement. If the imaginary part is only composed of only noise (its mean is null) and has no intrinsic distribution, then the scene measurement will be considered as valid. Otherwise, a flag is raised and the scene is deleted by setting all of its elements to zero.

The scene quality verification is based on the examination of imaginary part of the radiometric scene signal:

$$S_j^{\mathrm{qual}}(m^r) = \mathrm{Imag}\left\{ S_j^{complex}(m^r) \right\} \tag{1}$$

If $S_j^{\mathrm{qual}}(m^r)$ is only noise (its mean is null) and has no intrinsic distribution, then the scene measurement will be considered as valid.

A mean and a standard deviation of this imaginary part must be computed for the purpose of measuring the quality of the scene.

$$\langle S_j^{\text{qual}} \rangle = \frac{1}{N_j^{req}} \sum_{m^r=0}^{N_j^{req}-1} S_j^{\text{qual}}(m^r) \tag{2}$$

$$S_j^{\text{rms}} = \sqrt{\frac{1}{N_j^{\text{req}}-1} \sum_{m^r=0}^{N_j^{\text{req}}-1} \left(S_j^{\text{qual}}(m^r) - \langle S_j^{\text{qual}} \rangle \right)^2} \tag{3}$$

A scene will be considered unsatisfactory if more than t_{SVAL}% of the values of $S_j^{\text{qual}}(m^r)$ do not respect the following inequality:

$$\left| S_j^{\text{qual}}\left(m^r\right) \right| < s_{SVAL}^{\text{thres}} \times S_j^{\text{rms}} \tag{4}$$

In this case, a flag is raised as an observational error for the scene. The real part of the output vector $S_j^{cal}(m^r)$ is kept. Otherwise the scene is considered satisfactory.

The constants s_{SVAL}^{thres} and t_{SVAL} are defined in auxiliary data.

4.5.3.16 Reporting NESR

The NESR is reported for the complete spectral width of MIPAS. Gaps between bands are set to 0. The reported vector is on a reduce grid. The spectral axis is defined as follow:

$\Delta\sigma^{NESR} = \Delta\sigma_{\text{A}}^{req} \cdot u$ NESR wavenumber spacing between spectral data points,

$\sigma_0^{NESR} = \sigma_{0_{\text{A}}}^{req} + \frac{\Delta\sigma^{NESR}}{2}$ NESR starting wavenumber,

$N^{NESR} = \text{Floor}\left(\frac{\sigma_{0\text{D}}^{req} + \left(N_{\text{D}}^{req} - 1\right) \cdot \Delta\sigma_{\text{D}}^{req} - \Delta\sigma^{NESR}/2 - \sigma_0^{NESR}}{\Delta\sigma^{NESR}} \right) + 1$ NESR number of points.

The NESR is averaged for each interval of length *u* for all bands as follow:

$$S^{NESR}(m^N) = \sqrt{\frac{1}{u} \sum_{i=0}^{u-1} \left(S_j^{qual}\left(u \cdot \left(m^N - k_j\right) + i\right)\right)^2} \tag{1}$$

for $u = 1$ and

$$S^{NESR}(m^N) = \sqrt{\frac{1}{u}\left(\sum_{i=0}^{u-1} \left(S_j^{qual}\left(u \cdot \left(m^N - k_j\right) + i\right)\right)^2 - \frac{1}{u}\left(\sum_{i=0}^{u-1} S_j^{qual}\left(u \cdot \left(m^N - k_j\right) + i\right)\right)^2 \right)} \tag{2}$$

for $u > 1$ where $k_j = \text{Floor}\left(\frac{\sigma_{0\,j}^{req} - \sigma_{0\,\text{A}}^{req}}{\Delta\sigma^{NESR}}\right)$ and $m^N = 0,\ldots,N^{NESR}-1$. Note that in the case where the NESR intervals are only partly occupied with valid measurements (start and end of bands), the NESR value should be the averaged of available data points.

4.5.4 Computational sequence

The *Calculate Radiance* function receives control from the Load Data function when scene data have been found. The *Calculate Radiance* function processes this data and sends control to the Calculate Pointing function.

The output, i.e. a radiometrically calibrated spectrum, is delivered prior to control transfer.

The *Calculate Radiance* function assumes that gain, offset and spectral calibrations are available as soon as they are produced, so that they can be used for the processing of all scene measurements following these calibrations. If this is not the case, then processing will proceed with the latest available calibration.

The computational sequence for normal processing of the *Calculate Radiance* is illustrated by the flowchart of Figure 4.5.4-1.

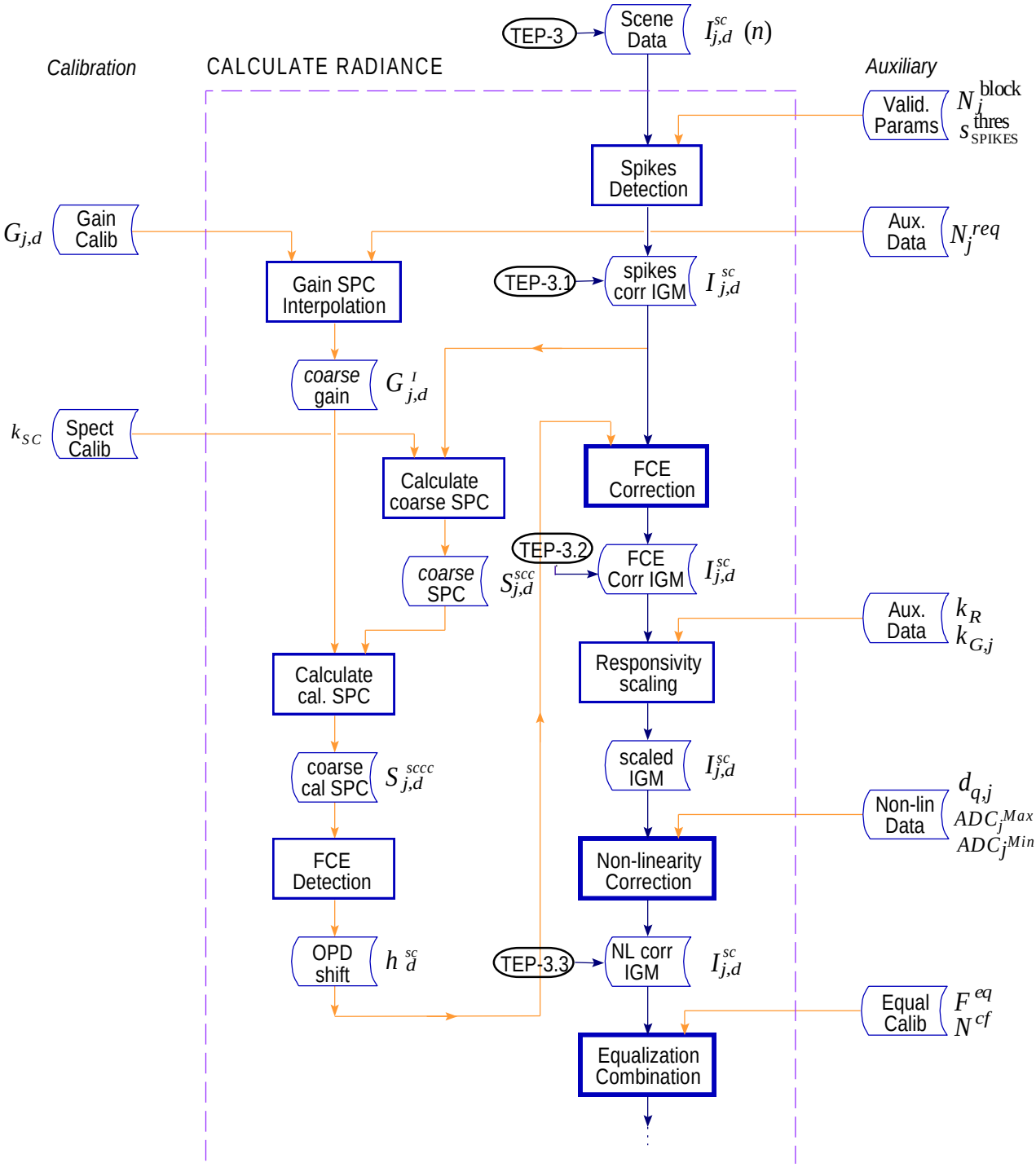

Figure 4.5.4-1 *Calculate Radiance Calibration* flowchart (*first part*)

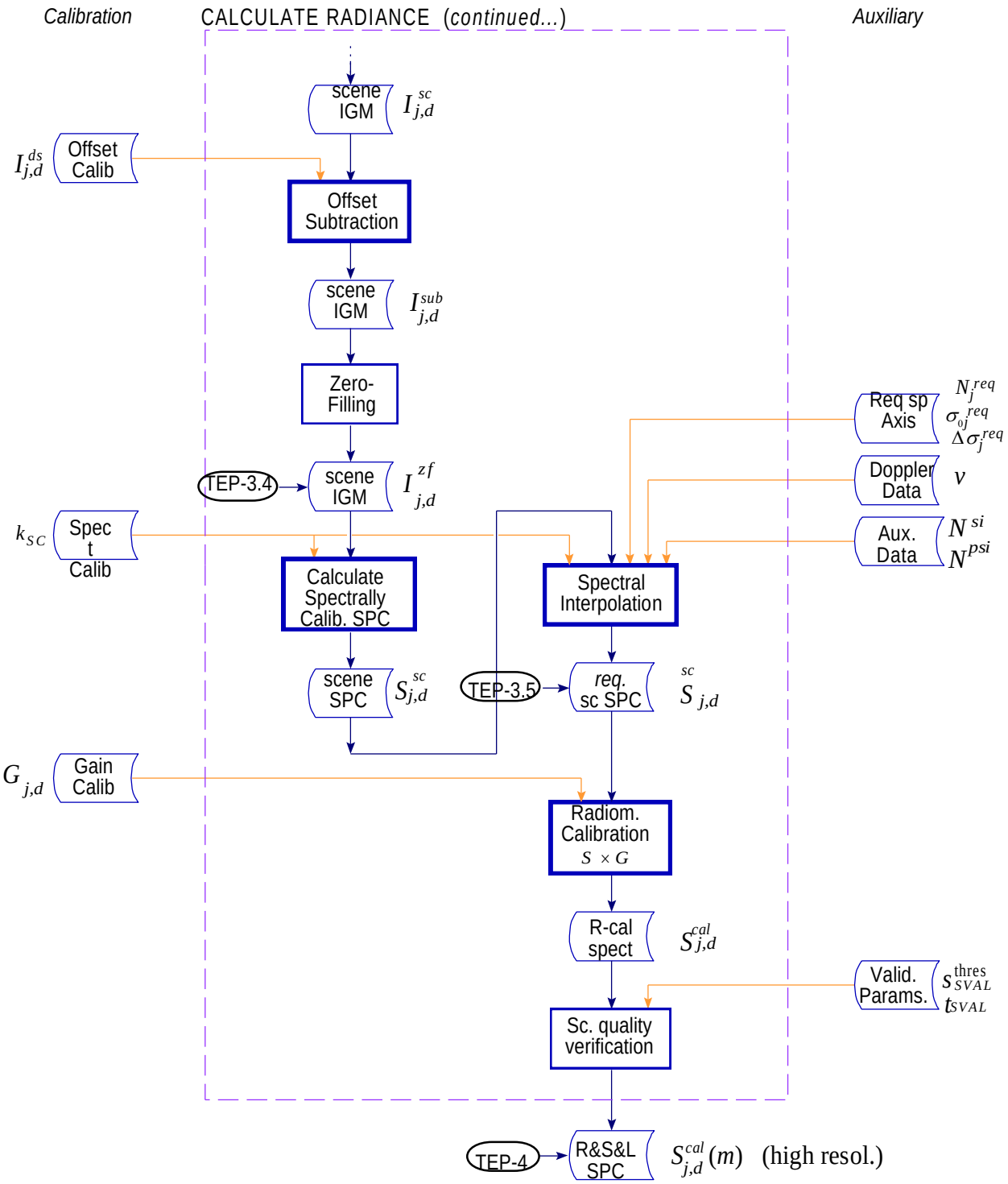

Figure 4.5.4-1 *Calculate Radiance Calibration* flowchart (*second part*)

4.6 CALCULATE ILS RETRIEVAL

This Section describes the *Calculate ILS Retrieval* function that performs, as its name implies, the necessary processing to retrieve the instrument line shape (ILS) from measured spectra. The data flowchart of this function is provided in Figure 4.6.4-1.

ILS retrieval has been studied extensively in the technical note [RD 4]. The deconvolution approach has shown to be inadequate, but a second approach has shown to give good enough results. The chosen ILS retrieval method is called the "Parametric ILS Fitting Method" (PIFM). This method proceeds with a theoretical ILS, obtained by a modelization with a limited number of parameters, convoluted with the theoretical line and iteratively fits the results onto the experimental data.

Appropriate peaks for spectral calibration that represent known features of standard scene measurements have been identified and studied in the document [RD 4]. The present algorithm works on such or equivalent spectral lines. The precision of the peak identification algorithm is proportional to the number of equivalent scenes that are coadded, as the noise affecting the signal decreases when multiple readings are superposed. This number will probably vary between 2 and 10, and will be defined in auxiliary data. We suppose for the present algorithm that five scenes per peak are used for each ILS retrieval.

The operation of ILS retrieval is more computer intensive than others tasks presented up to here, but this operation will be requested only from time to time, not on a regular basis as the computation of spectral calibration for example. Topics of the exact frequency at which the ILS retrieval shall be done is addressed here.

It has been chosen to extract the ILS in each detector band of the instrument on an appropriate spectral line located anywhere inside the band. The list of reference spectral lines will be stored in a table kept as auxiliary data.

The auxiliary data file containing retrieved ILS parameter data and spectral calibration data shall be produced by the Level 1B processor according to the processing parameter file. An initial ILS and spectral calibration auxiliary file will be given as an input to the processor at all processing stations and shall be used until the next file will be made available. ILS and spectral calibration data will be written to the auxiliary file simultaneously (i.e., only ca. once per week). Otherwise the file shall not be modified by the processor.

The processing parameters file contains control parameters for ILS and spectral calibration processing. For ILS:

- The time since ascending node crossing from which the search for first valid scene data shall start in seconds,
- The tangent height interval within which scene shall be extracted,
- The number of scenes to be coadded,
- The maximal number of subsequent scans from which scenes are to be extracted.

For spectral calibration:

- The time since ascending node crossing from which the search for first valid scene data shall start in seconds,
- Update period (number of scans),
- The tangent height interval within which scene data shall be extracted,
- The number of scenes to be coadded.

4.6.1 Objective

The main objectives of the Calculate ILS Retrieval function are the *fitting* of the convolution of the theoretical spectral line *by a parametric* ILS in the purpose of finding the ILS that matches the most closely the raw data.

- Select specific microwindows containing precisely one reference peak of well-known wavenumber.
- Obtain or generate the reference theoretical spectral line corresponding to this microwindow.
- Fit an ILS to the incoming raw spectrum by minimizing residuals between the reference line and the parametric ILS.
- Store the iterated parameter set and the specific wavenumbers as a Level 1B product.

The assumptions on the format of the ILS retrieval that are used in the definition of the other function of the present document are the same as those for spectral calibration, listed in Section 4.4.2.

The number of points in the spectral axis definition of a band from any spectral calibration shall be the smallest power of two larger than the actual number of points measured in that band. The reason for this is that standard FFT algorithms require a number of points that is an integer power of two. Thus, the calculated spectra have such a number of points and it is more appropriate that the spectral calibration is adjusted consequently.

4.6.2 Definition of variables

Calculate ILS Retrieval

Variable	Descriptive Name	I/O	Type	Ranges / References / Remarks
	General variables & indices			
N_j^{req}	Number of points in band *j* for the requested spectral axis	a	i	MIP_PS1_AX(7)
m^r	Numerical index of points in vector	l	i	$m^r = 0,\ldots,N_j^{req}-1$
$N^{\mu w}$	Number of points in the μw	t	r	= 1024
m^w	Numerical index data points in working vector	l	i	$m^w = 0,\ldots,N^{\mu w}-1$
n	Index of line	l	i	$n = 1,\ldots,N^{\text{lines}}$
$\Delta\sigma_j^{req}$	Spacing between spectral data points in the band	t	r	Computed with MIP_PS1_AX(7, 8, 9)
σ_{0j}^{req}	Starting wavenumber of the band	a	r	MIP_PS1_AX(8)
$\Delta\sigma_n^{\mu w}$	Spacing between spectral data points in working vector	t	r	$= 1/N^{\mu w}$
$\sigma_{0_n}^{\mu w}$	Starting wavenumber of working vector	t	r	
4.6.3.1	*Selection of microwindows*			
s	Index of elevation scans	l	i	$s = 1,\ldots,N_n^{\text{coadd}}$
N^{lines}	Number of spectral lines to be identified Number retrieved	a o	i	Equal to the number of to be used during ILS retrieval in file MIP_MW1_AX MIP_CS1_AX(3.3)
N_n^{coadd}	Number of equivalent scenes that must be coadded	a	i	Practical values are $1 \le N_n^{\text{coadd}} \le 10$ MIP_PS1_AX(45.6)
$S_{j,d}^{cal}(m^r)$	Radiometrically and spectrally calibrated input spectrum	i	r	Input from *Calculate Radiance* function
$S_j^{coadd}(m^r)$	Coadded spectrum band *j*	t	r	
σ_n^{exp}	Experimental peak position in working vector	t	r	
$S_n^{\mu w}(m^w)$	Working vector	t	r	
4.6.3.2	*Generate theoretical spectral line*			
$S_n^{\text{ref}}(m^w)$	Reference theoretical spectral line	t	r	
a, *b*, *c*	Theoretical function parameters	a	r	*a* = height, *b* = position, *c* = HWHM MIP_MW1_AX(11, 7, 12)

Variable	Descriptive Name	I/O	Type	Ranges / References / Remarks
model	Line model	a	i	MIP_MW1_AX(13)
4.6.3.3	*Fit ILS*			
`axz, ay`	Final parameters of Simplex fitting	o	r	MIP_CS1_AX(3.9, 3.10)
a_0, d_0, $\texttt{axz}_0$, $\texttt{ay}_0$	Initial guesses of Simplex fitting parameters	a	r	Must be different than 0 MIP_PS1_AX(47.5, 54, 73.2)
`shift`	ILS frequency shift	o	r	MIP_CS1_AX(3.10.1)
$S_n^{\text{model}}(m^w, params)$	Modelized spectrum to be fitted with experimental data	t	r	
σ_n^{uw}	Microwindow central frequency	i	r	MIP_MW1_AX
$E_{n,k}$	Sum of square residuals	t	r	local to Simplex routine
Simp^{tol}	Simplex convergence tolerance	a	r	Set to about 1×10^{-6} to 1×10^{-8} MIP_PS1_AX(46)
$\text{Simp}^{\text{itermax}}$	Maximum number of iterations for the simplex	a	i	Set to about 1000 MIP_PS1_AX(47)
k	Simplex iteration index	l	i	$k = 0,\ldots, N_n^{\text{iter}}$
N_n^{iter}	Number of Simplex iterations done to reach convergence tolerance for line n	t	i	
R_n^2	Coefficient of correlation for the fit	t	r	computed value: $R_n^2 \le 1$
$R_{\min}^2$	Threshold of validity for R_n^2	a	r	Set to about 0.5 MIP_MW1_AX(15)

4.6.3 Detailed structure and formulas

4.6.4.1 Selection of microwindows

This subfunction selects pre-defined portions of the observed pre-calibrated spectrum that contain reference lines, as defined in an auxiliary database (see Table 4.4.3-1). If no line can be identified, because no one correspond to the current altitude for example, the subfunction gives back control to the main processing flow and waits for another pass.

In the database are stored N^{lines} reference lines with their natural characteristics and the associated microwindows details. An example of a given line would be following the structure given in Table 4.4.3-1. The same description of each parameter also applies, except that the given width of the line is strictly the natural HWHM of the natural line, with no ILS widening. The chosen lines for ILS retrieval should correspond to measurements made at sufficiently high altitude that no offset is present in the measurements. The selected lines should also have a sufficiently high SNR to make the process feasible (see more discussions on the selection of microwindows in document [RD 4]).

The minimal case would consist of only two reference peaks, one present in band A and one in band D, at both extremities of the spectrum covered by the MIPAS detectors ($N^{\text{lines}} = 2$). This requirement comes from the fact that interpolation of ILS can be done between extrema reference points [RD 4]. But the more reference lines can be identified, more precise the method will be. A practical case would consist of at least one reference peak in each band. The exact number of reference lines required in each band is still TBD, but it can be taken as one for the current baseline.

In order to reduce noise, N_n^{coadd} equivalent scenes are coadded, i.e., scenes with altitude included in the range (MIP_PS1_AX(45.4)) for the last number of elevation scans (MIP_PS1_AX(45.8)) specified in the processing parameter file. The band *j* is the one that contains the microwindow *n*.

$$S_j^{coadd}(m^r) = \frac{1}{N_n^{coadd}} \sum_{s=1}^{N_n^{coadd}} S_{j,s}^{cal}(m^r) \tag{1}$$

Before the extraction of the microwindow, a peak fit (see section 4.9.6) is done in the range of the microwindow interpolated with a sinc interpolation as follow in order to find the experimental peak position $\sigma_n^{\exp}$.

$$S_n'^{\mu w}(m^w) = \text{ Interpolate} \left\{ S_j^{coadd}(m^r); \Delta\sigma_j^{req}, \sigma_{0j}^{req}, N_j^{req} \rightarrow \Delta\sigma_n^{\mu w}, b - \frac{\Delta\sigma_n^{\mu w} \cdot N^{\mu w}}{2}, N^{\mu w} \right\} \tag{2}$$

with $N^{\mu w} = 1024$ and $\Delta\sigma_n^{\mu w} = 1/N^{\mu w}$.

Then a new interpolation is done in order to obtain the peak position exactly on a point at the center of the working vector:

$$S_n^{\mu w}(m^w) = \text{ Interpolate } \left\{ S_j^{coadd}(m^r); \Delta\sigma_j^{req}, \sigma_{0j}^{req}, N_j^{req} \rightarrow \Delta\sigma_n^{\mu w}, \sigma_n^{\exp} - \frac{\Delta\sigma_n^{\mu w} \cdot N^{\mu w}}{2}, N^{\mu w} \right\} \quad (3)$$

Finally, the origin of the working vector is simply set to $\sigma_{0_n}^{\mu w} = b - \frac{\Delta\sigma_n^{\mu w} \cdot N^{\mu w}}{2}$. This re-centering is done in order to compensate the residual error of the spectral calibration. Since we only are interest to fit the shape of the ILS, this is legitimate.

The range of data points index of the microwindow is defined by:

$$m^w = 0, \ldots, N^{\mu w} - 1$$

Before this vector is sent to the next processing step, a re-centering is done using the algorithm defined in appendix B. The shift is determined with a parabolic fit.

4.6.4.2 Generate theoretical spectral line

This subfunction generates a theoretical model of the reference spectral line according to the data stored in auxiliary data. This reference line is used as a base for the convolution with the ILS for fitting with experimental data. The reference line and the model ILS are generated at the highest possible resolution, and the result is transformed to match the measurement sampling.

This subfunction generates a numerical vector containing the theoretical shape of the reference spectral line under study, according to the mathematical model and the associated parameters.

If model = 1, then $$S_n^{\text{ref}}(m^w) = a\, e^{-\left(\frac{\sigma - b}{c}\right)^2 \ln(2)} \quad (1)$$

If model = 2, then $$S_n^{\text{ref}}(m^w) = \frac{a}{\left(\frac{\sigma - b}{c}\right)^2 + 1} \quad (2)$$

(No sinc model is used to modelize a reference spectral line)

with $$\sigma = \sigma_{0_n}^{\mu w} + m^w \cdot \Delta\sigma_n^{\mu w}$$

The amplitude *a*, the spectral line position *b* and the width *c* are taken as the data values stored in the microwindows database.

The reference line $S_n^{\text{ref}}(m^w)$ is used as a base for the convolution with the ILS for fitting with experimental data.

4.6.4.3 Fit ILS

This subfunction minimizes residuals between selected raw spectral lines and the convolution of the reference theoretical line model with a parametric ILS. The fitted model will represent the instrument line shape that best represent the observed scene.

This subfunction contains in itself many other functions of lower level that will be discussed more thoroughly in Section 4.6.4.

The main core of the iterative fitting approach (PIFM) can be segmented in the following way:

1– Computes convolution between the reference spectrum $S_n^{\text{ref}}(m^w)$ and the model ILS, function of an initial set of characteristic parameters.

The instrument line shape function *ILS*(parameters) is described in appendix C and should be accordingly implemented.

The two chosen parameters are the following ones:

`axz`: Linear shear variation along z axis
`ay`: Systematic IR misalignment angle along y axis

They consist of two orthogonal imperfections that model the most important perturbations that affect the global aspect of the ILS. They are used more as modeling knobs than indications of instrument's performances.
They are initialized with the most probable values expected from theory and a prior analysis of the instrument characteristics.

$$\texttt{axz}_0 = 1.0\times10^{-3} \quad (1)$$
$$\texttt{ay}_0 = 0.2\times10^{-3} \text{ mrad} \quad (2)$$

The exact guess values for these parameters will have to be adjusted in function to the real incoming data coming from the instrument.

The other intrinsic parameters modeling the ILS are defined as auxiliary data and are considered fixed throughout the ILS retrieval operation.

A scaling factor a (which initial primer guess is set as $a_0 = 1.0$) is also needed because of the unavoidable error on the height of the theoretical line. Even if the measured lines for the ILS retrieval are taken at a sufficiently high altitude and that no continuum is present, an offset parameter d_0 is taken into account because of potential errors due to imperfect offset subtraction of the instrument contribution.

The ★ symbol represents here the convolution operator.

$$S_n^{\text{model}}(m^w, params) = a\left(S_n^{\text{ref}}(m^w) \bigstar ILS(m^w, \texttt{axz}, \texttt{ay})\right) + d \quad (3)$$

Note that the *ILS* vector is re-centered before the convolution using the algorithm defined in appendix B. The shift is determined with a parabolic fit.

2– Minimize the next residual with the Simplex iterative method that uses the variation of the vector $params_k$ = axz$_k$, ay$_k$, a_k, and d_k:

$$E_{n,k} \leftarrow \sum_{m^w = m_{left}}^{m_{right}} \left[S_n^{\text{model}}(m^w, params_k) - S_n^{\mu w}(m^w) \right]^2 \tag{4}$$

where $m_{left} = (N^{\mu w}/2) - \Delta m$, $m_{left} = (N^{\mu w}/2) + \Delta m$ and $\Delta m = \min\left(b - \sigma_{l_n}^{\mu w}, \sigma_{r_n}^{\mu w} - b\right) / \Delta\sigma_n^{\mu w}$

The Simplex algorithm is performed until a predefined tolerance Simp^{tol} is reached on the residual values. If a maximum number of iterations is reached, expressed as

$$N_n^{\text{iter}} > \text{Simp}^{\text{itermax}}$$

then the algorithm is stopped and an error is dispatched. If a_k is pushed to 0 by the Simplex, calculate eq.(4) with $a_k = 10^{-7}$.

3– Characterize the final result by the computation of the coefficient of correlation R_n^2, defined as follows:

$$R_n^2 = 1 - \frac{E_{n,N_n^{\text{iter}}}}{\sum_{m^w = m_{left}}^{m_{right}} \left(S_n^{\mu w}(m^w) \right)^2} \tag{5}$$

This number indicates a perfect fit when $R_n^2 = 1$, while $R_n^2 = 0$ means that the data is completely uncorrelated (negative values indicate an anti-correlation trend but should never occur). For an appropriate fit, the value of R_n^2 shall be higher than $R_{\min}^2$ (set at about 0.5). If the value computed is less than $R_{\min}^2$, the fit should be rejected.

This statistical test can be performed to check for the validity of the operation.

4– Calculate the shifted position of the maximum amplitude ILS frequency vs the central ILS frequency:

$$shift(m^w) = MaxFreq\left(ILS(m^w, \text{axz}, \text{ay})\right) - \sigma_n^{uw} \tag{6}$$

4.6.4.4 Store results

For each of the N^{lines}, the output products will be specified as the set of the two final iterated parameters axz and ay and a reference to auxiliary data containing the whole set of ILS parameters. The iterated parameters have priority to values in the auxiliary table. Also stored will

be the associated wavenumber at which the ILS retrieval have been computed. The storage of only these parameters has been preferred to the storage of the whole ILS for practical reasons of storage space savings and also for flexibility of the interpolation at different wavenumbers.

To obtain the ILS at levels higher than 1B, this data will be needed, and also will be the ILS function generator itself. This will enable the calculation of ILS profiles at the few specific wavenumbers of the reference lines. To obtain the ILS profiles anywhere on the spectrum, the ILS interpolation procedure will be needed (see [RD 4]). This algorithm is not reproduced here because of its complexity and because it is exterior to the present procedure and can not be considered as data but instead as an operator.

4.6.4 Computational sequence

The computational sequence is illustrated by the flowchart of Figure 4.6.4-1.

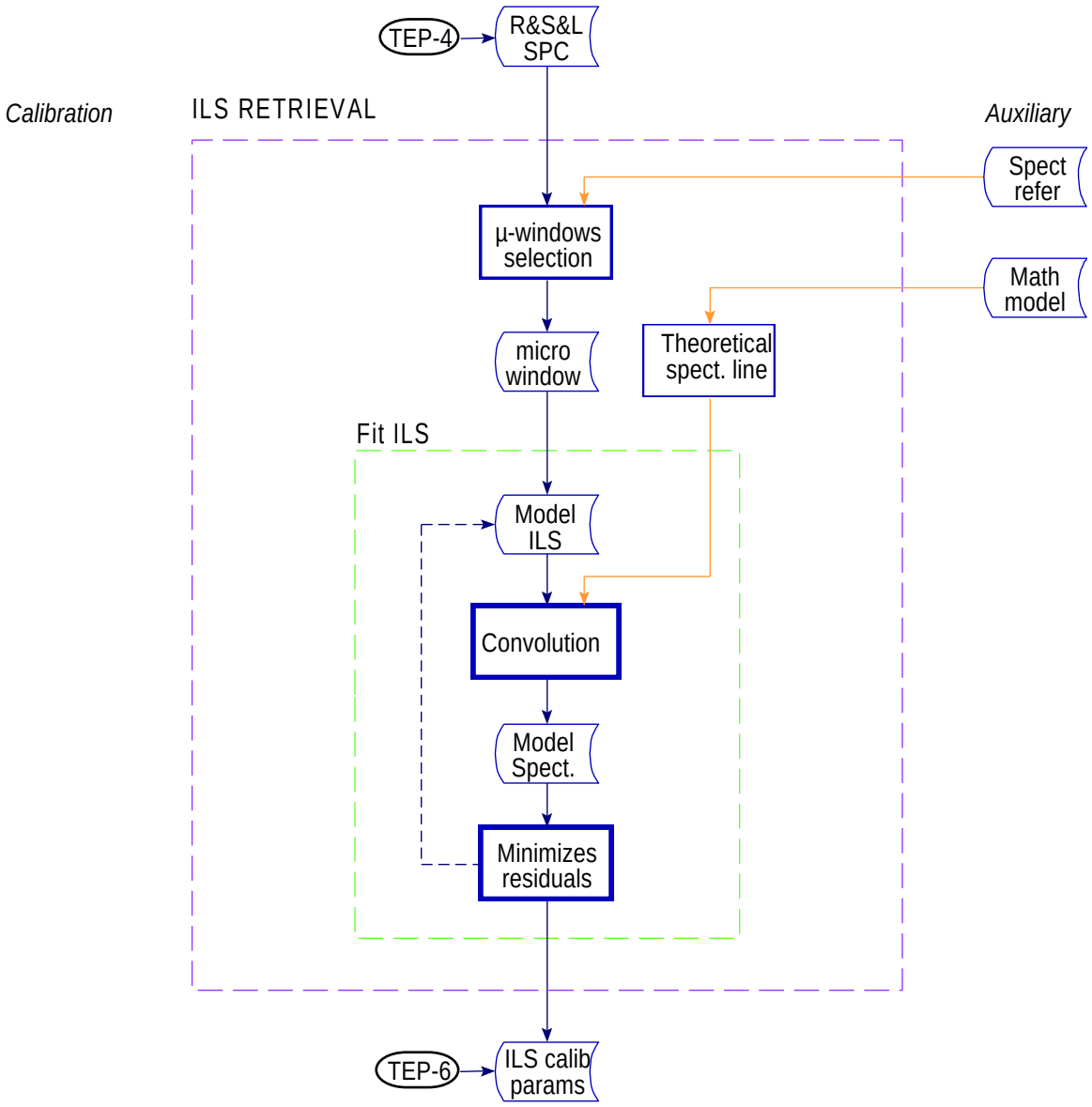

Figure 4.6.4-1 Calculate ILS Retrieval flowchart

4.7 CALCULATE POINTING

The *Calculate Pointing* function performs the processing necessary for line of sight pointing calibration in order to generate corrected LOS pointing angles.

The algorithms are covered in details in Section 7.3.11 of document [RD 1]. The Section is recopied here for completeness of the document.

This section describes the Calculate Pointing Function that performs the processing necessary to generate LOS, radiometrically and spectrally calibrated spectra (L, R & S spectrum).

4.7.1 Objective

The main objectives of the Calculate Pointing function are

- Compute correction of elevation pointing angle,
- Compute elevation angle corrections due to scan mirror non-linearity
- Compute corrected pointing angles of actual scene (sweep).

The Calculate Pointing function is based on the following assumptions. It is assumed that commanded elevation angles are only partially corrected with respect to known pointing errors according to the best knowledge based on-ground characterization and LOS calibration measurements. The remaining elevation error, obtained from LOS calibration measurements, shall be computed in the ground segment (PDS) and be used to correct in measurement mode the measured elevation angles. The corrected elevation angles and the measured azimuth angles are used to compute the geolocation (height/longitude/latitude) of the actual scene (target).

4.7.2 Definition of Variables

Calculate Pointing

Variable	Descriptive Name	I/O	Type	Ranges / References / Remarks
	Calculate Pointing			
$\bar{\bar{x}}$	Vector of averaged unknown pointing error $\bar{\bar{x}} := \left(\bar{\xi}_0, \bar{c}_\xi, \bar{\Phi}_\xi, \bar{\eta}_0, \bar{c}_\eta, \bar{\Phi}_\eta\right)$	a	r	MIP_CL1_AX(5 to 10)
t_0^{ref}	Reference time used to compute the phase of the harmonic pointing error	i	r	Time of last ascending node crossing From *Geolocation* function
t^{scene}	Onboard time related to actual scene measurement data	i	r	Time of actual ZPD crossing From *Load Data* function
ω_ξ	Angular frequency of first order harmonic pointing error related to x-axis (pitch)	a	r	MIP_CL1_AX(3)
ω_η	Angular frequency of first order harmonic pointing error related to y-axis (roll)	a	r	MIP_CA1_AX(4)
$\Delta\bar{\alpha}$	Azimuth offset, correction of azimuth angle	a	r	MIP_CA1_AX(46)
$\Delta\bar{\varepsilon}(t^{scene})$	Correction of elevation angle at time t^{scene}	t	r	
$\varepsilon^{meas}(t^{scene})$	Measured elevation angle at time t^{scene}	i	r	From *Load Data* function
$\alpha^{meas}(t^{scene})$	Measured azimuth pointing at time t^{scene}	i	r	From *Load Data* function
elev and *corr*	MIPAS scan mirror non-linearity elevation angle corrections	i	r	MIP_CA1_AX (field 45.1) *elev* and angle corrections (field 45.2) *corr*
$\varepsilon^{nl}(t^{scene})$	Corrected elevation angle for non-linearity at time t^{scene}	o	r	Corrected elevation angles
ε^{yc}	Corrected elevation angle due to yearly pointing variation	o	r	Depends only of orbit number and MIP_CA1_AX fields (48-55)
$\varepsilon^{act}(t^{scene})$	Actual elevation angle at time t^{scene}	O	r	MIP_NL__1P(5) MDS 1
$\alpha^{act}(t^{scene})$	Actual azimuth angle at time t^{scene}	O	r	MIP_NL__1P(5) MDS 1

4.7.3 Detailed structure and formulas

The actual elevation pointing angle related to each interferometer sweep (scene) is given by the measured elevation angle and the computed correction at the time of ZPD crossing.

4.7.4.1 Compute the actual pointing error at time of ZPD crossing

This subfunction computes the actual pointing error with respect to pitch and roll at the time of scene measurement.

The actual pointing error of the satellite and the instrument based on LOS calibration measurement is given by:

a) Pointing error related to x-axis (pitch)

$$\bar{\xi}(t^{scene}) = \bar{\xi}_0 + \bar{c}_\xi \cdot \cos\left(\omega_\xi \cdot (t^{scene} - t_0^{ref}) - \bar{\Phi}_\xi\right) \quad (1)$$

b) Pointing error related to y-axis (roll)

$$\bar{\eta}(t^{scene}) = \bar{\eta}_0 + \bar{c}_\eta \cdot \cos\left(\omega_\eta \cdot (t^{scene} - t_0^{ref}) - \bar{\Phi}_\eta\right) \quad (2)$$

where t^{scene} is the time related to a measurement which may be the time of Zero Path Difference.

4.7.4.2 Compute actual azimuth pointing angle

This subfunction computes for each scene (sweep) the actual azimuth angle. Pointing errors in azimuth will not be calibrated during flight operation. However, a correction based on on-ground characterization/alignment measurements must be performed.

The actual azimuth pointing angle at time t^{scene} is given by:

$$\alpha^{act}(t^{scene}) = \alpha^{meas}(t^{scene}) - \Delta\bar{\alpha} \quad (1)$$

where $\Delta\bar{\alpha}$ is an azimuth offset characterized on-ground.

4.7.4.3 Compute correction of elevation angle

This subfunction computes the correction to be applied to the measured elevation angle of a scene (sweep). Inputs to this function are the estimated bias and harmonic pointing errors for rearward and sideways measurement, the commanded azimuth angle, and the time of data acquisition.

Note: Estimated pointing errors may be based on a single orbit LOS calibration measurement. In the following it is assumed that estimated pointing errors are the result of an averaging process over multiple orbits.

The correction to be applied to the measured elevation angle is given by:

$$\Delta\bar{\varepsilon}(t^{scene}) = \left[-\bar{\xi}(t^{scene})\cdot\cos\left(\alpha^{act}(t^{scene})\right) + \bar{\eta}(t^{scene})\cdot\sin\left(\alpha^{act}(t^{scene})\right)\right] \quad (1)$$

where $\alpha^{act}(t^{scene})$ is the actual azimuth pointing angle.

4.7.4.4 Compute scan mirror non-linearity elevation angle correction

Find the index *i* in the angle correction table *elev* (MIP_CA1_AX) where $elev[i] > el \geq elev[i-1]$ and $el = \varepsilon^{meas}(t^{scene}) + 90$. Then interpolate the elevation angle correction. No correction is done if *el* is outside the angle correction table.

$$\varepsilon^{nl}(t^{scene}) = \varepsilon^{meas}(t^{scene}) - \left(corr[i-1] + \frac{(corr[i]-corr[i-1])\times(el-(elev[i-1]+corr[i-1]))}{((elev[i]+corr[i])-(elev[i-1]+corr[i-1]))} \right) \quad (1)$$

4.7.4.5 Compute annual pointing elevation angle correction

Compute a mispointing annual variation where the coefficients a_s, ω_s, p_s, a_c, ω_c, p_c, m and *offset* are defined in MIP_CA1 fields (48-55).

$$\varepsilon^{yc} = a_s \sin((\omega_s + orbno)2\pi / p_s) + a_c \cos((\omega_c + orbno)2\pi / p_c) + m\times orbno + offset \quad (1)$$

4.7.4.6 Compute actual elevation pointing angle

The actual elevation pointing angle at time t^{scene} is given by:

$$\varepsilon^{act}(t^{scene}) = \varepsilon^{nl}(t^{scene}) - \Delta\bar{\varepsilon}(t^{scene}) + \varepsilon^{yc} \quad (1)$$

4.7.4 Computational Sequence

The *Calculate Pointing* function receives control from the *Load Data* function when nominal measurement data have been found in source packets. The *Calculate Pointing* function processes pointing data belonging to radiometrically and spectrally processed spectra and send control back to the *Load Data* function.

The output is generated if the instrument is commanded in measurement mode.

The computational sequence of the *Calculate Pointing* function is illustrated by the flowchart of figure 4.7.4-1.

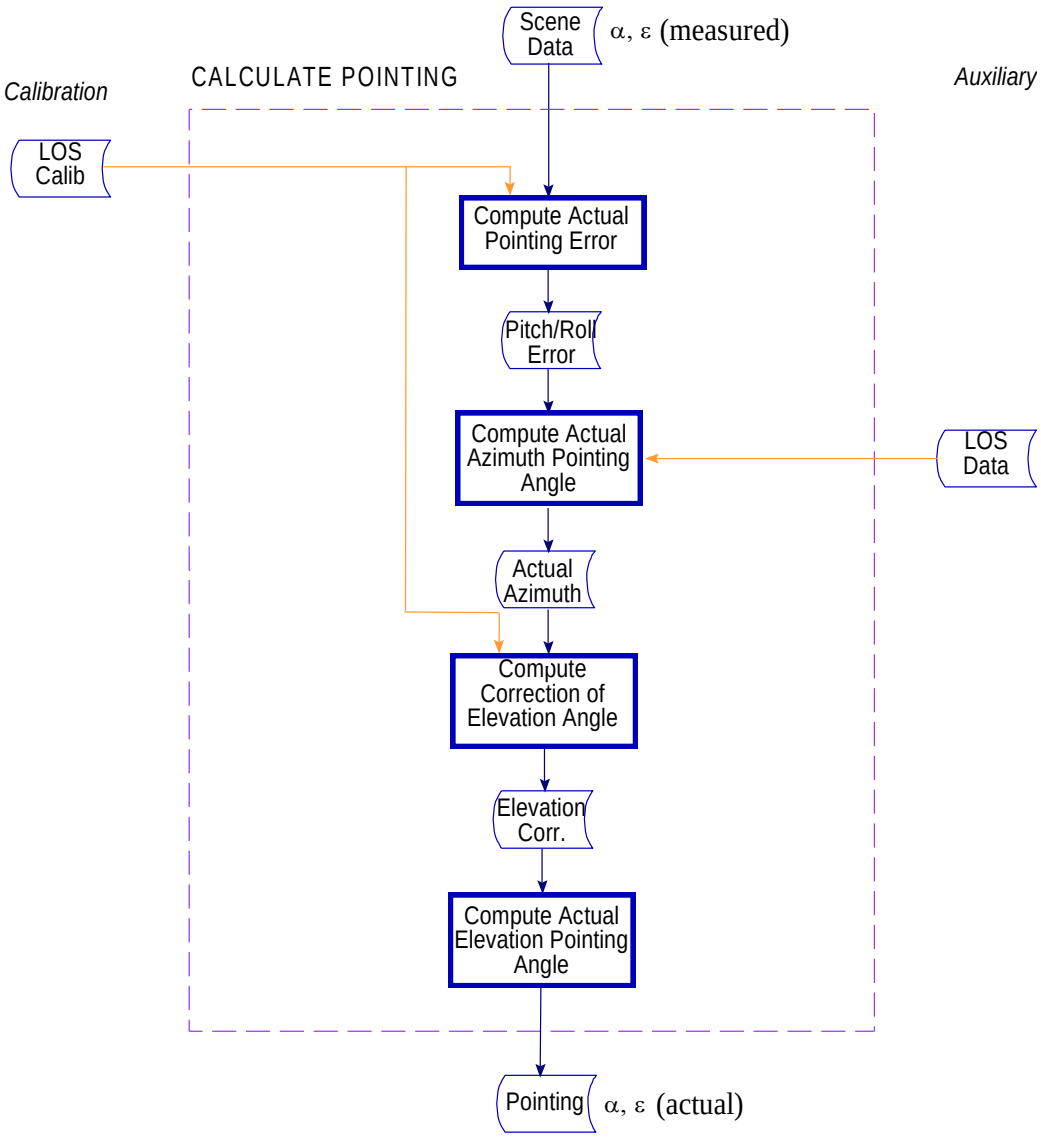

Figure 4.7.4-1 *Calculate Pointing* flowchart

4.8 CALCULATE GEOLOCATION

The *Calculate Geolocation* function calculates the tangent point geolocation and related information. The function has as input the orbit state vector and corrected pointing angles and it makes use of the CFI softwares [RD 20] and [RD 19].

4.8.1 Objective

The main objectives of the Calculate Geolocation function are

- Compute the effective mispointing angles taking into considerations the MIPAS alignment matrices defined in the MIP_CA1_AX,
- Compute tangent height of actual scene,
- Compute rms error of tangent height of actual scene,
- Compute longitude / latitude of actual scene,
- Retrieve day/night flag from CFI S/W

4.8.2 Definition of Variables

Calculate Geolocation

Variable	Descriptive Name	I/O	Type	Ranges / References / Remarks
	Calculate Geolocation			
4.8.3.1	*Compute orbital position*			
PTIME	Time of initial state vector	I	r	From MPH state vector
RR	Initial state vector position	I	r	
RRD	Initial state vector velocity	I	r	
t^{scene}	Onboard time related to actual scene measurement data	i	r	Time of actual ZPD crossing From *Load Data* function
t_0^{ref}	Reference time used to compute the phase of the harmonic pointing error	o	r	Time of last ascending node crossing Output MJDR of Orbit Propagator s/w
4.8.3.2	*Compute effective attitude information*			
f	Flag if pointing is calculated according to restituted attitude file method	i	i	MIP_PS1_AX(85.1)
AlignMat	MIPAS alignment matrix	i	d	MIP_CA1_AX (field 44.1)
M_char	MIPAS mispointing characterization (same as used for planning)	i	r	MIP_CA1_AX bias (field 44.5), a vector of 3 values: pitch.bias, roll.bias and yaw.bias. MIP_CA1_AX harmonics (field 44.6) 3 vectors(pitch, roll, yaw) of 9 values : pitch_harm[9] roll_harm[9], yaw_harm[9] This x_harm[] vector (where x stands for pitch, roll and yaw) is equivalent to a cos, sin and freq harmonics vector where j varies from 0 to nharmonics -1. x.harm[j].cos = x_harm[3*j] x.harmo[j].sin = x_harm[3*j+1] x.harm[j].freq = x_harm[3*j+2]
dtype	Derivative type	i	i	MIP_CA1_AX (no derivative or 1st derivative) (field 44.7)
nharmonics	Number of harmonics	i	i	MIP_CA1_AX (field 44.8) possible values: 0 to 3
att0 and *datt0*	Constant mispointing angle inputs	i	r	MIP_PS1_AX (81,82)
e_att and *e_datt*	Effective attitude information angle outputs at t^{scene}	i	r	

4.8.3.3	*Compute tangent height*			
$\varepsilon^{act}(t^{scene})$	Actual elevation angle at time t^{scene}	i	r	From *Calculate Pointing* function
$\alpha^{act}(t^{scene})$	Actual azimuth angle at time t^{scene}	i	r	From *Calculate Pointing* function
$h(t^{scene})$	Geodetic altitude (tangent height) at t^{scene}	O	r	Output RES[6]/(7) of Payload to Target Parameters Calculation s/w MIP_NL__1P(6) MDS 1
$long(t^{scene})$	Geographic longitude at time t^{scene}	O	r	Output RES[3]/(4) of Payload to Target Parameters Calculation s/w MIP_NL__1P(7) MDS 1
$lat(t^{scene})$	Geodetic latitude at time t^{scene}	O	r	Output RES[5]/(6) of Payload to Target Parameters Calculation s/w MIP_NL__1P(7) MDS 1
$S/C(t^{scene})$	S/C position at time t^{scene}	O	r	Output POS of Orbit Propagator s/w MIP_NL__1P(4) MDS 1
R	Radius of curvature in looking direction at nadir of target	O	r	Output RES[15]/(16) of Payload to Target Parameters Calculation s/w MIP_NL__1P(8) MDS 1
v	Earth-fixed target to satellite range-rate	O/o	r	Output RES[37]/(38) of Orbit Propagator s/w. Needed for Doppler shift MIP_NL__1P(9) MDS 1
v_g	Geodetic altitude-rate of the target	O	r	Output RES[23]/(24) of Payload to Target Parameters Calculation s/w MIP_NL__1P(10) MDS 1
AziTopo	Target to satellite azimuth angle (Topocentric CS)	o	r	Output RES[8] of Payload to Target Parameters Calculation s/w MIP_NL__1P(24.11) MDS 1
ElevTopo	Target to satellite elevation angle (Topocentric CS)	o	r	Output RES[9] of Payload to Target Parameters Calculation s/w MIP_NL__1P(24.10) MDS 1
day_night	Day/night flag	o	r	Output RES[71]/(72) of Payload to Target Parameters Calculation s/w MIP_NL__1P(25.2) MDS 1
4.8.3.4	*Estimate error on tangent height*			
$\alpha_{\min}^{rear}$	Minimum azimuth angle in rearward observation geometry	a	r	MIP_PS1_AX(77)
$\alpha_{\max}^{rear}$	Maximum azimuth angle in rearward observation geometry	a	r	MIP_PS1_AX(78)
$\alpha_{\min}^{side}$	Minimum azimuth angle in sideways observation geometry	a	r	MIP_PS1_AX(76.1)
$\alpha_{\max}^{side}$	Maximum azimuth angle in sideways observation geometry	a	r	MIP_PS1_AX(76.2)

ω_ξ	Angular frequency of first order harmonic pointing error related to x-axis (pitch)	a	r	MIP_CL1_AX(3)
ω_η	Angular frequency of first order harmonic pointing error related to y-axis (roll)	a	r	MIP_CL1_AX(4)
$\vec{\bar{\sigma}}^2_{\bar{x}}$	Vector of averaged variances of unknown pointing error $\vec{\bar{\sigma}}^2_{\bar{x}} := \left(\sigma^2_{\bar{\xi}_0}, \sigma^2_{\bar{c}_\xi}, \sigma^2_{\bar{\Phi}_\xi}, \sigma^2_{\bar{\eta}_0}, \sigma^2_{\bar{c}_\eta}, \sigma^2_{\bar{\Phi}_\eta}\right)$	a	r	MIP_CL1_AX(11 to 16)
$\sigma(h)$	RMS error of tangent height at t^{scene}	O	r	MIP_NL__1P(6) MDS 1

4.8.3 Detailed structure and formulas

4.8.3.1 Compute orbital position of S/C at ZPD time

This sub-function computes from ZPD time and state vector the satellite position and velocity.

The orbital position can be calculated using the orbit propagator or the orbit interpolation.

A) *No DOR_VOR ADF file available*

The orbital position and velocity of S/C shall be computed using the Envisat CFI software PPF_ORBIT (po_ppforb) [RD 19] and the initial state vector in auxiliary data and the ZPD time.

First, the orbit propagator (po_ppforb) shall be initialized in the longitude dependent mode with the following input parameters:

Parameters	Values
mode	PO_INIT
mjdp	PTIME
pos	RR
vel	RRD

Table 4.8.3.1-1 Input parameters for orbit propagator s/w initialization

Next, it shall be propagated at t^{scene} using absolute time with the following input parameters:

Parameters	Values
mode	PO_PROPAG
mjdr	MJDR output of orbit propagator initialization
xm	XM output of orbit propagator initialization
mjdp	t^{scene}

Table 4.8.3.1-2 Input parameters for orbit propagator s/w

B) *Using DOR_VOR ADF file*

The orbital position and velocity of S/C shall be computed using the Envisat CFI software PPF_ORBIT (po_interpol) [RD 20] and the closest state vector in auxiliary data and the ZPD time.

First, the orbit interpolation (po_interpol) shall be initialized with the following input parameters:

Parameters	Values
mode	PO_INIT_FILE + PO_INTERPOL_RES_BAS + PO_INTERPOL_RES_AUX
Choice	0, automatic selection depends on file provided
Ndc	1
Doris_precise_file	DOR_VOR filename
Mjdr0	MPH SENSING START (decimal days)
Mjdr1	MPH SENSING STOP (decimal days)

Table 4.8.3.1-3 Input parameters for orbit interpolation s/w initialization

Next, it shall be propagated at t^{scene} using absolute time with the following input parameters:

Parameters	Values
mode	PO_INTERPOLATE + PO_INTERPOL_RES_BAS + PO_INTERPOL_RES_AUX
Mjdr0	t^{scene}

Table 4.8.3.1-4 Input parameters for orbit interpolation s/w propagation

4.8.3.2 Compute MIPAS effective attitude information

The S/C attitude information (pitch, roll and yaw angles and rates) must be corrected by the MIPAS alignment matrix *AlignMat* to get the effective attitude information *e_att* and *e_datt*.

The MIPAS alignment matrix *AlignMat* is a [3,3] dimension matrix and is defined in the characterization ADF MIP_CA1_AX. The baseline values are the following:

+0.9999997427	+0.0000697013	-0.0007105313
-0.0000699291	+0.9999999978	-0.0001720573
+0.0007105465	+0.0002174480	+0.9999997087

4.8.3.2.1 Calculate the attitude information at the time of the scene measurement.

A) Using planned attitude information ($f = 0$)

When $f = 0$, the S/C attitude information is the one used during the planning (commanding). Parameters *M_char* to calculate *sc_att* and *sc_datt* are stored in the MIP_CA1_AX file. The *sc_aocs* is retrieved from the MIP_PS1_AX field (80). The baseline is {-0.1672, +0.0501, +3.9284}.

$$sc\_att[1] = \sum_{i=0}^{nharmonics-1} M\_char.pitch.harm[i].sin \times \sin(fp\_t) + M\_char.pitch.harm[i].cos \times \cos(fp\_t) \quad (1)$$

where $fp\_t = \text{PL\_to\_rad}(M\_char.pitch.harm[i].freq) \times t^{anx}$,
and $t^{anx} = t^{scene} - t_0^{ref}$ is the time since ascending node crossing in second.

$$sc\_att[1] = sc\_att[1] + M\_char.pitch.bias \quad (2)$$

$$sc\_att[2] = \sum_{i=0}^{nharmonics-1} M\_char.roll.harm[i].sin \times \sin(fr\_t) + M\_char.roll.harm[i].cos \times \cos(fr\_t) \quad (3)$$

where $fr\_t = \text{PL\_to\_rad}(M\_char.roll.harm[i].freq) \times t^{anx}$.

$$sc\_att[2] = sc\_att[2] + M\_char.roll.bias \quad (4)$$

$$sc\_att[3] = \sum_{i=0}^{nharmonics-1} M\_char.yaw.harm[i].sin \times \sin(fy\_t) + M\_char.yaw.harm[i].cos \times \cos(fy\_t) \quad (5)$$

where $fy\_t = \text{PL\_to\_rad}(M\_char.yaw.harm[i].freq) \times t^{anxne}$.

$$sc\_att[3] = sc\_att[3] + M\_char.yaw.bias \quad (6)$$

PL_to_rad is a function to convert from degrees/sec to radians/sec.

In addition if the *dtype* = 1 (1st derivative), the rates are calculated for the pitch, roll and yaw, otherwise the rates are set to 0 if the *dtype* = 0 (no derivative)

$$sc\_datt[1] = \sum_{i=0}^{nharmonics-1} fp \times (-M\_char.pitch.harm[i].cos \times \sin(fp\_t) + M\_char.pitch.harm[i].sin \times \cos(fp\_t)) \quad (7)$$

where $fp = \text{PL\_to\_rad}(M\_char.pitch.harm[i].freq)$.

$$sc\_datt[2] = \sum_{i=0}^{nharmonics-1} fr \times (-M\_char.roll.harm[i].cos \times \sin(fr\_t) + M\_char.roll.harm[i].sin \times \cos(fr\_t)) \quad (8)$$

where $fr = \text{PL\_to\_rad}(M\_char.roll.harm[i].freq)$

$$sc\_datt[3] = \sum_{i=0}^{nharmonie-1} fy \times \left(-M\_char.yaw.harm[i].cos \times \sin(fy\_t) + M\_char.roll.harm[i].sin \times \cos(fy\_t)\right) \quad (9)$$

Where $fy = \text{PL\_to\_rad}\left(M\_char.yaw.harm[i].freq\right)$

B) Using Restituted Attitude file ($f = 1$)

First, the restituded attitude file (AUX_FRA_AX) corresponding to the desired orbit must be obtained and the Envisat CFI software PPF_ORBIT [RD 20] module (po_init_attitude_file) shall be called once after calling the "Load_data" function with the following input parameters:

Parameters	Values
mode_out	PP_ATT_HARMONIC
mode_perf	PP_NO_PERFO
mode_stat	PP_STATISTIC
perf_param[0]	100
perf_param[1]	100
perf_param[2]	100
perf_param[3]	1
perf_param[4]	0
perf_param[5]	0

Table 4.8.3.2-1 Input parameters for attitude s/w initialization

The S/C attitude information *sc_aocs*, *sc_att*, *sc_datt* are obtained from the Envisat CFI software PPF_POINTING (pp_get_attitude_aocs). It shall be called with the following parameters:

Parameters	Values
utc_time	mjdp output of orbit propagator

Table 4.8.3.2-2 Input parameters for get attitude s/w

4.8.3.2.2 Calculate the effective attitude information

1) Calculate the mispointing matrix corresponding to the input mispointing angles by three consecutive rotations over the pitch, roll and yaw to the relative satellite coordinate system. At this stage, additional attitude angles and rates may be specified in processing parameter file MIP_PS1_AX (*att0* and *datt0*) and added to the overall angles/rates.

pitch =PL_to_rad(*att0*[*1*] + *sc_att*[*1*])
roll = PL_to_rad(*att0*[*2*] + *sc_att*[*2*])
yaw = PL_to_rad(*att0*[*3*] + *sc_att*[*3*])

$M[1][1] = \cos(yaw)\times\cos(roll) + \sin(roll)\times\sin(yaw)\times\sin(pitch)$
$M[1][2] = \sin(yaw)\times\cos(pitch)$
$M[1][3] = \cos(yaw)\times\sin(roll) - \cos(roll)\times\sin(yaw)\times\sin(pitch)$
$M[2][1] = -\sin(yaw)\times\cos(roll) + \sin(roll)\times\sin(pitch)\times\cos(yaw)$
$M[2][2] = \cos(yaw)\times\cos(pitch)$
$M[2][3] = -\sin(yaw)\times\sin(roll) - \sin(pitch)\times\cos(yaw)\times\cos(roll)$
$M[3][1] = -\sin(roll)\times\cos(pitch)$
$M[3][2] = \sin(pitch)$
$M[3][3] = \cos(roll)\times\cos(pitch)$

$pitchd$ = PL_to_rad($datt0[1] + sc\_datt[1]$)
$rolld$ = PL_to_rad($datt0[2] + sc\_datt[2]$)
$yawd$ = PL_to_rad($datt0[3] + sc\_datt[3]$)

$$\begin{aligned}
M'[1][1] = &-\sin(yaw)\times\cos(roll)\times yawd - \cos(yaw)\times\sin(roll)\times rolld + \\
&\cos(roll)\times\sin(yaw)\times\sin(pitch)\times rolld + \\
&\sin(roll)\times\cos(yaw)\times\sin(pitch)\times yawd + \\
&\sin(roll)\times\sin(yaw)\times\cos(pitch)\times pitchd \\
M'[1][2] = &\cos(yaw)\times\cos(pitch)\times yawd - \sin(yaw)\times\sin(pitch)\times pitchd \\
M'[1][3] = &-\sin(yaw)\times\sin(roll)\times yawd + \cos(yaw)\times\cos(roll)\times rolld + \\
&\sin(roll)\times\sin(yaw)\times\sin(pitch)\times rolld - \\
&\cos(roll)\times\cos(yaw)\times\sin(pitch)\times yawd - \\
&\cos(roll)\times\sin(yaw)\times\cos(pitch)\times pitchd \\
M'[2][1] = &-\cos(yaw)\times\cos(roll)\times yawd + \sin(yaw)\times\sin(roll)\times rolld + \\
&\cos(roll)\times\sin(pitch)\times\cos(yaw)\times rolld + \\
&\sin(roll)\times\cos(pitch)\times\cos(yaw)\times pitchd - \\
&\sin(roll)\times\sin(pitch)\times\sin(yaw)\times yawd \\
M'[2][2] = &-\sin(yaw)\times\cos(pitch)\times yawd - \cos(yaw)\times\sin(pitch)\times pitchd \\
M'[2][3] = &-\cos(yaw)\times\sin(roll)\times yawd - \sin(yaw)\times\cos(roll)\times rolld - \\
&\cos(pitch)\times\cos(yaw)\times\cos(roll)\times pitchd + \\
&\sin(pitch)\times\sin(yaw)\times\cos(roll)\times yawd + \\
&\sin(pitch)\times\cos(yaw)\times\sin(roll)\times rolld \\
M'[3][1] = &-\cos(roll)\times\cos(pitch)\times rolld + \sin(roll)\times\sin(pitch)\times pitchd \\
M'[3][2] = &\cos(pitch)\times pitchd \\
M'[3][3] = &-\sin(roll)\times\cos(pitch)\times rolld - \cos(roll)\times\sin(pitch)\times pitchd
\end{aligned}$$

2) Calculate the effective mispointing matrix E by multiplying the MIPAS alignment matrix *AlignMat* with the mispointing matrix M.

$$[E] = [AlignMat] \times [M]$$

- If $dtype = 0$ (no derivative)

$$[E'] = 0$$

- If *dtype* = 1 (1st derivative)

[E'] = [AlignMat'] ×[M] + [AlignMat] × [M'],

but since [*AlingMat*] is constant, the [*AlignMat*'] = 0 and [*E*'] matrix is simplified to

[E'] = [AlignMat] × [M']

3) Calculate the effective mispointing angles from the effective mispointing matrix

pitch = asin(*E*[*3*][*2*])
roll = -atan2(*E*[*3*][*1*], *E*[*3*][*3*])
yaw = atan2(*E*[*1*][*2*], *E*[*3*][*3*])

e_att[*1*] = PL_to_deg(*pitch*)
e_att[*2*] = PL_to_deg(*roll*)
e_att[*3*] = PL_to_deg(*yaw*)

where PL_to_deg is a function to convert from radians to degrees

Note: *e_att*[*1*], *e_att*[*2*] and *e_att*[*3*] range is [-180, 180]

pitchd = *E'*[*3*][*2*] / cos(*pitch*)

rolld = - (*E'*[*3*][*1*] – sin(*roll*)×sin(*pitch*)×*pitchd*) / (cos(*roll*)×cos(*pitch*))
or
rolld = - (*E'*[*3*][*3*] + cos(*roll*)×sin(*pitch*)×*pitchd*) / (sin(*roll*)×cos(*pitch*))
When | sin(*roll*)×cos(*pitch*)| > | cos(*roll*)×cos (*pitch*) |

yawd = - (*E'*[*1*][*2*] – sin(*yaw*)×sin(*pitch*)×*pitchd*) / (cos(*yaw*)×cos(*pitch*))
or
yawd = - *(E'*[*2*][*2*] + cos(*yaw*)×sin(*pitch*)×*pitchd*) / (sin(*yaw*)×cos(*pitch*))
When | sin(*roll*)×cos(*pitch*)| > | cos(*roll*)×cos (*pitch*) |

e_datt[*1*] = PL_to_deg(*pitchd*)
e_datt[*2*] = PL_to_deg(*rolld*)
e_datt[*3*] = PL_to_deg(*yawd*)

4.8.3.3 Compute tangent height, longitude and latitude

This sub-function computes from actual pointing angles the actual geolocation of the target.

The geolocation (tangent height $\sigma(h)$, latitude and longitude) of the target shall be computed using the Envisat CFI software PPF_POINTING (pp_target) [RD 20] and the actual pointing $\varepsilon^{act}(t^{scene})$

after scan miror non-linearity correction and $\alpha^{act}(t^{scene})$. It shall be called with the following input parameters:

Parameters	Values
mjdp	mjdp output of orbit propagator
pos	pos output of orbit propagator
vel	vel output of orbit propagator
acc	acc output of orbit propagator
aocs	*sc_aocs*
att	*e_att*
datt	*e_datt*
idir	MIP_PS1_AX(83) = 7 (baseline)
dir	$\{\alpha^{act}(t^{scene}), \varepsilon^{act}(t^{scene}),0,0,0,0,0,0\}$
iray	MIP_PS1_AX(84) = 10 (baseline)
freq	$1550 \times c$
ieres	MIP_PS1_AX(85) = 1 (baseline)

Table 4.8.3.3-1 Input parameters for payload to target s/w

4.8.3.4 Estimate error on computed tangent height

Beside the tangent height also the error of the tangent height shall be computed using the information on estimated rms pointing errors.

In order to compute the tangent height error in rearward viewing geometry $\left(\alpha_{\min}^{rear} \le \alpha^{act}\left(t^{scene}\right) \le \alpha_{\max}^{rear}\right)$, the Envisat CFI Software has to be run another time at elevation angle $\varepsilon^{act}(t^{scene}) + \sqrt{\sigma_{\bar{\xi}_0}^2 + \left(\sigma_{\bar{c}_\xi} \cdot \cos\left(\omega_\xi\right)\right)^2}$. The rms error of the tangent height $\sigma(h)$ is approximately equal to the modulus of the difference between the two heights. In sideways viewing geometry $\left(\alpha_{\min}^{side} \le \alpha^{act}\left(t^{scene}\right) \le \alpha_{\max}^{side}\right)$ the tangent height errors may be computed accordingly using $\sigma_{\bar{\eta}_0}$ and $\sigma_{\bar{c}_\eta}$ for the rms pointing error, respectively.

4.8.4 Computational Sequence

The *Calculate Geolocation* function receives control from the *Calculate Pointing* function when actual pointing have been determined. The *Calculate Geolocation* function processes pointing data belonging to radiometrically and spectrally processed spectra and send control back to the *Calculate Radiance* function.

The output is generated if the instrument is commanded in measurement mode.

The computational sequence of the *Calculate Geolocation* function is illustrated by the flowchart of figure 4.8.4-1.

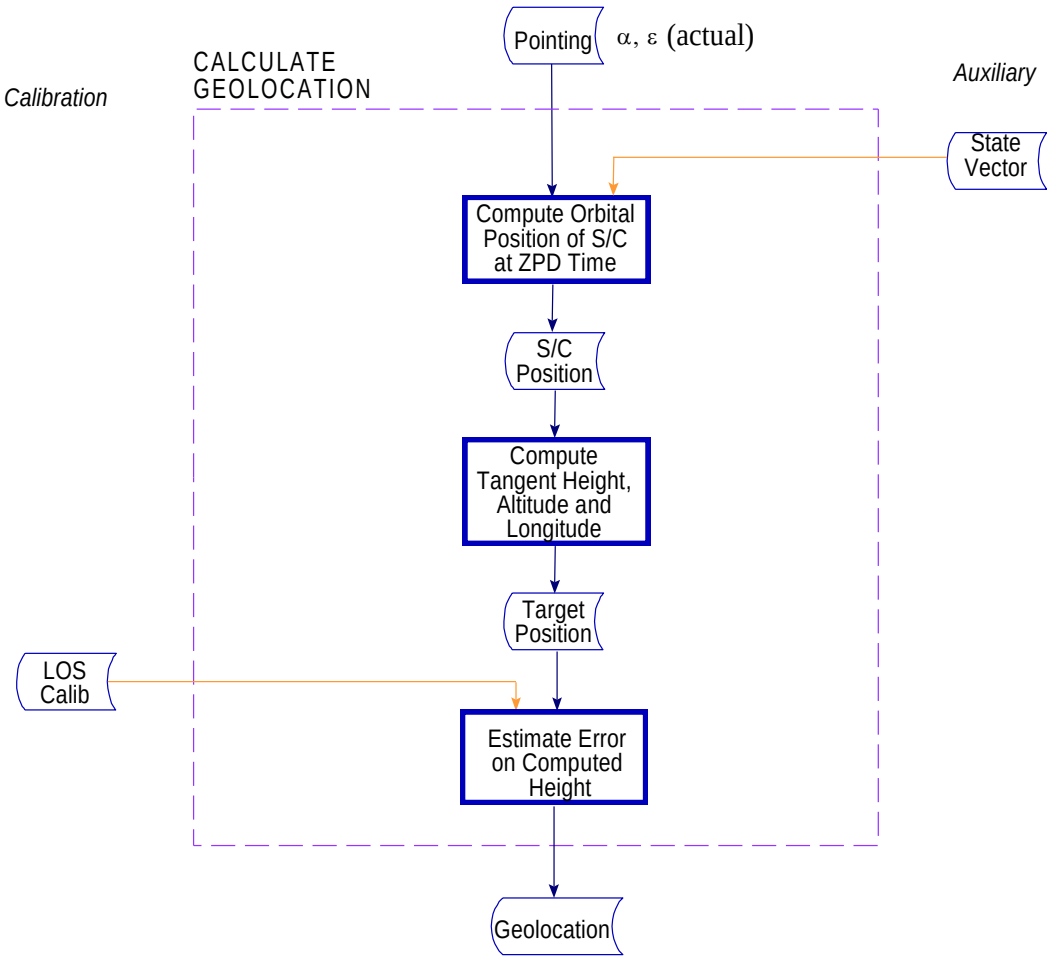

Figure 4.8.5-1 *Calculate Geolocation* flowchart

4.9 MAIN PROCESSING SUBFUNCTIONS

The following subfunctions are processing units defined throughout the document and assembled in specific subfunctions for more clarity and ease of implementation. Tables are given for the local variables used for each subfunction described.

In all the following subfunctions, the prime ($'$) symbol signifies the output modified variable. For example, in:

$$I'(n) = \text{CorrectSpikes}\{I(n), N\} \quad (1)$$

$I(n)$ is the incoming interferogram and $I'(n)$ is the corrected one.

4.9.1 Spikes detection

This subfunction has the purpose of detecting spurious spikes in an interferogram. The presence of spikes in an interferogram can be caused by cosmic radiation or transmission errors. This scene will be flagged of having corrected for one or more spikes. Is a spike is detected in a gain or in an offset measurement, this measurement will be discarded in order to avoid corrupting all of the subsequent calibrated spectra.

4.9.1.1 Definition of variables

Variable	Descriptive Name	I/O	Type	Ranges / References / Remarks
	Spikes detection			
$I(n)$	Input complex IGM	i / o	c	correction is done directly on the given IGM
N_{zpd}	Number of data points to reject on each side of ZPD	t	i	= 10
N_{mpdp}	Number of data points to reject near MPD (if required)	t	i	= 10
τ	Threshold for spike identification	i	r	= 5, MIP_PS1_AX (32)
n_{std}	Number of samples on each side of detected spike for statistics computation	i	i	= 40, MIP_PS1_AX (31)
is_spike	Flag for spike identification	o	i	
k_{spike}	Spike position	o	i	
$r(k)$	Ratio of spike amplitude to noise	o	r	
D	Decimation factor	i	i	input from given IGM
$NFilter_{zpd}$	Number of data points to filter in central part of phase interferogram	t	i	= (4000 / D) + D

The spike detection/correction, is an iterative process that is performed for a maximum number of corrected spikes. First the spike detection algorithm is applied to find the highest spike exceeding the threshold τ. If a spike is found, the spike correction algorithm is applied to the interferogram to get the corrected interferogram $I'(n)$, otherwise the iterative detection/correction process is stopped. At the next iteration, the corrected interferogram $I'(n)$ is used as the input of the DetectSpike function and the next highest spike exceeding the threshold is found. If a spike is found at the same location as in the previous iteration, the detection/correction process is stopped

$$is\_spike = \mathrm{DetectSpike}\{I(n), N_{zpd}, N_{mpd}, n_{std}, k_{spike}, \tau, r\} \quad (1)$$

$$I'(n) = \mathrm{CorrectSpike}\{I(n), k_{spike}\} \quad (2)$$

4.9.1.2 Implementation of the spike detection

The spike detection algorithm relies on a signal characteristic that is specific to FTS data: the strong phase relationship (correlation) between all frequencies. Interferograms are ideally symmetric signals that have a real spectrum without imaginary part. Although the correlation between the amplitude of the different spectral components can be very week, the phase correlation is strong. With an ideal interferogram, the phase of all spectral components is null. For an actual spectrometer, the phase of the spectrum is slowly varying due to optical and electrical dispersion (and possibly numerical dispersion due to numerical filtering). Other phenomena affecting the phase are the delay (non centered ZPD) and the noise, which has a non-symmetric signature in the interferogram. The delay do not change the correlation level (linear phase).

Whenever a spike occurs in the interferogram, it will break the interferogram symmetry around the ZPD and create an oscillation in the phase of the spectrum. Even though the interferogram is not truly symmetric due to dispersion, the phase variations due to the dispersion will be easily discerned from the spike induced phase, unless the spike occurs in the vicinity of the ZPD. Note that the phase of the spectrum cannot be analyzed directly due to SNR variations. The phase is more revealing when looking at its Fourier transform.

Relying on the phase information has another advantage. The filtering and decimation do not alter significantly the phase of the spectrum (although the interferogram becomes complex), except for the dispersion of the filter.

The algorithm to perform this operation can be described as follows:

Step 1: Compute a spectrum from the (complex) interferogram using FFT. There is no need to re-center the ZPD in the interferogram at this step:

$$\mathbf{spc}[n] = \mathrm{FFT}\{\mathbf{igm}[k]\}. \quad (2)$$

Step 2: To compute the interferogram of the phase, $\mathbf{igm}_{phase}[k]$, perform the ratio of the spectrum and its modulus:

$$\mathbf{phase}[n] = \frac{\mathbf{spc}[n]}{|\mathbf{spc}[n]|}. \quad (3)$$

Then, an optional high pass filter, $\mathbf{filter}_{highpass}[n]$ can be applied to remove the low frequency phase variations due to the spectrometer. Afterwards perform the inverse Fourier transform of the filtered phase to get the phase interferogram.
Applying the filter after performing the inverse Fourier transform of the phase, has the advantage to use only a vector multiplication instead of a convolution. Note that it is highly recommended to add a delay to the filter such that the position of the 'DC' value is shifted at the position of the ZPD.

$$\mathbf{igm}_{phase}[k] = \mathrm{IFT}\{\mathbf{phase}[n]\}, \tag{4}$$

$$\mathbf{F}_{highpass}[k] = \mathrm{IFT}\{\mathbf{filter}_{highpass}[n]\}. \tag{5}$$

The high pass filter chosen is a first order derivative filter since its Fourier transform is readily computed.

$$\mathbf{F}_{highpass}[k] = k - k_{zpd}\,. \tag{5}$$

Step 3: Identify the position k_{zpd} of the ZPD from the maximum value of the phase interferogram modulus, in order to apply the high pass filter and later to identify the position of the potential spike, To cover cases where spikes occur closed to ZPD position and have a magnitude greater than ZPD itself, a low pass apodizing function is applied at the center of the phase interferogram before finding the ZPD position.

$$W_{howpass}[x] = 1 - \frac{|x|}{NFilter_{zpd}} \quad \text{for} - NFilter_{zpd} < x < NFilter_{zpd} \tag{6a}$$

$$W_{howpass}[x] = 0 \quad \text{for} - NFilter_{zpd} \le x \;\; and \; x \ge NFilter_{zpd} \tag{6b}$$

Find the maximum value of the following equation

$$Max_{zpd} = \max_{k} \left| \mathbf{igm}_{phase}[k] W_{howpass}[k - N/2] \right|, \quad k = 1,...,N\,. \tag{6c}$$

k_{zpd} is the index position of Max_{zpd}

$$Max_{zpd} = \left| \mathbf{igm}_{phase}[k_{zpd}] W_{howpass}[k_{zpd} - N/2] \right| \tag{6d}$$

Step 4: Apply the high pass filter properly delayed to be centered at the ZPD position to get a phase interferogram with a lower weight to the ZPD region:

$$\mathbf{igm}_{phaseh.p.}[k] = \mathbf{igm}_{phase}[k]\mathbf{F}_{highpass}[k - k_{zpd}]. \tag{7}$$

Step 5: Compute the standard deviation σ[k] of the phase interferogram on each side of each position k, excluding the position k itself, using n_{std} points on each side (we assume zero mean interferogram):

$$\boldsymbol{\sigma}[k] = \sqrt{\frac{1}{2n_{std} - 1} \sum_{k'=k-n_{std}}^{k-1} \left| \mathbf{igm}_{phaseh.p.}[k'] \right|^2 + \frac{1}{2n_{std} - 1} \sum_{k'=k+1}^{k+n_{std}} \left| \mathbf{igm}_{phaseh.p.}[k'] \right|^2} \tag{8}$$

In order to speed up the calculation, the computation may be done through a convolution using Fourier transforms (similar to a moving average):

$$\mathbf{filter}_{m.a.}[k] = \begin{cases} 1/(2n_{std}-1) & k = 2,...,n_{std}+1; N-n_{std}+1,...,N \\ 0 & \text{elsewhere} \end{cases} \tag{9}$$

$$\boldsymbol{\sigma}[k] = \sqrt{\left| \mathrm{IFT}\left\{ \mathrm{FFT}\left\{ \left| \mathbf{igm}_{phaseh.p.}[k] \right|^2 \right\} \times \mathrm{FFT}\{ \mathbf{filter}_{m.a.}[k] \} \right\} \right|} \tag{10}$$

Step 6: Compute the amplitude ratio of the phase interferogram for each position *k*:

$$\mathbf{r}[k] = \frac{\left| \mathbf{igm}_{phaseh.p.}[k] \right|}{\boldsymbol{\sigma}[k]}. \tag{11}$$

Step 7: Identify the position k_{left} and k_{right} of the highest feature of the amplitude | **igm**[*k*] | on each side of the ZPD, excluding points when **r**[*k*] <= τ, and n_{zpd} points near ZPD and n_{mpd} points near MPD if required. Spikes will leave signatures in the amplitude ratio of the phase interferogram symmetrically positioned on both side of ZPD in most cases:

If $r = \mathbf{r}[k] > \tau$ then

$$\begin{aligned} k_{left} &= \max_k |\mathbf{igm}[k]|, \quad k = n_{mpd},...,k_{ZPD} - n_{zpd} \\ k_{right} &= \max_k |\mathbf{igm}[k]|, \quad k = k_{ZPD} + n_{zpd},...,N - n_{mpd} + 1 \end{aligned} \tag{12}$$

Step 8: In order to identify on which side of the ZPD the spike is located, we select the position k_{left} or k_{right} for which the modulus of the interferogram is maximum:

$$k_{spike} = \max_k |\mathbf{igm}[k]|, \quad k = k_{left}, k_{right} \tag{13}$$

Step 9: If the ratio at the largest spike is larger than the threshold τ, $r = \mathbf{r}[k_{spike}] > \tau$, then a spike has been identified at position k_{spike}. Set *is_spike* to 1

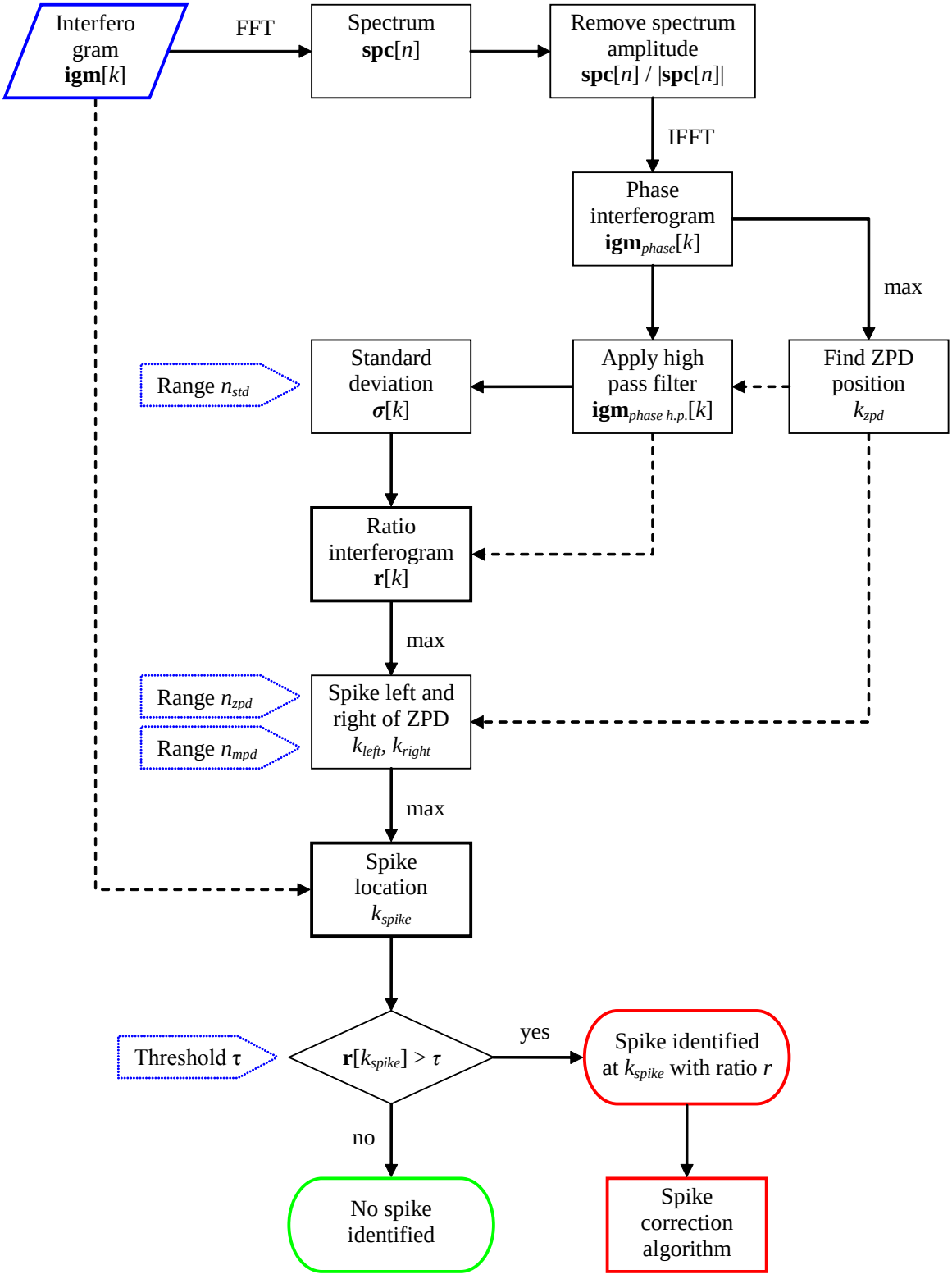

Figure 4.9.1-1 Spike Detection flowchart

4.9.1.3 Implementation of the spike correction

If *is_spike* is set to 1, at least one spike has been detected and the spike correction algorithm must be applied.

At the detected spike position, shrink the spike vector [k_{spike} - 3 , k_{spike} + 3] at an amplitude level determined by the average of the modulus at k_{spike} - 4 and at k_{spike} + 4. Each data point of the spike vector is iteratively divided by a factor 2 until the modulus of the point is smaller than the noise level.

$$Noise\_Level = \frac{|Igm[k_{spike}-4]| + |Igm[k_{spike}+4]|}{2} \quad (1)$$

Set the initial value of I'[n]:

$$I'_{imag}[n] = Igm_{imag}[n] \text{ and } I'_{real}[n] = Igm_{real}[n] \quad (2)$$

For *n* between [k_{spike} - 3 , k_{spike} + 3], stop reducing the amplitude of the data point when the modulus of *I'* is smaller than *Noise_Level*, otherwise keep reducing *I'* by a factor of 2.

$$|I'[n]| \le Noise\_Level \quad (3)$$

$$I'_{imag}[n] = \frac{I'_{imag}[n]}{2} \text{ and } I'_{real}[n] = \frac{I'_{real}[n]}{2} \quad (4)$$

4.9.2 Interpolation

For a given vector $f(x_k)$ defined on N points, the ideal interpolation function is the *sinc* function:

$$f(x) = \sum_{i=-w}^{w} f(x_{k+i})\,\mathrm{Sinc}[i-\delta] \qquad (1)$$

with the following definition: $\mathrm{Sinc}[a\,x] \equiv \dfrac{\sin(\pi\,a\,x)}{\pi\,a\,x}$

x is limited inside the vector: $x_0 \le x \le x_{N-1}$

k is the interpolation coefficient index: $k = \mathrm{Floor}\left\{\dfrac{x-x_0}{\Delta x}\right\}, \quad 0 \le k \le N-1$

δ is the offset between two discrete points: $\delta = \dfrac{x-x_k}{\Delta x}, \quad 0 \le \delta < 1$

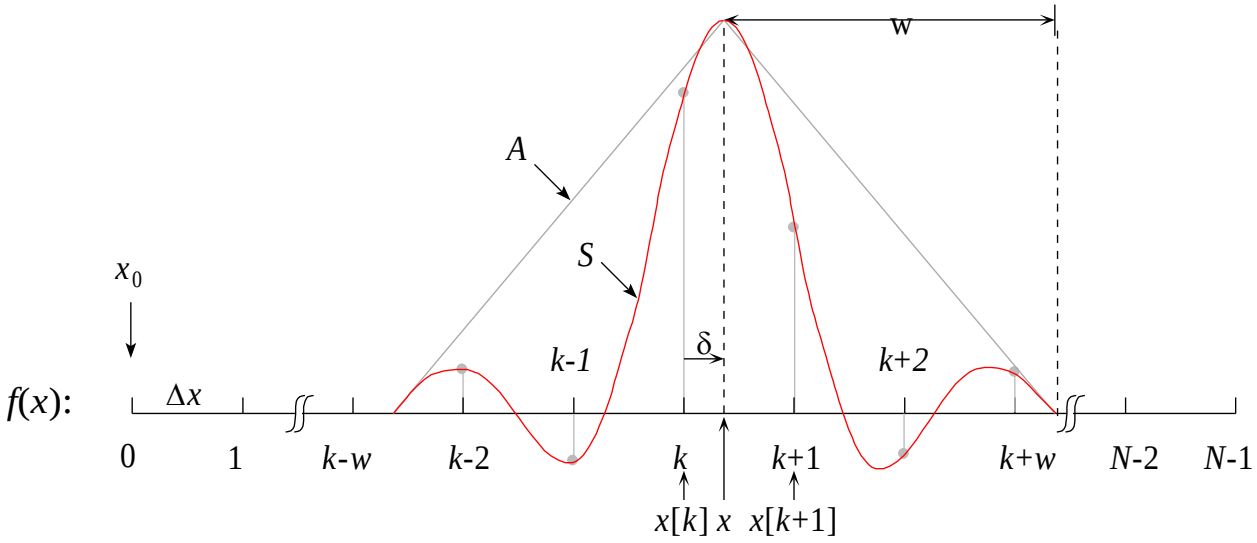

with $x_k = x_0 + k\Delta x$

The values of the interpolation function at arbitrary positions within integer sampling positions, occurs at fractional δ values.

The sinc function by itself decays very slowly, and it needs to be evaluated over a wide range of the spectral axis in order to provide good accuracy. Ideally, the span of the sinc would be infinite ($W \to \infty$), so that the function would decrease to zero at the extremities. In practice however, numerical vectors are of finite extent and contain a limited number of points. An apodization function is useful to compensate for this effect. A simple triangular Bartlett function

could be successfully used, but more sophisticated ones like the Hanning and the Blackman functions lead to more precise results for same *w*.

The apodized interpolation function can be written as:

$$f(x) = \sum_{i=-w}^{w} f(x_{k+i})\, S(w,\delta,i) \tag{2}$$

where *w* is an integer defining the extent of the width of the apodizing window. With the definition $N^{si} = 2w+1$, N^{si} is the number of sampling intervals defining the range over which we want to evaluate the interpolation function. It can also be seen as the number of zeroes that the sinc function encompasses.

The interpolating function *S* is given by:

$$S(w,\delta,i) = \frac{\mathrm{Sinc}\left[i-\delta\right] A\left(\dfrac{i-\delta}{w}\right)}{\displaystyle\sum_{j=-w}^{w} \mathrm{Sinc}\left[i-\delta\right] A\left(\dfrac{i-\delta}{w}\right)} \tag{3}$$

The area of the *S* function needs to be unitary in order to give correct results (with no introduction of excessive energy). This requires that the sum of the coefficients used by the interpolation function be unitary. The argument of the apodizing function *A* is defined between –1 and +1.

According to the numerical precision requirements, the accuracy of the interpolation of a spectrum can be substantially increased by zero filling the corresponding interferogram to the double of its original width. This doubles the density of the vector to be interpolated, and lowers the errors caused by the apodizing function. One way to see this is in the spatial domain, where the lateral parts of the filter function (where the error is maximal) now multiply the added zeroes on the lateral parts of the extended interferogram.

In the extreme case of the interpolation of a single impulsion, the different apodizing functions lead to the following maximum relative error, in comparison with an ideal infinite sinc interpolation. Results are given in the case of a double-width zero filling.

Bartlett: $$A(p) = \begin{cases} 1-|p| & -1 \le p \le 1 \\ 0 & \text{otherwise} \end{cases} \qquad \text{err} = 1\times10^{-3} \tag{4}$$

Hanning: $$A(p) = \begin{cases} 0.5\left[1+\cos(\pi p)\right] & -1 \le p \le 1 \\ 0 & \text{otherwise} \end{cases} \qquad \text{err} = 5\times10^{-5} \tag{5}$$

Blackman: $$A(p)=\begin{cases}0.42+0.5\cos(\pi p)+0.08\cos(2\pi p) & -1\le p\le 1\\ 0 & \text{otherwise}\end{cases}$$ err = 1×10^{-5} (6)

Gaussian: $$A(p)=\begin{cases}e^{-10p^2} & -1\le p\le 1\\ 0 & \text{otherwise}\end{cases}$$ err = 1×10^{-5} (7)

4.9.2.1 Definition of variables

The various variables used by the sinc interpolation algorithm are given in the following table with their description and ranges.

Variable	Descriptive Name	I/O	Type	Ranges / References / Remarks
	Sinc interpolation			
$S(n^{in})$	Input signal	i	c	can be a SPC or also an IGM
n^{in}	Index points of input signal	i	i	$n^{in} = 0,\ldots,N^{in}-1$
$\Delta\sigma^{in}$	Sampling of input signal	i	r	
σ_0^{in}	Origin of input signal	i	r	
N^{in}	Number of points of input signal	i	i	
$f(x_k)$	Input vector to be interpolated	i	r	
$S(w,\delta,i)$	Apodized sinc interpolating function	t	r	Total area of the function must be unitary
$A(p)$	Apodizing window function	t	r	$-1 \le p \le 1$
N	Number of points of the input vector	i	i	N needs not to be a power of 2
k	Index of data points in the input vector	l	i	$k = 0,\ldots,N-1$
Δx	Spacing between data points	i	r	Can be in cm^{-1} or cm
x_0	Starting value of abscissa axis	i	r	
x_k	Abscissa value of point k	t	r	$x_k = x_0 + k\,\Delta x$
N^{si}	Number of sampling intervals defining the range	a	i	MIP_PS1_AX(35)
N^{psi}	Number of points per sampling intervals	a	i	$4 \le N^{psi} \le 1024$ N^{psi} = MIP_PS1_AX(36) – 1
δ	Offset between two discrete points	t	r	$\delta \in [0..1]$
w	Width of the apodizing function	t	r	$w = (N^{si}-1)/2$
i	Index in the interp. table	l	i	$i = -w,\ldots,+w$
l	Index in the interp. table	l	i	$l \in [0..N^{psi}]$
Coef	Interpolation coefficients table	a	r	Dimension $N^{si} \times (N^{psi}+1)$ MIP_PS1_AX(37)
$S'(n^{out})$	Output signal	o	c	output of *Interpolate*
n^{out}	Index points of output signal	l	i	$n^{out} = 0,\ldots,N^{out}-1$
$\Delta\sigma^{out}$	Requested sampling of output signal	i	r	
σ_0^{out}	Requested origin of output signal	i	r	
N^{out}	Requested number of points in output signal	i	i	

4.9.2.2 Tabulation of the sinc function

In order to speed up the numerical computation by avoiding the re-evaluation of the interpolation function each time an interpolated value is needed, a lookup table needs to be built for the calculated values. For this operation, the offset δ is limited to N^{psi} discrete values extending between 0 and 1. One lookup table column contains all the coefficients for interpolation for a given offset from the sampled point of the vector. The table contains many columns for different offsets.

We then have:

$$f(x) = \sum_{i=-w}^{w} f(x_{k+i})\,\mathrm{Coef}(i,l) \tag{1}$$

l is the index in the interpolation table: $l = \mathrm{Floor}\left(\delta\, N^{psi} + \frac{1}{2}\right), \quad l \in [0..N^{psi}]$

(+1/2 ensures the rounding to the correct position)

$$\mathrm{Coef}(i,j) = \frac{\mathrm{Temp}(i,j)}{\sum_{n=-w}^{w}\mathrm{Temp}(n,j)} \quad \begin{matrix} i = -w,\ldots,w & (2w+1 = N^{si}\ \text{points}) \\ j = 0,\ldots,N^{psi} & (N^{psi}+1\ \text{points}) \end{matrix} \tag{2}$$

$$\mathrm{Temp}(i,j) = \mathrm{Sinc}\left[i - \frac{j}{N^{psi}}\right] A\left(\frac{i - j/N^{psi}}{w}\right) \tag{3}$$

4.9.2.3 Linear interpolation of coefficients in lookup table

To ensure minimal precision the parameter w should large enough in order to leave a minimal number of oscillations from the sinc function ($w \geq 4$). The number of different precomputed offsets in the table will also determine (in a less important manner) the precision of the interpolation. For a given value of N^{psi}, the precision could be further increased by using linear interpolation between coefficients from adjacent columns. This requires a little more computation, but it needs a smaller value of N^{psi} in order to achieve the same accuracy.

$$\mathrm{Coef}(i,l) \rightarrow (1-\delta')\cdot\mathrm{Coef}(i,l') + \delta'\,\mathrm{Coef}(i,l'+1) \tag{1}$$

l' is the index of the interpolation table: $l' = \mathrm{Floor}\left(\delta\, N^{psi}\right), \quad l \in [0..N^{psi}[$

δ' is the new offset: $\delta' = \delta N^{psi} - l', \quad \delta \in [0..1[$

4.9.2.4 Use of half of the lookup table

Coming from the fact that the interpolation function is even, the lookup table contains redundant information and only half of its values are really needed for the computation. The last column can also be deleted because it corresponds to a shifted equivalent of the first column.

$$f(x) = \underbrace{\sum_{i=0}^{w} f(x_{k+i-w})\ \mathrm{Coef}'(i,l)}_{\text{if } (l<N^{psi})} + \underbrace{\sum_{i=1}^{w} f(x_{k+i})\ \mathrm{Coef}'(1-i+w, N^{psi}-l)}_{\text{if } (l>0)} \quad (1)$$

where:

$$\mathrm{Coef}(i,j) = \frac{\mathrm{Temp}(i,j)}{\mathrm{Temp}(w,j) + 2\sum_{n=0}^{w-1}\mathrm{Temp}(n,j)} \quad \begin{matrix} i=0,\ldots,w & (w+1=(N^{si}+1)/2 \text{ points}) \\ j=0,\ldots,N^{psi}-1 & (N^{psi} \text{ points}) \end{matrix} \quad (2)$$

$$\mathrm{Temp}(i,j) = \mathrm{Sinc}\left[\, i-w-\frac{j}{N^{psi}} \,\right] A\left(\frac{i-w-j/N^{psi}}{w}\right) \quad (3)$$

However, this option does not represents a significant gain in required computing versus storage space.

The lookup table would be provided as an input file for the normal ground processing. N^{si} and N^{psi} need to be available during normal ground processing for the correct use of the interpolation table. The optimum values used for these two parameters (leading to correct results with the fastest computation time) depend on the signal to interpolated and need to be investigated.

4.9.2.5 Implementation of the interpolation

The following function call defined throughout the present document:

$$S'(n^{out}) = \mathrm{Interpolate}\left\{S(n^{in});\ \Delta\sigma^{in}, \sigma_0^{in}, N^{in} \rightarrow \Delta\sigma^{out}, \sigma_0^{out}, N^{out}\right\} \quad (1)$$

represents $S(n^{in})$ as is the input function defined on N^{in} points, with numerical spectral axis values starting from σ_0^{in} and separated by $\Delta\sigma^{in}$. The spectral indices range of the input function is $n^{in}=0,\ldots,N^{in}-1$. The output interpolated function $S'(n^{out})$ will be computed on N^{out} points, on a requested spectral axis starting from σ_0^{out} and separated by $\Delta\sigma^{out}$. Spectral indices range of the output function will be $n^{out}=0,\ldots,N^{out}-1$.

Numerical interpolation shall be implemented as:

$$S'(n^{out}) = \sum_i S(k+i)\cdot Coef(i,l) \quad (2)$$

where $i = -w,...,+w \qquad w = \left(N^{si} - 1\right)/2 \quad \text{if } N^{si} \text{ is odd}$

$i = -w+1,...,+w \qquad w = N^{si}/2 \quad \text{if } N^{si} \text{ is even}$

and the following parameters:

$$\begin{cases} k = \text{Floor}\left(\dfrac{\sigma_0^{\text{out}} + n^{out}\Delta\sigma^{out} - \sigma_0^{\text{in}}}{\Delta\sigma^{in}} \right) \\ \delta = \dfrac{\sigma_0^{\text{out}} + n^{out}\Delta\sigma^{out} - \sigma_0^{\text{in}} - k\,\Delta\sigma^{in}}{\Delta\sigma^{in}} \\ l = \text{Floor}\left(\delta \cdot N^{psi} + 0.5\right) \end{cases}$$

and the previous definition of *Coef*.

4.9.3 Fringe count error detection and correction

4.9.3.1 Definition of variables

Variable	Descriptive Name	I/O	Type	Ranges / References / Remarks
	Fringe count error detection			
h_j^{sys}	Systematic OPD shift for a given band	i	i	
$S_{j,d}(m)$	Input spectrum	i	c	given in argument to the function
m	Input SPC data point index	l	i	$m = 0,\ldots,N_j - 1$
$\sigma_j(m)$	Spectral axis vector of the input spectrum	i	r	wavenumber values
Δx	Sampling interval	i	r	given in argument to the function
$\phi_{j,d}(m)$	Spectral phase of the spectrum	t	r	j is limited to the B and C bands
$\delta\phi_{j,d}$	Slope of the spectral phase	t	r	
$\phi_{0,j,d}$	Ordinate at the origin of the spectral phase	t	r	
s_h	Standard deviation of the fit	t	r	used for FCE detection validation
$h_{j,d}$	Computed OPD shift	t	i	integer giving the measured FCE for a given band
h_d	Computed OPD shift	o	i	integer output of *FCE Detect* giving the measured FCE
	Fringe count error correction			
$I_{j,d}(n)$	Input spectrum and corrected output	i / o	c	correction is done directly on the given IGM
$S_{j,d}^{FCE}(m)$	Spectrum used in convolution	t	c	
$\sigma_j(m)$	equivalent wavenumber vector	i	r	computed from the IGM by the unscrambling method
$C_{j,d}(m)$	Phase correction spectral function	t	c	

4.9.3.2 Implementation of the FCE detection

The fringe count error detection, as defined throughout the document by the following function call:

$$h_d = \text{FCE Detect}\left\{S_{j,d}(m), \sigma_j(m), \Delta x, h_j^{sys}\right\} \quad (1)$$

computes the OPD shift from a given spectrum, returning the number of fringe count errors identified in the corresponding interferogram. Δx is the current value of the IGM sampling (before decimation) given in argument.

The first step for the FCE detection is the calculation of the spectral phase:

$$\phi_{j,d}(m) = \tan^{-1}\left(\frac{\mathrm{Im}\{S_{j,d}(m)\}}{\mathrm{Re}\{S_{j,d}(m)\}}\right) \tag{2}$$

with *j* limited to the B and C bands.

This calculation should include an "un-wrapping" of the phase in case it exceeds the range [-π,+π]. Compensations of ±2π are added to the phase where discontinuities (absolute difference greater than π) are noticed between two consecutive points.

The second step is a linear regression of the phase $\phi_{j,d}(m)$ versus the wavenumber $\sigma_j(m)$.

$$\phi_{0\,j,d}, \delta\phi_{j,d} = \mathrm{LinearFit}\left\{\phi_{j,d}(m), \sigma_j(m)\right\} \tag{3}$$

The output consists of two values per band and sweep direction.

$\delta\phi_{j,d}$	the slope
$\phi_{0\,j,d}$	the origin, i.e. the value of the fit at *m* = 0. (shall be approximately 0)

The validity of the slope can be checked by verifying the linear dispersion of the calculated points. This check is performed to confirm that the phase compensation has been correctly performed and that the fringe count has been properly identified. The approach is to compute the standard deviation of the points along the computed line:

$$s_h = \sqrt{\frac{1}{N_j - 1}\sum_{m=0}^{N_j-1}\left[\phi_{j,d}(m) - (\delta\phi_{j,d}\cdot\sigma_j(m) + \phi_{0,j,d})\right]^2} \tag{4}$$

An error should be reported if the value of s_h is larger than 0.1 (hard coded value) after a maximum of 5 iterations. Between each iteration, an elimination of the data points exceeding 1 standard deviation is done before recalculating the phase slope by linear regression.

$$abs(\phi_{j,d}(m) - (\delta\phi_{j,d}\cdot\sigma_j(m) + \phi_{0,j,d})) > s_h \tag{4a}$$

The calculated OPD shift shall be the same for all detectors. The OPD shift shall be an integer giving the number of fringe count displacement in the measured interferogram:

$$h_{j,d} = \mathrm{Round}\left\{\frac{\delta\phi_{j,d}}{2\pi\cdot\Delta x}\right\} + h_j^{sys} \tag{5}$$

Finally, if $h_{B,d}$ and $h_{C,d}$ are equal then the output value is $h_d = h_{B,d} = h_{C,d}$. If they are different, then the output value corresponds to the one of band *j* where the ratio of data point kept in the phase is higher i.e., $h_d = h_{j,d}$ for which N'_j / N_j is larger. Then an error should be reported but the sweep is still valid.

4.9.3.3 Implementation of the FCE correction

The fringe count error correction, as defined throughout the document by the following function call:

$$I'_{j,d}(n) = \text{FCE Correct}\left\{ I_{j,d}(n), h_d, \Delta x \right\} \quad (1)$$

corrects for the OPD shift present in a given interferogram according to the pre-computed FCE value h_d. Δx is the current value of the IGM sampling (before decimation) given in argument.

The current approach is to perform a convolution with a shifting function, by means of Fourier multiplication to interpolate the interferogram back to its original centered position.

The first step is to zero-fill the interferogram (to a power of 2) and compute the corresponding spectrum with a Fourier transform:

$$S^{FCE}_{j,d}(m) = \text{FFT}\left\{ I_{j,d}(n) \right\} \quad (2)$$

The spectrum vector is computed with the unscrambling method described in Section 4.10.2, and spectral axis vector $\sigma_j(m)$ corresponds to equation (4) of that same section.

Then, the phase correction shifting spectral function is computed on the same spectral axis:

$$C_{j,d}(m) = \exp(-2\pi i \cdot \sigma_j(m) \cdot h_d \cdot \Delta x) \quad (3)$$

A convolution of the interferogram is then performed by a point by point multiplication of the spectrum by the shifting function:

$$S'^{FCE}_{j,d}(m) = S^{FCE}_{j,d}(m) \cdot C_{j,d}(m) \quad (4)$$

The interferogram is finally restored by doing an inverse Fourier transform. Before the inverse Fourier transform, a scrambling (inverse of the method described in Section 4.10.2) must be done:

$$I_{j,d}(n) = \mathrm{IFFT}\left\{S_{j,d}^{FCE}(m)\right\} \tag{5}$$

The final step is to remove the points added by the zero-filling of the IGM, in order to discard the artifacts that appeared on these points.

4.9.4 Non-linearity correction

4.9.4.1 Definition of variables

Variable	Descriptive Name	I/O	Type	Ranges / References / Remarks
	Non-linearity correction			
$I_j(n)$	IGM to be corrected	i/o	c	correction is done directly on the given IGM
ADC_j^{Max} ADC_j^{Min}	Maximum and minimum values of the digitized IGM	i	i	input from *Load Data* function. Integer values as given by the ADC before filtering and decimation.
Δx_j^{dec}	Sampling interval	i	r	input from *Load Data* function.
N_j^{req}	Number of points in band *j* for requested spectral axis	a	i	MIP_PS1_AX(7)
$\Delta\sigma_j^{req}$	Wavenumber spacing in band *j* for requested spectral axis	a	i	Computed from MIP_PS1_AX(7,8,9)
φ_{DC}	Total photon flux on detector	t	r	In units of [d.u.]
φ_j^{Max} φ_j^{Min}	Validity limits of photon flux associated the fit coefficients	a	r	In units of [d.u.] MIP_CA1_AX(13.1)
$c_{q,j,d}$	Responsivity polynomial fit coefficients corresponding to a given non-linear detector and sweep direction	a	r	Polynomial order is 4 *j* covers only the index of non-linear detectors, A1, A2, AB and B MIP_CA1_AX(13)
k_R	Responsivity scaling factor	i	r	function of temperature at the DTUs. From *Load Data* function
$k_{G,j}$	Gain scaling factor	i	r	defined by PAW gain switching. From *Load Data* function
q	index of polynomial coefficient	l	i	The range of q is $q = 0,\ldots,3$
SF	Scaling factor	t	r	scalar value
$I'_j(n)$	Corrected IGM	o	c	output of *CorrectNL*

4.9.4.2 Implementation of the correction

The non-linearity correction, as defined throughout the document by the following function call:

$$I'_j(n) = \text{CorrectNL}\left\{I_j(n), ADC_j^{Min}, ADC_j^{Max}, c_{q,j,d}\right\} \quad (1)$$

can be implemented according to the ASCM method, defined as follows.

The first step for non-linearity correction is to compute the total incoming photon flux φ_{DC} (in digitalization units [d.u.]) at the origin of the present interferogram. This meaningful parameter

can be estimated with the minimum and maximum values of the digitized IGM by the ADC before filtering and decimation, noted as ADC_j^{Max} and ADC_j^{Min}.

$$\varphi_{DC} = \left(ADC_j^{Max} - ADC_j^{Min} \right) \cdot k_{G,j} \cdot k_R \tag{2}$$

Then the scaling factor and the constant flux coefficient can be computed from this total photon flux φ_{DC} and the responsivity coefficients $c_{q,j,d}$ of detector j expressed in digitalization units:

$$SF\left(\varphi, c_{q,j,d}\right) = 1 + c_{0,j,d}\varphi + c_{1,j.d}\varphi^2 + c_{2,j,d}\varphi^3 + c_{3,j,d}\varphi^4 \quad \text{[n.u.]} \tag{3}$$

The real and imaginary parts of the incoming interferogram can then be independently corrected with the following equation:

$$I'_j(n) = \frac{I_j(n)}{SF} \tag{4}$$

Note that if the incoming photon flux is out of range i.e., not in the validity limits $\varphi_j^{Min} \le \varphi_j^{DC} \le \varphi_j^{Max}$ then an error message should be issued and the corresponding PCD set.

4.9.5 Equalization and combination

4.9.5.1 Definition of variables

Variable	Descriptive Name	I/O	Type	Ranges / References / Remarks
	Equalization and combination			
$I_{j,d}(n)$	Input IGMs to be equalized and combined	i	c	for j = A1 and A2
j_A^{eq}	Index of equalized channel in band A	a	i	j_A^{eq} = A1 or A2 MIP_CA1_AX(17)
$F_j^{eq}(c)$	Complex equalization filter coefficient vector	a	c	MIP_CA1_AX(19)
N^{cf}	Number of coefficients in the equalization filter	a	i	16 or 32 MIP_CA1_AX(18)
c	Index of the equalization filter coefficient	t	l	$c = -N^{cf}/2,\ldots,N^{cf}/2-1$
$I_{A,d}(n)$	IGM of band A after equalization and combination	o	c	output of *EqualizeCombine*

4.9.5.2 Implementation of the equalization and combination function

The equalization and combination is defined throughout the document by the following function call:

$$I'_{j,d}(n) = \text{EqualizeCombine}\left\{I_{j,d}(n)\right\} \tag{1}$$

For channel A1 and A2, the equalization and combination must be performed. The equalization is performed only on one channel, either A1 or A2.

$$I'_{j_A^{eq},d}(n) = \sum_{c=-N^{cf}/2}^{N^{cf}/2-1} I_{j_A^{eq},d}(n+c+1)\cdot F_{j_A^{eq}}^{eq}(c-1) \tag{2}$$

where j_A^{eq} = A1 or A2.

Before equalization, the range of the interferogram is n. With values of n close to extremities of the interferogram, the indexing in above equation refers to values outside the range of n. In this case, the interferogram value is taken as 0. Therefore, the range after equalization is the same as before.

If j_A^{eq} = A1 the combined interferogram is:

$$I_{A,d}(n) = \frac{I'_{A1,d}(n) - I_{A2,d}(n)}{2} \tag{3}$$

and if j_A^{eq} = A2, the combined interferogram is:

$$I_{\mathrm{A},d}(n) = \frac{I_{\mathrm{A1},d}(n) - I'_{\mathrm{A2},d}(n)}{2} \tag{4}$$

4.9.6 Peak fitting

This general subfunction is used for the characterization of the peak in a given signal. The main characteristics are the peak height, position, width, and the constant DC offset.

This function is used in the spectral calibration for the localization of the reference peaks in the scene spectra, and is also used in the ILS retrieval function for the evaluation of the peak position and the offset.

4.9.6.1 Definition of variables

Variable	Descriptive Name	I/O	Type	Ranges / References / Remarks
	Peak fitting			
$y(i)$	Input data vector	i	r	
x_0	Horizontal axis origin	i	r	
Δx	Sampling of horizontal axis	i	r	
N	Number of points in signal	i	i	
i	index of points in signal	l	i	$i = 0,\ldots,N-1$
a	peak height	o	r	
b	peak horizontal position	o	r	
c	half width at half maximum	o	r	
d	offset	o	r	
p_c	Index of maximum point in $y(i)$	l	i	
A, B, C	Parabola coefficients	t	r	
$p_l,\ p_r,\ p_w$	Indices at left and at right of central peak, and full width	l	i	Used for HWHM finding

4.9.6.2 Implementation of the peak fitting

The peak fitting is defined by the following function call:

$$a,b,c,d \leftarrow \mathrm{FitPeak}\{y(i),\ x_0,\ \Delta x,\ N\} \tag{1}$$

The steps required for the evaluation of the characteristic parameters are the following:

1– Finds index of maximum point p_c in spectrum $y(i)$

2– Fits a parabola ($Ax^2 + Bx + C$) over the three maximum points (See Section 4.10.3).

$$A, B, C \leftarrow \text{ParabolaFit}\left\{\begin{array}{l} x_0 + (p_c - 1)\Delta x,\ y(p_c - 1), \\ x_0 + p_c \Delta x,\ y(p_c), \\ x_0 + (p_c + 1)\Delta x,\ y(p_c + 1) \end{array}\right\} \tag{2}$$

$$a = C - \frac{B^2}{4A} \qquad \text{found maximum height of signal} \tag{3}$$

$$b = \frac{-B}{2A} \qquad \text{found center of signal} \tag{4}$$

3– Starting from p_c, scan vector at right of peak until the magnitude of $y(i)$ becomes less than $a/2$. Note the found position p_r. Starting from p_c, scan vector at left of peak until the magnitude of $y(i)$ becomes less than $a/2$. Note the found position p_l.

$$p_w = p_r - p_l \qquad \text{FWHM in number of points}$$

$$c = \frac{p_w}{2}\Delta x \qquad \text{found HWHM} \tag{5}$$

4– The last parameter corresponding to the DC offset of the signal. If the signal is well conditioned, its evaluation can be done by taking the mean of all the radiance values outside twice the previously found width p_w:

$$d = \frac{1}{N - 2p_w}\left(\sum_{i=0}^{i<p_l - p_w/2} y(i) + \sum_{i=p_r + p_w/2}^{i<N} y(i)\right) \qquad \text{initial guess for DC offset} \tag{6}$$

Corrects the height of the peak by taking into account this offset:

$$a' = a - d \tag{7}$$

4.10 AUXILIARY SUBFUNCTIONS

4.10.1 Fast Fourier transforms

The definitions of the scaled discrete direct and inverse Fourier transforms are:

$$S(m) = \Delta x \sum_{n=0}^{N-1} I(n) \cdot e^{-2\pi i\, n\, m/N} \tag{1}$$

$$I(n) = \Delta\sigma \sum_{n=0}^{N-1} S(m) \cdot e^{+2\pi i\, n\, m/N} \tag{2}$$

where N = number of data points in numerical vectors

with

n and m the index data points ranging from: $0,\ldots,N-1$

and Δx the sampling of the interferogram: $\Delta x = \dfrac{\text{IGM width}}{N}$ [cm] (3)

and $\Delta\sigma$ the sampling of the spectrum: $\Delta\sigma = \dfrac{\text{SPC width}}{N}$ [cm^{-1}] (4)

The relation coupling the two spaces is: $\Delta x \Delta\sigma = \dfrac{1}{N}$ (5)

Fast Fourier Transform (FFT) algorithms exist that implement the same transformation in a much more efficient manner. Standard FFT algorithms are available in different programming languages. Care must be taken when considering the exponent sign (±) and the normalization constant ($1/N$ or $1/\sqrt{N}$ employed in the direct or inverse transform particular implementation. They will not be reproduced here. Moreover, we should mention that the present document assumes the standard type of algorithms that requires a number of points corresponding to an integer power of two for the input vector.

The choice of the FFT algorithm is an important issue for ground processing accuracy. From an accuracy point of view, no specific FFT algorithm is imposed and different algorithms are possible that use different optimization techniques. Consult [RD A] for a thorough study and various implementations of discrete FFTs.

Double precision computation is preferable for adequate numerical accuracy. This is especially true if a trigonometric recurrence algorithm is chosen, where the last points may be totally corrupted due to “rounding effect” in single precision. On modern computers, double precision algorithms requires almost the same computing time as the single precision algorithms, so there should be no penalty using maximum precision.

4.10.1.1 Data translation and centering

When using numerical Fourier transforms, special care must be taken about the data points ordering. Results from the direct FFT are usually returned in "normal" order (as opposed to the "bit reverse" sometimes seen):

If the input data to the FFT is a spectral series of length N with linear time spacing Δx:

$$x_i = \Delta x \times [0..N-1] \tag{6}$$

then the corresponding frequencies after execution of the FFT are:

$$\sigma_i = \frac{[0..N/2[,-[N/2..0[}{N\ \Delta\sigma} \tag{7}$$

i.e., the first half of the result corresponds to positive increasing frequencies; the second half of the result corresponds to negative frequencies (decreasing in absolute values). This is why an unswapping of the interferogram is required for adequate phase computation. An alternative way to avoid this operation is to introduce a linear phase shift into the input data to change the position of the transform. Since the easiest way to store the data is to put the origin at the center of the array, it is necessary the multiply the array by a phase factor of $(-1)^i$ to end up with a centered function after the transform is taken. For phase shifted, centered data, we have:

$$S(\sigma_i - N/2) \times (-1)^i = F\left\{I(x_i - N/2) \times (-1)^i\right\} \tag{8}$$

Therefore to obtain the correct result, the transform must also be multiplied by a $(-1)^i$ phase factor. For more information, consult [RD B].

References

[RD A] M. Frigo and S. G. Johnson, "The Fastest Fourier Transform in the West", Massachusetts Institute of Technology, fftw@theory.lcs.mit.edu, http://theory.lcs.mit.edu/~fftw/

[RD B] E. O. Brigham, "The Fast Fourier Transform", Prentice hall, Englewood Cliffs, New Jersey, 1974. ISBM 0-13-307496-X.

4.10.2 Alias unfolding

After the operation of decimation on an interferogram, the spectral range of the corresponding changes and must be precisely determined. To assign correct spectral axis one must perform *alias unfolding* (also called spectrum unscrambling or spectrum re-ordering) in order to remove the down conversion to a zero IF (intermediate Frequency) introduced at the satellite level

Let us suppose an original spectrum of N points with frequencies ranging from 0 to σ_L, where σ_L is the sampling frequency of the reference laser. Using a decimation frequency D_j (j for channel/band index), the apparent frequencies range from 0 to σ_L/D_j. The spectral range determination implies the reordering of the spectrum and a shift to the original band (consult [RD 17] for more details).

The reordering point k is determined with the following:

$$\sigma_{\min j} = \sigma_{\min j}^{\text{req}} - \frac{\left(\sigma_L / D_j\right) - \left(\sigma_{\max j}^{\text{req}} - \sigma_{\min j}^{\text{req}}\right)}{2} \tag{1}$$

$$k = \left(\text{Floor}\left\{ \frac{\sigma_{\min j} D_j N}{\sigma_L} \right\} \right) \bmod N \tag{2}$$

Equation (1) calculates a new $\sigma_{\min j}$ in order to center the band of interest (requested) in order to have an equal number of points on each side for the interpolation (to follow).

The location r of the band with regards to positions of folding in set with the following:

$$r = \text{Floor}\left\{ \frac{\sigma_{\min j} D_j}{\sigma_L} \right\} \tag{3}$$

The relation between m and σ reads as follows:

$$\sigma(m) = \begin{cases} \dfrac{\sigma_L}{D_j}\left(\dfrac{m}{N} + r + 1\right) & \text{for } 0 \le m < k \\ \dfrac{\sigma_L}{D_j}\left(\dfrac{m}{N} + r\right) & \text{for } k \le m \le N \end{cases} \tag{4}$$

An example of the effect aliasing of decimation after complex numerical filtering is provided in Figure 4.10.2-1. Another example has already been given in Figure 3.4.4-2.

The numerical operation of unscrambling must be executed after each Fourier transform on decimated signals.

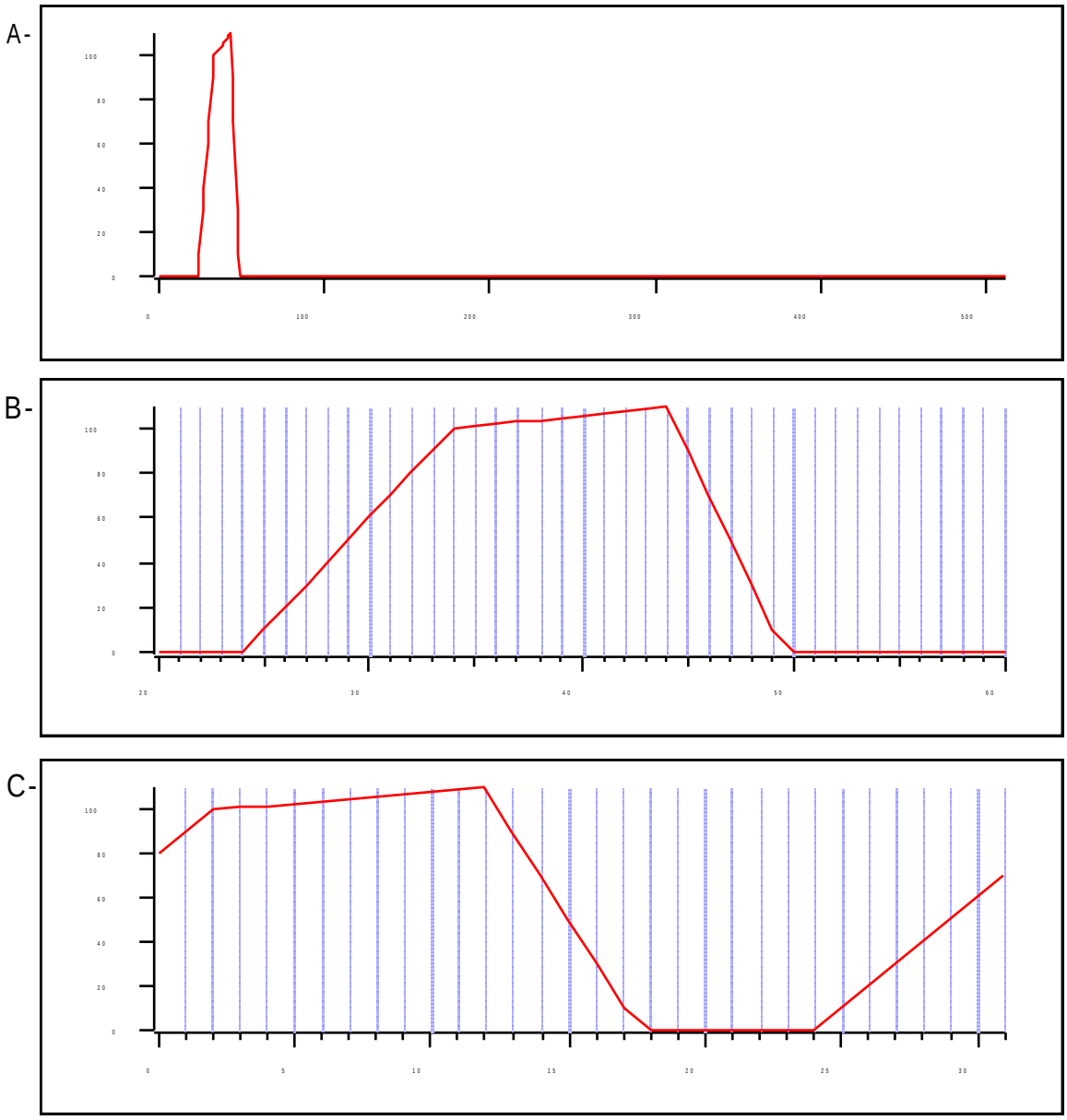

Figure 4.10.2-1: Aliasing by decimation (undersampling).

A– A band spectrum after complex numerical filtering. The sampling frequency is 512 (arbitrary units). There is no image above the Nyquist frequency (256).

B– Enlarged view of the band of interest. For a decimation factor of 16, the effective sampling frequency will be 32 and there will be a folding frequency within the band.

C– The resulting spectrum after decimation by a factor of 16. The folding frequency is now at the origin and the part of the spectrum that was below that frequency is now swapped to the top of the band.

Aliasing spike removal

If the numerical filter used for the decimation does not remove completely the DC level, an undesired aliasing spike occurs in the spectrum. To remove this spike, the first spectrum data point before reordering the data is replaced by the average of the last data point and the second data point.

$$S(0)=(S(1)+S(N-1))/2 \qquad (5)$$

4.10.3 Linear fitting

Description:

This subfunction is used for the determination of the slope and the ordinate of a straight line through a set of data points. It will be used for the determination of the slope in the coarse spectra phases for the fringe count error detection.

We give here a general description for the implementation of the algorithm, that is independent of the type of data used as input.

Processing:

Variable	Descriptive Name	I/O	Type	Ranges / References / Remarks
N	Dimension of vectors to fit	i	i	No restriction on the size of N
x_i	Abscissa data values	i	r	could also be specified by: $x_i = x_0 + i\Delta x = \Delta x(-N/2 + i)$
y_j	Ordinate data values	i	r	
m	Computed slope of the fitted line	o	r	
b	Computed ordinate at origin of the fitted line	o	r	

One of the simplest implementation of the linear fitting is defined as follows:

$$y = mx + b \tag{1}$$

$$t = N \times \sum_{i=0}^{N-1} x_i^2 - \left(\sum_{i=0}^{N-1} x_i \right)^2 \tag{2}$$

$$m = \frac{1}{t}\left[N \times \sum_{i=0}^{N-1} x_i y_i - \sum_{i=0}^{N-1} x_i \times \sum_{i=0}^{N-1} y_i \right] \tag{3}$$

$$b = \frac{1}{t}\left[\sum_{i=0}^{N-1} y_i \times \sum_{i=0}^{N-1} x_i^2 - \sum_{i=0}^{N-1} x_i \times \sum_{i=0}^{N-1} x_i y_i \right] \tag{4}$$

When the abscissa data is uniformly distributed at Δx intervals, the previous expression can be further simplified:

$$y = mx + b$$

$$\begin{aligned} x &= x_0,\ x_0+\Delta x,\ x_0+2\Delta x,\ \ldots,\ x_0+(N-1)\Delta x \\ &= x_0+[0,1,2,\ldots(N-1)]\ \Delta x \end{aligned} \tag{5}$$

$$t_1 = \frac{6}{\Delta x N(N+1)}, \tag{6}$$

$$t_2 = t_1 \sum_{i=0}^{N-1} y_i\ , \tag{7}$$

$$t_3 = \frac{2t_1}{N-1} \sum_{i=0}^{N-1} i\, y_i \tag{8}$$

$$m = t_3 - t_2, \tag{9}$$

$$b = t_2\left(x_0 + \Delta x \frac{2N-1}{3}\right) - t_3\left(x_0 + \Delta x \frac{N-1}{2}\right) \tag{10}$$

4.10.4 Parabolic fitting

Description:

This subfunction is used for the computation of the horizontal and vertical position of the maximum of a parabola defined by three points. It can be used as an example for the finding of the approximate position of a peak in spectrum or an interferogram. The method is to scan the vector to find the highest point, and then to compute a parabola that fits on that point and its two immediate neighbors.

Processing:

Variable	Descriptive Name	I/O	Type	Ranges / References / Remarks
(x_k, y_k)	Input coordinate pairs	i	r	k = 0, 1, 2
x_{max} and y_{max}	Coordinate of maximum	o	r	

The parabolic fitting is defined by the following function call:

$$x_{\max}, y_{\max} \leftarrow \text{ParabolaFit}\{(x_0, y_0),(x_1, y_1),(x_2, y_2)\} \quad (1)$$

The analytic form of the fit can be computed with help of an algebraic calculator like *Mathematica* for example:

Computes coefficients of a parabola: $y = Ax^2 + Bx + c$

passing through 3 points (x_0, y_0), (x_1, y_1), and (x_2, y_2)

```
M := {{x0^2,x0,1}, {x1^2,x1,1}, {x2^2,x2,1}};
MatrixForm[M]
v = {y0, y1, y2}
Simplify[LinearSolve[M, v]]
Simplify[% * (x1 - x0)(x2 - x1)(x2 - x0)]
```

the found analytical form is:

$$t = (x_1 - x_0)(x_2 - x_1)(x_2 - x_0) \quad (2)$$

$$A = \frac{1}{t}\left[y_0(x_2 - x_1) + y_1(x_0 - x_2) + y_2(x_1 - x_0)\right] \quad (3)$$

$$B = \frac{1}{t}\left[y_0(x_1^2 - x_2^2) + y_1(x_2^2 - x_0^2) + y_2(x_0^2 - x_1^2)\right] \quad (4)$$

$$C = \frac{1}{t}\left[y_0 x_1 x_2(x_2 - x_1) + y_1 x_0 x_2(x_0 - x_2) + y_2 x_0 x_1(x_1 - x_0)\right] \quad (5)$$

and the maximum point is then given by:

$$x_{\max} = \frac{-B}{2A} \tag{6}$$

$$y_{\max} = C - \frac{B^2}{4A} \tag{7}$$

4.10.5 Linear interpolation

Description:

Interpolates a value in a vector corresponding to a given abscissa value using a straight line model.

Processing:

Variable	Descriptive Name	I/O	Type	Ranges / References / Remarks
N	Dimension of input vectors	i	i	$k = 0..N-1$
x_k	Abscissa data values	i	r	is specified by x_0 and Δx
$f(x_k)$	Ordinate input data points	i	r	
x	Interpolation abscissa point	i	r	point at which interpolation is to be computed. Must be between input vector limits. Otherwise, extrapolation must be computed.
$f(x)$	Interpolated value	o	r	

The following description supposes a uniform points distribution:

For a given vector $f(x_k)$ defined on N points, *linear* interpolation can be expressed as:

$$f(x) = f(x_k) + \delta\left[f(x_{k+1}) - f(x_k)\right] \tag{1}$$

with the following definitions:

x is limited inside the vector: $x_0 \le x \le x_{N-1}$

k is the interpolation coefficient index: $k = \text{Floor}\left\{\dfrac{x - x_0}{\Delta x}\right\}, \quad 0 \le k \le N-1$

δ is the offset between two discrete points: $\delta = \dfrac{x - x_k}{\Delta x}, \quad 0 \le \delta < 1$

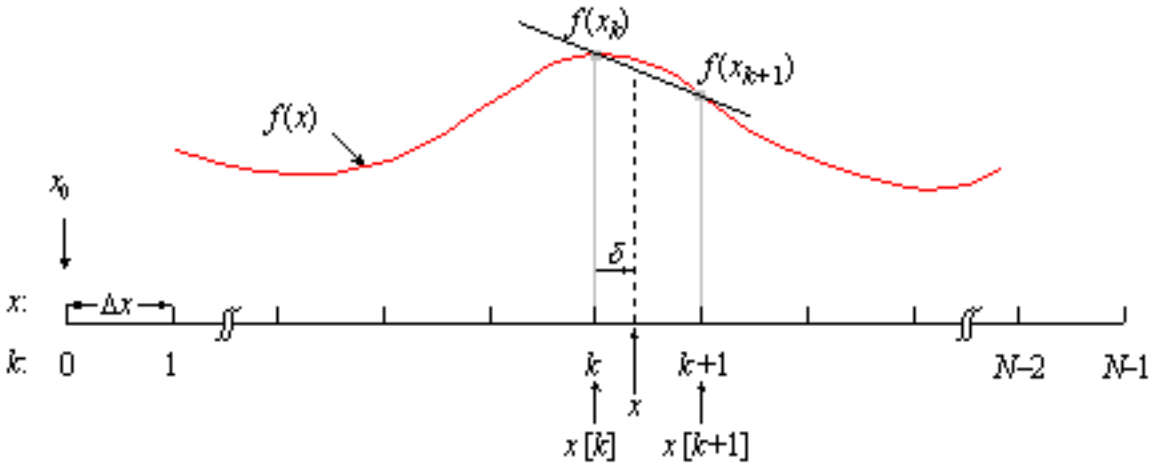

with $x_k = x_0 + k\,\Delta x$

The values of the interpolation function at arbitrary positions within integer sampling positions, occurs at fractional δ values.

4.10.6 Parabolic interpolation

Description:

Interpolates a value in a vector corresponding to a given abscissa value using a parabolic fit model.

Processing:

Variable	Descriptive Name	I/O	Type	Ranges / References / Remarks
N	Dimension of input vectors	i	i	$k = 0..N-1$
x_k	Abscissa data values	i	r	is specified by x_0 and Δx
$f(x_k)$	Ordinate input data points	i	r	
x	Interpolation abscissa point	i	r	point at which interpolation is to be computed. Must be between input vector limits. Otherwise, extrapolation must be computed.
$f(x)$	Interpolated value	o	r	

The following description supposes a uniform points distribution:

For a given vector $f(x_k)$ defined on N points, *parabolic* interpolation can be expressed as:

$$f(x) = A\delta^2 + B\delta + C \tag{1}$$

with the following definitions:

x is limited inside the vector: $x_0 \le x \le x_{N-1}$

k is the interpolation coefficient index: $k = \text{Floor}\left\{\frac{x - x_0}{\Delta x} + 0.5\right\}, \quad 0 \le k \le N-1$

δ is the offset between two discrete points: $\delta = \frac{x - x_k}{\Delta x}, \quad -\frac{1}{2} \le \delta < \frac{1}{2}$

and the parabolic coefficients:

$$A = \frac{f(x_{k-1}) - 2f(x_k) + f(x_{k+1})}{2}$$

$$B = \frac{f(x_{k+1}) - f(x_{k-1})}{2}$$

$$C = f(x_k)$$

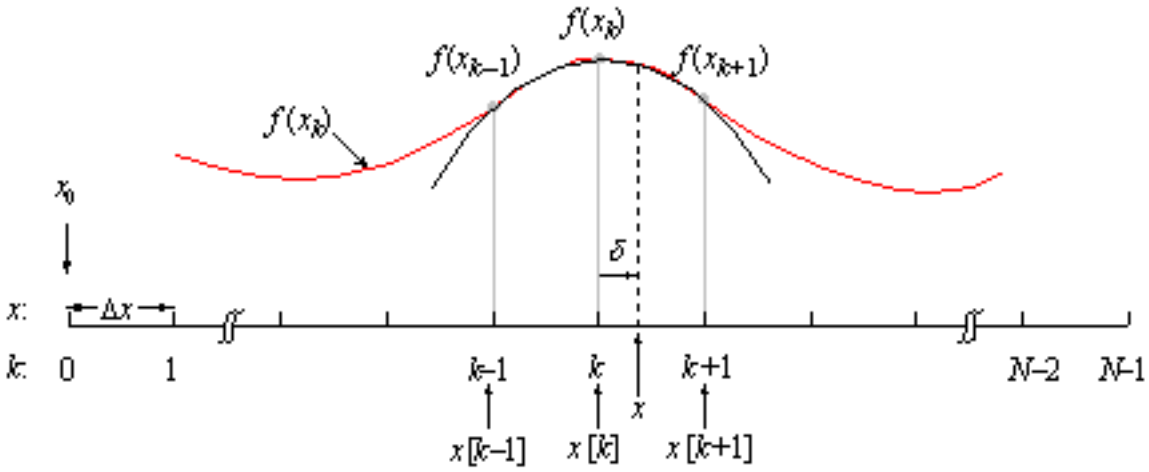

with $x_k = x_0 + k\Delta x$

The values of the interpolation function at arbitrary positions within integer sampling positions, occurs at fractional δ values.

A special care must be taken at the extremities of the vector, where indiciation can exceed the numerical limits. In this case, a linear interpolation can be used at the extremity points, or a cyclic indiciation can be supposed with the use of modulus.

4.10.7 Simplex minimization

Description:

For the solution of arbitrary algebraic equations, it is often useful to use minimization algorithms. This strategy, based on a convergent minimization of residuals between the reference data and the fit, enables the resolution of complex equations that some times would be unsolvable otherwise.

Different algorithms can be used for the minimization of residuals between experimental points and a mathematical model according to a set of independent parameters. The most common alternatives for the search of a minimum are [RD C, RD D, RD E]:

1– *The stepwise descent strategy*

Easy to program and converges virtually all the time, but can be extremely slow to run.

2– *The steepest descent methods*

Involve fewer iterations, but require knowledge or computation (by numerical differentiation) of the first derivative of the sum of square residuals.

3– *The Newton-Raphson algorithm*

The most popular nonlinear, least-square fitting algorithm today; it is fast, but always prone to divergence (if started from inaccurate initial guesses).

4– *The Marquart algorithm*

This algorithm and more recent methods (like *Powell's quadratically convergent method*) are mathematically equivalent to a mixture of methods 2 and 3. They avoid divergence problems of Newton-Raphson without unacceptable losses in speed. The amount and complexity of code generated can become substantial.

5– *The Simplex algorithm*

Proposed in 1965 [RD F], this method has the following advantages.

- Divergence is impossible
- Response value need to be computed only once or at most a few times for each iteration.
- No previously required knowledge of derivatives or numerical differentiation. This avoids rounding-off errors and allows the handling of non continuous functions.
- The number of data points and the number of parameters (m) are only limited by the speed and memory limitations of the machine on which the program will be run.
- Very generally speaking, the simplex algorithm usually converges in less than $20 \times m^2$ iterations.

Note that even if the Simplex never diverges, this does not guarantee that no problem will develop. Failure to converge and premature conclusion are usually the results of using the wrong input parameters (or with truncation/round-off errors in the machine's arithmetic when working with single precision numbers). But with appropriate guesses, this should never happen.

Sometimes, the Simplex gives results far from expected, but the fitted curve matches the experimental data excellently. This happens when a particular function can be equally satisfied with more than one set of parameters.

The big advantages of the Simplex algorithm are its remarkable speed, the fact that the program can never diverge, and the compactness of its implementation. Implemented in a curve-fitting algorithm, it is capable of handling virtually any function, no matter how complex, with any number of variables and parameters. It is the chosen tool for the current task of spectral calibration and ILS retrieval, because of its remarkable speed, simplicity, and reliability.

Processing:

Variable	Descriptive Name	I/O	Type	Ranges / References / Remarks
N	Dimension of input vectors	i	i	$i = 0..N-1$
Ncoeffs	Number of coefficients to fit	i	i	*Ncoeffs* < 10
p_j	Initial values for coefficients	i	r	
x_i	Abscissa input data values	i	r	
y_i	Ordinate input data values	i	r	
E	Merit value	t	r	Sum of squared residuals
tol	Tolerance for convergence	i	r	Relative convergence definition; $10^{-10} < tol < 10^{-3}$
model_fit	Residual minimization function	i	fnc	Sub-function computing SSR
p_j	Fitted coefficients	o	r	j: 0.. *Ncoeffs*–1
ftol	Residual error of fit	o	r	information parameter
iters	Number of iterations for convergence	o	i	informs about the speed of convergence

The Simplex method presume the existence of a “black-box” sub-algorithm, whose role is to compute the merit value, or the amplitude of what one is trying to minimize. In our case, we want to lessen the sum of the squares of the differences E between the fitted model and the reference data points. For random errors randomly distributed, this is the best criterion of all.

$$E = \sum_{i=0}^{N-1} \left[\text{model\_fit}(i, p_0, p_1, p_2, \ldots) - y_i\right]^2$$

where p_1, p_2, ... are a set of input parameters that characterize the theoretical model. For such an algorithm to work correctly, one must input initial values for these parameters. These initial values will be computed according to the physics of each specific problem.

By setting a suitable precision or a maximum number of iterations, the Simplex algorithm will modify the parameters and compute a residual value for each set until a minimum residual (or least square) is produced, yielding the “optimum” set of parameters for the considered case.

References:

[RD C] W. H. Press, S. A. Teukolsky, W. T. Vetterling, and B. P. Flannery, *Numerical Recipes in C: The art of scientific computing*, Second Ed., Cambridge University Press, 994 p., 1992.

[RD D] M. S. Caceci and W. P. Cacheris, *Fitting curves to data: The Simplex algorithm is the answer*, BYTE Magazine, May 1984, pp. 340–362.

[RD E] R. Beer, *Cross with your spectra? Cross-correlate instead!*, 5th Workshop on Atmospheric Science from Space using Fourier Transform Spectroscopy, Proceedings of the ASSFTS, Nov 30th–December 2nd, 1994, pp. 311–329

[RD F] J. A. Nedeler and R. Mead, "A simple method for function minimization", Computer Journal, 7, 308, 1965.

4.10.8 Determination of the goodness of fit

Description:

After a given fit has been computed, the standard deviation can be computed to evaluate the dispersion of the fit. The standard deviation is the root mean square of the deviations, and is associated with the *second moment* of the data about the mean [RD G].

A goodness of fit indicator can also be computed between the reference points and the fit to determine with which validity they are similar. A useful operator used to evaluate the goodness of fit criteria is mathematically derived as follows:

$$r = \frac{\sum_{i=0}^{N-1}(f_i - \bar{f})(y_i - \bar{y})}{\sqrt{\sum_{i=0}^{N-1}(f_i - \bar{f})^2}\sqrt{\sum_{i=0}^{N-1}(y_i - \bar{y})^2}} \quad [-1\ldots1] \qquad (1)$$

where f_i is the fitted data, or the experimental spectrum
y_i is the model data, or the reference spectrum
and $\bar{f}$ and $\bar{y}$ are the means of the vectors *f* and *y*.

Correlation coefficient *r*

r is the *linear-correlation coefficient*, also called the *product-moment correlation coefficient*, or *Pearson's r*. It indicates the strength of the association between the dependent and independent variables. The magnitude of the coefficient is not easy to interpret (see definition of coefficient of determination), but the sign (+ or –) indicates the direction of the relationship. The coefficient of correlation varies from –1 to +1, with –1, for example, indicating a reversed relationship (as one grows larger, the other grows smaller).

Coefficient of determination r^2

Measures the proportion of the variation of the dependent variable about its mean that is explained by the independent or predictor variable(s). The coefficient r^2 can vary between 0 and 1, inclusive. If the regression model is properly applied and estimated, the higher the value of r^2, the greater the explanatory power of the regression equation, and therefore the better the prediction of the criterion variable [RD H]. It takes a value of 1, termed "complete correlation", when the model and the experimental points match one-by-one.

r^2 has the following properties:

$r^2 = 1$ when input functions (the model and the experimental points) match perfectly.

$r^2 = 0$ when input functions are completely uncorrelated.

When a correlation is known to be significant, r^2 is one conventional way of summarizing its strength. In fact, the value of r^2 can be translated into a statement about what residuals (root mean square deviations) are to be expected if the data are fitted to a straight line by the least-squares method. This value is always bounded, but it does not indicate when a fit departs linearly from the reference.

Another similar determination coefficient is R^2, that is closely related to the c^2 criteria, and is defined as:

$$R^2 = 1 - \frac{\sum_{i=0}^{N-1}(f_i - \bar{f})^2}{\sum_{i=0}^{N-1}(y_i - \bar{y})^2} \tag{2}$$

$$R^2 = 1 - \frac{\text{unexplained variation}}{\text{total variation about the mean}} \quad [-\infty \ldots 1]$$

R^2 has the following properties:

$R^2 = 1$ when input functions (the model and the experimental points) match perfectly.

$R^2 = 0$ when input functions are completely uncorrelated.

$R^2 = -\infty$ when input functions are completely anti-correlated.

An ill conditioned case occurs when the model y is distributed around zero in an horizontal line: this causes both correlation factors to take small values even in the presence of good fits.

In summary, r and R are the correlation coefficients, while r^2 and R^2 are the determination factors. It is on the last two values that the present analysis is based. The squared values are used to simplify the understanding, and both r^2 and R^2 are used to get as much information as possible for the goodness of the fit. At the end of the study, maybe it will be judged that only one identificator is sufficient for a correct identification.

Further details regarding the correlation/determination coefficient can be found at the following references: [RD G, Chap. 11], [RD H, Chap. 11], [RD I, Chap. 15], [RD J, Sect. 24.12].

Processing:

Variable	Descriptive Name	I/O	Type	Ranges / References / Remarks
N	Dimension of input vectors	i	i	$i = 0..N-1$
y_i	Ordinate values of reference data points	i	r	
f_i	Ordinate values of fitted data	i	r	
s	Standard deviation	o	r	
r^2	Determination factor	o	r	$-1 \le r^2 \le 1$
R^2	Determination factor	o	r	$-\infty < R^2 \le 1$

The expression for the standard deviation s of the sample fit is given by:

$$s = \sqrt{\frac{1}{N-1}\sum_{i=0}^{N-1}(f_i - y_i)^2}$$

where f_i is the fitted data
y_i is the model data, or the reference points

References

[RD G] P. R. Bevington and D. K. Robinson, *Data reduction and error analysis for the physical sciences*, Second Edition, McGraw-Hill, Inc., New York, 328 p., 1992.

[RD H] J. F. Hair, Jr., R. E. Anderson, R. L. Tatham, *Multivariate Data Analysis*, with readings", Second Ed., Macmillan Publishing Company, London, 449 p., 1987.

[RD I] W. H. Press, S. A. Teukolsky, W. T. Vetterling, and B. P. Flannery, *Numerical Recipes in C: The art of scientific computing*, Second Ed., Cambridge University Press, 994 p., 1992.

[RD J] Erwin Kreyszig, *Advanced Engineering Mathematics*, Seventh Ed., John Wiley & Sons, Inc., New York, 1400 p., 1993.

5. GROUND PROCESSING ACCURACIES

5.1 Sources of processing errors

There are two main sources of processing errors

- Algorithm accuracy
- Finite precision of (real) numbers

5.1.1 Algorithm accuracy

An algorithm is the set of operations performed on data for a specific purpose; for example, algorithm for Fourier transform, algorithm for numerical integration, etc.

Algorithms can be exact or approximated. Exact algorithms introduce no errors on the data. For example, the algorithm for scalar product of two vectors is exact, i.e. the result is intrinsically accurate.

On the other hand, approximated algorithms have a limited accuracy depending on the level of approximation. For example, the algorithm for the numerical integration of an analytical function on a certain range by the method of rectangles is approximated. The result normally converges to the exact solution when the number of rectangles goes to infinity (on a finite range). The accuracy of the result for a given number of rectangles depends on that number, on the range of integration and on the behavior of the function in the range.

When the use of an approximated algorithm is necessary, the limitation on accuracy is normally the result of a trade-off between accuracy and computing time or storage space.

5.1.2 Finite precision

Because of the finite precision of the representation of real numbers in a computer, arithmetic operations can introduce errors on the results.

In a computer, floating point numbers are represented in a base β with an exponent e and a mantissa with precision p.

$$\pm \underbrace{ddd\ldots d}_{p} \times \beta^{\pm e}$$

For example in *IEEE* standard 754, β=2 and p=24 for single precision and β=2 and p=53 for double precision [RD X][RD Y].

In the *IEEE* standard, the result of an operation (e.g. addition, subtraction, multiplication, division, etc.) must be the same as if the operation was done exactly and then rounded to the precision used. This is called an "*exactly rounded operation*".

With finite precision, a first effect to consider is the fact that rounding errors can propagate toward higher digits when several successive operations are performed. For instance, if n operations are done, then the $q = log_2\ n$ lower digits can possibly be corrupted. This is the worst case (an upper limit) where all the rounding are cumulated. In general, some rounding errors are canceled with others. Nevertheless, the more operations are done, the more lower digits are possibly corrupted. If very long sums or products are done, the result obtained can be totally wrong. For example, if a sum of 2^{24} terms in single precision is done, all the digits can be corrupted and the result can be totally meaningless.

In addition, there are also "pathological cases" that need special attention when developing a computer software. A first case occurs when two very close numbers need to be subtracted (or added with one negative operand). The condition can be written as

$$x - y \leq \beta^{e-p+1}$$

To illustrate this case, let's take for example β=10 (base 10), e=2, p=3 (precision of 3 digits), $x = 1.01\times10^{e}$ and $y = 1.00\times10^{e}$ where the last digit of x is corrupted. Then $x - y = 0.01\times10^{e}$. In floating-point representation, numbers are normalized, i.e., the first digit must be different from 0. It means that the result will be shifted and represented as 1.00×10^{0}. Then, all the digits are wrong! A well known case is the quadratic formula, if b^2 is close to $4ac$ then the roots can be affected greatly.

Another case happen with the successive addition of numbers with important variations of the exponent. For example, taking $a_1 = 2.00\times10^{-10}$, $a_2 = 1.00\times10^{10}$, $a_3 = -1.00\times10^{10}$ and $a_4 = -1.00\times10^{-10}$, the exact sum is 1.00×10^{-10}. Because of the finite precision, $a_1 + a_2 = a_2$ and the final result will be -1.00×10^{-10}.

References

[RD X] "*What every computer scientist should know about floating-point arithmetic*" Computer Surveys, Association for Computing Machinery, Inc. March 1991.

[RD Y] "*IEEE Standard 754–1985 for Binary Floating-point arithmetic*", IEEE, 1985. Reprinted in SIGPLAN 22 (2) pp. 9–25.

5.2 General assumptions

The accuracy of the ground segment processing must be sufficient to allow the instrument to meet its performance requirements, i.e. the contribution from ground processing errors must be small in comparison with the contributions from the instrument.

5.2.1 Key Instrument performance requirements

According to the MIPAS Instrument Specification [RD 3], three basic requirements must be met:

- Radiometric Accuracy requirement
- Spectral Accuracy requirement
- LOS Accuracy requirement

Care must be taken to avoid the possibility of pathologic precision errors. It should be mentioned that increasing the precision *p* (taking double precision instead of single precision) does not eliminate these cases, it only extend the domain where they will not occur. The range of values must be checked and controlled as much as possible.

The algorithms used for ground processing should be exact wherever this is possible. When approximated algorithms are used, their accuracy should be checked against the performance requirements mentioned above.

In principle, the use of single precision should be sufficient as long as the number of operation done that affect one point of the spectrum is lower than 2^{14} =16384. That is, we need a relative error smaller than 0.1%, i.e., 10 higher bits of precision not contaminated. In the algorithm contain in the document, the average number of operations that affect one point of the spectrum is lower than 5000 (TBC). However, double precision arithmetic on today's computer is as fast as single precision. Therefore, double precision should be used for calculation. Also, pathological cases are not expected because the domain of values are conservatives, that is, interferogram and result of FFT range is [–32768, 32767], while the range of radiance, in appropriate units, is about $[10^{-4}, 10^{-9}]$.

Taking *IEEE* standard increases portability of software using floating-point numbers, i.e., the chance to obtain the same result on another platform. However, transcendental functions (e.g., exponential) are not ruled by the standard. They can give different results (on the lower digit) on different platforms because of the different techniques used (rational approximation, CORDIC, tables).

Special attention shall be paid to compiler optimizers. They can be a source of problems with floating-point arithmetic. They can modify the algorithms in an undesirable way.

APPENDIX A ILS ALGORITHM

A.1 Input Parameters

In the following, the main factors contributing to the ILS and spectral characteristics are listed together with their corresponding input parameters. Default values are also given.

Finite field of view

$\Delta\alpha_y$	Interferometer divergence (total angle) along *y* axis	0.0054 radians
$\Delta\alpha_z$	Interferometer divergence (total angle) along *z* axis	0.009 radians
N_y	Number of field of view subdivisions along *y* axis	13
N_z	Number of field of view subdivisions along *z* axis	20

Blur dimensions

b_y	Blur angular width along *y* axis	0.00052 radians
b_z	Blur angular width along *z* axis	0.00033 radians

Systematic IR misalignment

a_{Iy}	Misalignment angle along *y* axis	0.0002 radians
a_{Iz}	Misalignment angle along *z* axis	0.0002 radians

Systematic laser misalignment

a_{Ly}	Misalignment angle (radians) along *y* axis	0.00015 radians
a_{Lz}	Misalignment angle (radians) along *z* axis	0.00015 radians

Retroreflector shear

δ_y	Shear at ZPD along *y* axis	0.004 cm
δ_z	Shear at ZPD along *z* axis	0.004 cm
$\Delta\delta_y$	Linear shear variation (no units) along *y* axis	0
$\Delta\delta_z$	Linear shear variation (no units) along *z* axis	0

Sampling perturbation at turnaround

dx_0	Sampling perturbation on the first sample	4×10^{-8} cm
τ_s	Time constant for attenuation of sampling perturbation	0.16 second
MPD	Maximal optical path difference	8.2 cm
N_{opd}	Number of points in OPD	17 = 2 * *MPD* + 1

Optical speed profile

v	Nominal optical speed	10 cm/second
dv_0	Relative speed fluctuation (no units) on the first sample	0.03
τ_v	Time constant for attenuation of speed fluctuation	0.016 second
p	Slope of relative gain versus relative frequency (no units)	-0.22
Δt	Delay mismatch between IR electrical response and ADC trigger signal	1.4×10^{-6} second

Drift of laser frequency

σ_L	Nominal laser wavenumber	7606.6 cm^{-1}
$d\sigma_L$	Relative drift rate of laser wavenumber (maximum drift during one scan)	1×10^{-8} $second^{-1}$

White frequency noise on laser signal

BW_{Lw}	Laser bandwidth due to white frequency noise	2×10^{7} Hz

A.2 Formulas

For most of the following integrals, there is no analytical solution. They are computed numerically for discrete values. The optical path difference x varies from –Round(MPD) to +Round(MPD) for N_{opd} values, i.e., x_n = –Round(MPD) + $n \times \Delta x$
where Δx = 2Round(MPD) / (N_{opd} − 1) and $0 \le n < N_{opd}$. Sigma (σ) is the wavenumber at which the ILS is computed..

A.2.1 Integration on a Finite Field of View

With shear, misalignment and blur.

$$M_{IR}(\sigma,x)=\frac{1}{A}\int_{\alpha_{y1b}}^{\alpha_{y2b}}\int_{\alpha_{z1b}}^{\alpha_{z2b}} B(\alpha_y,\alpha_z)\,\mathrm{e}^{i2\pi\sigma\left\{x\left(\cos(\alpha_z)\cdot\cos(\alpha_y)-1\right)+\delta_y(x)\cdot\cos(\alpha_z)\cdot\sin(\alpha_y)+\delta_z(x)\cdot\sin(\alpha_z)\right\}}d\alpha_y d\alpha_z \qquad (1)$$

$$\delta_y(x)=2\delta_y+x\cdot\Delta\delta_y,\ \delta_z(x)=2\delta_z+x\cdot\Delta\delta_z \text{ and} \qquad (2)$$

$$A=\int_{\alpha_{y1b}}^{\alpha_{y2b}}\int_{\alpha_{z1b}}^{\alpha_{z2b}} B(\alpha_y,\alpha_z)\,d\alpha_y d\alpha_z \qquad (3)$$

where

$\alpha_{y1b}=a_{Iy}-\Delta\alpha_y/2-b_y/2$ $\quad$ $\alpha_{y2b}=a_{Iy}+\Delta\alpha_y/2+b_y/2$

$\alpha_{z1b}=a_{Iz}-\Delta\alpha_z/2-b_z/2$ $\quad$ $\alpha_{z2b}=a_{Iz}+\Delta\alpha_z/2+b_z/2$

The blur function is taken as $B(\alpha_y,\alpha_z)=B(\alpha_y)B(\alpha_z)$

$$B(\alpha_y) = 0 \qquad \text{for } \alpha_y \le \alpha_{y1b}$$
$$B(\alpha_y) = (\alpha_y - \alpha_{y1b}) / b_y \qquad \text{for } \alpha_{y1b} < \alpha_y < a_{Iy} - (\Delta\alpha_y - b_y)/2$$
$$B(\alpha_y) = 1 \qquad \text{for } a_{Iy} - (\Delta\alpha_y - b_y)/2 \le \alpha_y \le a_{Iy} + (\Delta\alpha_y - b_y)/2$$
$$B(\alpha_y) = 1 - (\alpha_y - (a_{Iy} + (\Delta\alpha_y - b_y)/2))/b_y \qquad \text{for } a_{Iy} + (\Delta\alpha_y - b_y)/2 < \alpha_y < \alpha_{y2b}$$
$$B(\alpha_y) = 0 \qquad \text{for } \alpha_y \ge \alpha_{y2b}$$

$$B(\alpha_z) = 0 \qquad \text{for } \alpha_z \le \alpha_{z1b}$$
$$B(\alpha_z) = (\alpha_z - \alpha_{z1b}) / b_z \qquad \text{for } \alpha_{z1b} < \alpha_z < a_{Iz} - (\Delta\alpha_z - b_z)/2$$
$$B(\alpha_z) = 1 \qquad \text{for } a_{Iz} - (\Delta\alpha_z - b_z)/2 \le \alpha_z \le a_{Iz} + (\Delta\alpha_z - b_z)/2$$
$$B(\alpha_z) = 1 - (\alpha_z - (a_{Iz} + (\Delta\alpha_z - b_z)/2))/b_z \qquad \text{for } a_{Iz} + (\Delta\alpha_z - b_z)/2 < \alpha_z < \alpha_{z2b}$$
$$B(\alpha_z) = 0 \qquad \text{for } \alpha_z \ge \alpha_{z2b}$$

Note : α_y and α_z are computed for N_y and N_z values respectively, i.e., $\alpha_{y,j} = \alpha_{y1b} + (j + 0.5) \times \delta\alpha_y$ where $\delta\alpha_y = (\alpha_{y2b} - \alpha_{y1b}) / N_y$, $0 \le j < N_y$ and $\alpha_{z,k} = \alpha_{z1b} + (k + 0.5) \times \delta\alpha_z$ where $\delta\alpha_z = (\alpha_{z2b} - \alpha_{z1b}) / N_z$ and $0 \le k < N_z$.

A.2.2 Laser Misalignment and Shear

$$M_L(\sigma, x) = \mathrm{e}^{-i2\pi\sigma\left\{x\left(\cos(a_{Lz})\cdot\cos(a_{Ly})-1\right)+\delta_y(x)\cdot\cos(a_{Lz})\cdot\sin(a_{Ly})+\delta_z(x)\cdot\sin(a_{Lz})\right\}} \qquad (1)$$

where $\delta_y(x) = 2\delta_y + x\cdot\Delta\delta_y$ and $\delta_z(x) = 2\delta_z + x\cdot\Delta\delta_z$

A.2.3 Optical Speed Profile

$$M_V(\sigma, x) = \left(1 + dv_0 \cdot p \cdot \mathrm{e}^{-\frac{x+MPD}{v\cdot\tau_v}}\right)\mathrm{e}^{i2\pi\sigma\cdot\Delta t\cdot v\cdot dv_0\cdot\mathrm{e}^{-\frac{x+MPD}{v\cdot\tau_v}}} \qquad (1)$$

A.2.4 Sampling Perturbation at Turn Around

$$M_{SP}(\sigma, x) = \mathrm{e}^{i2\pi\sigma\cdot dx_0\cdot\mathrm{e}^{-\frac{x+MPD}{v\cdot\tau_s}}} \qquad (1)$$

A.2.5 Drift of Laser Frequency

$$M_{Ld}(\sigma,x) = \mathrm{e}^{-i2\pi\sigma\cdot d\sigma_L\cdot x^2/v} \qquad (1)$$

A.2.6 White Frequency Noise on Laser Signal

$$M_{Lw}(\sigma,x) = \mathrm{e}^{-2\pi\frac{BW_{Lw}}{c}\cdot|x|\cdot\left(\frac{\sigma}{\sigma_L}\right)^2} \qquad (1)$$

where c is the light velocity (29979245800 cm/s)

A.2.7 Overall Modulation and ILS

The overall modulation function is

$$M(\sigma,x) = M_{IR}(\sigma,x)\cdot M_L(\sigma,x)\cdot M_V(\sigma,x)\cdot M_{SP}(\sigma,x)\cdot M_{Ld}(\sigma,x)\cdot M_{Lw}(\sigma,x) \qquad (1)$$

Before Fourier transform, points at extremities of modulation are normalized to take into account the fact that the sampling ends exactly at MPD.

$$M(\sigma,x_0) = M(\sigma,x_0)\times A \text{ and } M\left(\sigma,x_{N_{opd}-1}\right) = M\left(\sigma,x_{N_{opd}-1}\right)\times A$$
$$\text{where } A = 0.5 + MPD - Round(MPD) \qquad (2)$$

A normalization is done in order to obtain an area under the ILS curve equal to unity.

$$M(\sigma,x) = M(\sigma,x) / \mathrm{Real}\left\{M\left(\sigma,x_{(N_{opd}-1)/2}\right)\right\} \qquad (3)$$

Perform a zero-filling each side to 1024 points and a fast Fourier transform (FFT).

$$I(\sigma,\sigma') = \Delta x \sum_{x=-MPD}^{MPD} M(\sigma,x)\cdot e^{-i2\pi x\sigma'} \qquad (4)$$

The dual σ' dependence means that at each observed wavenumber σ, we may have a different ILS curve $I = f(\sigma')$.

APPENDIX B ADDITIONAL FUNCTIONALITY ALGORITHMS

This appendix describes the algorithms related to the additional functionalities of the MIPAS ground segment prototype software. For a description of the additional functionalities, see PO-SW-ESA-GS-0545.

B.1 ANALYZE INTERFEROGRAM

The present Section describes the *Analyze Interferogram* function that gives the ZPD peak position and height of the inputted interferogram.

B.1.1 Definition of variables

Analyze Interferogram

Variable	Descriptive Name	I/O	Type	Ranges / References / Remarks
	Global variables & indices			
N	Number of points in input IGM	i	i	
n	Input IGM data point index	l	i	$n = \begin{cases} -\frac{N}{2},\ldots,\frac{N}{2}-1, \text{if } N \text{ is even} \\ -\frac{N-1}{2},\ldots,\frac{N-1}{2}, \text{if } N \text{ is odd} \end{cases}$
B.1.2.1	*Calculate modulus*			
$I(n)$	Input IGM to be analyzed	i	c/r	
$I^M(n)$	Modulus of input IGMs	i	r	
B.1.2.2	*Fit ZPD Peak*			
n^{max}	Absolute maximum data point index	l	i	
x^{ZPD}	ZPD position	O	r	
I^{ZPD}	ZPD height	O	r	

B.1.2 Formulas

B.1.2.1 Calculate modulus

If the interferogram is complex, i.e., filtered and decimated, the modulus is calculated:

$$I^M(n) = |I(n)| \tag{1}$$

If it is real, i.e., raw:

$$I^M(n) = I(n) \tag{2}$$

B.1.2.2 Fit ZPD peak

Find data point index n^{max} of absolute maximum in $I^M(n)$ and fits a parabola over the three local points.

$$x^{ZPD}, I^{ZPD} \leftarrow \text{ParabolaFit}\left\{\begin{matrix}\left(x\left(n^{\max}-1\right), I\left(n^{\max}-1\right)\right), \\ \left(x\left(n^{\max}\right), I\left(n^{\max}\right)\right), \\ \left(x\left(n^{\max}+1\right), I\left(n^{\max}+1\right)\right)\end{matrix}\right\} \quad (1)$$

where $x(n)$ is the interferogram grid.

B.2 RAW TO NOMINAL

The present Section describes the *Raw to Nominal* function that applies numerical filtering, decimation and channel combination according to the on-board SPE model to data acquired in raw data mode.

B.2.1 Definition of variables

Raw to Nominal

Variable	Descriptive Name	I/O	Type	Ranges / References / Remarks
	Global variables & indices			
N	Number of points in raw IGM	i	i	
n	Input IGM data point index	l	i	$n = \begin{cases} -\frac{N}{2},\ldots,\frac{N}{2}-1, & \text{if } N \text{ is even} \\ -\frac{N-1}{2},\ldots,\frac{N-1}{2}, & \text{if } N \text{ is odd} \end{cases}$
j	Input channel index	l	i	j = A1, A2, B1, B2, C1, C2, D1 and D2
d	Direction index	l	i	d = Forward or Reverse
B.2.2.1	*Filtering and decimation*			
$I_{j,d}(n)$	Raw IGMs to be processed	i	r	
M	Number of points in complex filter	a	i	M = [1,..,512]
c	Filter data point index	l	i	$c = 0,\ldots,M-1$
$F_j(c)$	Complex numerical filter for channel j	a	c	The filter includes the equalization filter, see on-board SPE model.
$W_{n'}$	Decimated data point index	t	i	
D_j	Decimation factor of channel j	a	r	
P	Right shift position	a	i	$P = 0,\ldots,47$
B.2.2.2	*Channel combination*			
j'	Output band index	l	i	j' = A1, A2, AB, B, C and D
n'	Output IGM data point index	l	i	
N'	Number of points in decimated IGM	o	i	
$I'_{j',d}(n')$	Nominal IGMs	O	c	

B.2.2 Formulas

B.2.2.1 Filtering and decimation

The numerical filter should be applied to the following decimated positions on the raw interferograms:

$$W_0 = 0$$
$$W_{n'} = W_{n'-1} + D_j \quad (1)$$

Filtering is done as follow:

$$I_{j,d}^{FD}(n') = \sum_{c=0}^{M-1} I_{j,d}(W_{n'} + c) \cdot F_j(M - 1 - c) \quad (2)$$

The result is accumulated in a 48 bit register. After completion, only the higher 24 bits from position *P* are kept.

$$I_{j,d}^{Trunc}(n') = \left(\frac{I_{j,d}^{FD}(n')}{2^P} \right) \bmod 2^{24} \quad (3)$$

The number of points decimated is:

$$N' = \text{Floor}\left[\frac{N - M}{D_j} \right] + 1 \quad (4)$$

B.2.2.2 Channel combination

For channels *j* = A1, A2, B1, and B2, no signal combination is performed only truncation to 18 bits.

$$I'_{j',d}(n') = \text{Floor}\left(\frac{I_{j,d}^{Trunc}(n')}{2^6} \right) \quad (1)$$

where $(j', j) \in \{(A1, A1), (A2, A2), (AB, B1), (B, B2)\}$.

For channels *j* = C1, C2, D1, and D2, signal combination is performed before truncation to 18 bits.

$$I'_{j',d}(n') = \text{Floor}\left(\frac{I_{j1,d}^{Trunc}(n') + I_{j2,d}^{Trunc}(n')}{2^7} \right) \quad (2)$$

where $(j', j1, j2) \in \{(C, C1, C2), (D, D1, D2)\}$.

B.3 INTRODUCE FCE

The present Section describes the *Introduce FCE* function that applies a fringe count error to the inputted interferograms for different decimation factors.

B.3.1 Definition of variables

Introduce FCE

Variable	Descriptive Name	I/O	Type	Ranges / References / Remarks
	Global variables & indices			
N_j	Number of points in IGM	i	i	
n	Input IGM data point index	l	i	$n = \begin{cases} -\frac{N_j}{2},\ldots,\frac{N_j}{2}-1, & \text{if } N_j \text{ is even} \\ -\frac{N_j-1}{2},\ldots,\frac{N_j-1}{2}, & \text{if } N_j \text{ is odd} \end{cases}$
j	Input channel/band index	l	i	
d	Direction index	l	i	d = Forward or Reverse
B.3.2.1	*Fringe count error introduction*			
$I_{j,d}(n)$	IGMs to be processed	i	c	
Δx	Nominal sampling interval	a	r	$1/\sigma_L$
h_d	OPD shift to introduce	a	i	
$I'_{j,d}(n)$	FCE IGMs	O	c	

B.3.2 Formulas

B.3.2.1 Fringe count error introduction

The fringe count error introduction is done as the FCE correction but with the OPD shift in opposite direction, i.e., with a minus sign:

$$I'_{j,d}(n) = \text{FCE Correct}\left\{I_{j,d}(n), -h_d, \Delta x\right\} \quad (1)$$

B.4 COADD INTERFEROGRAMS

The present Section describes the *Coadd Interferograms* function that coadds interferograms (scene, *ds* or *bb* measurements) taking into account FCE.

NOTE: in the following, the "*S*" superscript stands for "*source*" and means that the measurement can be either a deep space (*ds*), a scene (*sc*) or a blackbody (*bb*) measurement.

B.4.1 Definition of variables

Coadd Interferograms

Variable	Descriptive Name	I/O	Type	Ranges / References / Remarks
	Global variables & indices			
N_j^S	Number of points in IGM	i	i	
N_j^{zpd}	Number of points to define the *coarse* spectra	a	i	Power of 2
N_k	Number of IGMs to coadd	i	i	
n	Input IGM data point index	l	i	$n = \begin{cases} -\frac{N_j^S}{2},\ldots,\frac{N_j^S}{2}-1, & \text{if } N_j^S \text{ is even} \\ -\frac{N_j^S-1}{2},\ldots,\frac{N_j^S-1}{2}, & \text{if } N_j^S \text{ is odd} \end{cases}$
n^c	Coarse IGM data point index	l	i	$n^c = -\frac{N_j^{zpd}}{2},\ldots,\frac{N_j^{zpd}}{2}-1$
m^c	Coarse spectrum data point index	l	i	$m^c = 0,\ldots,N_j^{zpd}-1$
j	Input channel/band index	l	i	
d	Direction index	l	i	d = Forward or Reverse
k	Index of IGM in a coaddition group	l	i	$k = 1,\ldots,N_k$
$\Delta\sigma_j^{Scc}$	Wavenumber spacing in band j of calibrated coarse spectrum	t	r	calibrated with correction factor
$\sigma_{0\,j}^{Scc}$	Starting wavenumber in band j of calibrated coarse spectrum	t	r	calibrated with correction factor
B.4.2.1	*Spikes detection*			
$I^S_{j,d,k}(n)$	IGMs to be coadded	i	c	
B.4.2.2	*Gain spectral interpolation*			
N_j^{req}	Requested number of points in spectrum	i	i	
m^r	Requested spectrum data point index	l	i	$m^r = 0,\ldots,N_j^{req}-1$
$\Delta\sigma_j^{req}$	Requested wavenumber spacing in band j of spectrum	i	r	

Variable	Descriptive Name	I/O	Type	Ranges / References / Remarks
$\sigma_{0\,j}^{req}$	Requested starting wavenumber in band *j* of spectrum	i	r	
$G_{j,d}(m^r)$	Previous gain	i	c	
$G^I_{j,d}(m^c)$	Previous gain, interpolated	t	c	
B.4.2.3	*Calculate coarse spectra*			
$S^{Sc}_{j,d,k}(m^c)$	Coarse spectrum	t	c	
$\Delta\sigma_j^{Sc}$	Wavenumber spacing in band *j* of coarse spectrum	t	r	
$\sigma_{0\,j}^{Sc}$	Starting wavenumber in band *j* of coarse spectrum	t	r	
k_{SC}	Spectral calibration correction factor	i	r	
B.4.2.4	*Calculate calibrated spectra*			
$S^{Scc}_{j,d,k}(m^c)$	Coarse calibrated spectrum	t	c	
B.4.2.5	*Fringe count error detection*			
N^{ADC}	Number of sample data points in IGM before decimation	i	i	Extracted from MIPAS source packet
D_j	Decimation factor of band *j*	i	i	Extracted from auxiliary data of MIPAS source packet
h_j^{sys}	Systematic OPD shift of IGM	t	i	$h_j^{sys} = \left(N^{ADC}/2 - 128\right) \bmod D_j$ if $\left(\left(N^{ADC} - 256\right)/D_j + 1\right) \bmod 2 = 0$ then $h_j^{sys} = h_j^{sys} - D_j$
$h^S_{d,k}$	OPD shift of IGM	t	i	
Δx	Nominal sampling interval	a	r	$1/\sigma_L$
B.4.2.6	*Fringe count error correction*			
B.4.2.7	*Interferogram coaddition*			
$I^S_{j,d}(n)$	Coadded IGMs	O	c	

B.4.2 Formulas

B.4.2.1 Spikes detection

The detection and correction of spikes caused by cosmic radiation or transmission errors is computed on the input interferogram, according to the procedure described in Section 4.9.1.2:

$$I'^S_{j,d,k}(n) = \text{CorrectSpikes}\left\{I^S_{j,d,k}(n), N^S_j\right\} \qquad (1)$$

B.4.2.2 Gain spectral interpolation

For *j* limited to band B and C, we do an interpolation of the actual gain to a coarser resolution by the operation:

$$G^{I}_{j,d}(m^c) = \text{Interpolate}\left\{G_{j,d}(m^r); \Delta\sigma^{req}_j, \sigma^{req}_{0_j}, N^{req}_j \rightarrow \Delta\sigma^{Scc}_j, \sigma^{Scc}_{0_j}, N^{zpd}_j\right\} \quad (1)$$

with the procedure described in Section 4.10.5 according to the *Linear Interpolation Method*.

The range of data points index of the input gain is defined by the *requested* spectral calibration:

$$m^r = 0,\ldots, N^{req}_j - 1$$

The computed range of data points index is defined by the *actual* spectral calibration, but at coarse resolution.

$$m^c = 0,\ldots, N^{zpd}_j - 1$$

B.4.2.3 Calculate coarse spectra

This subfunction computes a coarse spectrum of the interferograms. A Fourier transform is done at very low resolution, on the ZPD region of each interferogram:

$$S^{Sc}_{j,d,k}\left(m^c\right) = \text{FFT}\left\{I^{S}_{j,d,k}\left(n^c\right)\right\} \quad (1)$$

The range of data points index defined by the *coarse* spectral calibration is:

$$n^c = -\frac{N^{zpd}_j}{2},\ldots,\frac{N^{zpd}_j}{2} - 1$$

where N^{zpd}_j is an integer power of 2, and *j* is limited to the B and C bands. For a given measurement, the sweep direction may be either forward or reverse.

The radiometric vector is then unscrambled following the method described in Section 4.10.2. The corresponding spectral axis vector $\sigma^{Sc}_j\left(m^c\right)$ is computed according to equation (4) of that same section. This spectral vector is then calibrated by a multiplication by the current spectral calibration correction factor k_{SC}. If no spectral calibration is available yet, this scaling is taken as unity.

$$\begin{aligned}\Delta\sigma^{Scc}_j &= \Delta\sigma^{Sc}_j \cdot k_{SC}\\ \sigma^{Scc}_{0_j} &= \sigma^{Sc}_{0_j} \cdot k_{SC}\end{aligned} \quad (2)$$

In addition to this stretching of the spectral axis, an inverse stretching must be applied on the radiometric scale to ensure the conservation of energy in the signal. This compensation can be applied with the following spectral calibration.

B.4.2.4 Calculate calibrated spectra

For j = B and C, the coarse calibrated spectrum is obtained with:

$$S^{Scc}_{j,d,k}\left(m^c\right) = S^{Sc}_{j,d,k}\left(m^c\right) \cdot G^{I}_{j,d}\left(m^c\right) / k_{SC} \quad (1)$$

B.4.2.5 Fringe count error detection

The fringe count error detection can be computed from these calibrated spectra, according to the procedure described in Section 4.9.3.2 for j = B and C:

$$h^{S}_{d,k} = \text{FCE Detect}\left\{S^{Scc}_{j,d,k}\left(m^c\right), \sigma^{Scc}_{j}\left(m^c\right), \Delta x, h^{sys}_{j}\right\} \quad (1)$$

B.4.2.6 Fringe count error correction

The fringe count error correction is applied only if a non-zero OPD shift $(h^{S}_{d,k} - h^{sys}_{j})$ is calculated. It is applied on the current interferogram at the input resolution, according to the procedure described in Section 4.9.3.3:

$$I'^{S}_{j,d,k}(n) = \text{FCE Correct}\left\{I^{S}_{j,d,k}(n), (h^{S}_{d,k} - h^{sys}_{j}), \Delta x\right\} \quad (1)$$

The correction is applied to all detectors/bands so:

j = A1, A2, AB, B, C and D

B.4.2.7 Interferogram coaddition

The coaddition is performed on each interferograms. There is a separate coaddition for each band and sweep direction:

$$I^{S}_{j,d}(n) = \frac{1}{N_k} \sum_{k=1}^{N_k} I^{S}_{j,d,k}(n) \quad (1)$$

— End of document —